Technical Report Documentation Page

1. Report No.	2. Government Accession No.	3. Recipient's Catalog No.
FHWA/TX-98/1472-1F		

4. Title and Subtitle	5. Report Date
TIGHTENING PROCEDURES FOR LARGE-DIAMETER ANCHOR BOLTS	December 1996 Resubmitted: June 1997
	6. Performing Organization Code
7. Author(s) R. W. James, P. B. Keating, R. W. Bolton, F. C. Benson, D. E. Bray, R. C. Abraham, and J. B. Hodge	8. Performing Organization Report No. Research Report 1472-1F
9. Performing Organization Name and Address Texas Transportation Institute The Texas A&M University System College Station, Texas 77843-3135	10. Work Unit No. (TRAIS)
	11. Contract or Grant No. Study No. 0-1472
12. Sponsoring Agency Name and Address Texas Department of Transportation Research and Technology Transfer Office P. O. Box 5080 Austin, Texas 78763-5080	13. Type of Report and Period Covered Final Report: September 1994-August 1996
	14. Sponsoring Agency Code

15. Supplementary Notes

Research performed in cooperation with the Texas Department of Transportation and the U. S. Department of Transportation, Federal Highway Administration.
Research Study Title: Tightening Procedures for Large-Diameter Anchor Bolts

16. Abstract

Recent failures of cantilever overhead sign structures in Michigan and elsewhere, coupled with the absence of standards for tightening methods for the double-nut system used with large-diameter anchor bolts in similar structures in Texas have been the motivation for this study. Practices of various field offices were reviewed, a literature study was performed, and both laboratory studies and field studies were performed. Three questions were raised: How tight do the anchor bolt nuts need to be? What techniques and procedures are best suited for tightening? How can tightness best be inspected? Standards for tightening procedures for large-diameter anchor bolts are proposed.

In current TxDOT practice, the contractor is left to his or her own judgment concerning how tight to tighten the nuts on the double-nut anchor bolt system. Recent bolt failures in other states have raised concerns about nut tightening procedures. When the nuts of a double-nut system are not tightened sufficiently, fatigue loading, and even impact loading, can be factors in the performance of the bolts.

Three full-size test specimens were built in the laboratory to evaluate tightening methods and the fatigue performance of the double-nut system used for anchorage of cantilever overhead sign structures (COSS) and on high mast illumination poles (HMIP). Analytical and numerical studies were performed to identify and study parameters affecting the stresses in the anchor bolts. Field studies were conducted to measure the wind-load induced anchor bolt reactions and stresses in one specimen of each type. This report details these studies and the findings.

17. Key Words	18. Distribution Statement
Anchor Bolt, Double-Nut System, Fatigue, Tightening, Wind Loads	No restrictions. This document is available to the public through NTIS: National Technical Information Service 5285 Port Royal Road Springfield, Virginia 22161

19. Security Classif.(of this report)	20. Security Classif.(of this page)	21. No. of Pages	22. Price
Unclassified	Unclassified	206	

TIGHTENING PROCEDURES FOR LARGE-DIAMETER ANCHOR BOLTS

by

Ray W. James
Associate Research Engineer
Texas Transportation Institute

Peter B. Keating
Associate Research Engineer
Texas Transportation Institute

Robert W. Bolton
Assistant Research Engineer
Texas Transportation Institute

Fred C. Benson
Department of Civil and Mechanical Engineering
Texas A&M University - Kingsville

Don E. Bray
Department of Mechanical Engineering
Texas A&M University

Ryan C. Abraham
Research Assistant
Texas Transportation Institute

J. Blake Hodge
Research Assistant
Texas Transportation Institute

Research Report 1472-1F
Research Study Number 0-1472
Research Study Title: Tightening Procedures for Large-Diameter Anchor Bolts

Sponsored by the
Texas Department of Transportation
In Cooperation with
U. S. Department of Transportation,
Federal Highway Administration

December 1996
Resubmitted: June 1997

TEXAS TRANSPORTATION INSTITUTE
The Texas A&M University System
College Station, Texas 77843-3135

IMPLEMENTATION RECOMMENDATIONS

This research report presents various findings and recommendations which may be implemented in different ways. Most significantly, a proposed method for tightening large-diameter anchor bolts is codified in the form of a proposed specification, suitable for inclusion into the existing standard construction specifications. The proposed specification is included as an appendix to this research report.

1) It is recommended that the Department adopt a standard specification for tightening large-diameter anchor bolts by the contractor at the time of installation. A draft specification is given in Appendix D.

2) It is recommended that the Department identify twenty to thirty COSS structures for field inspection. Candidate structures should be selected based on time in service in areas subject to frequent high wind loadings. The anchor bolts in these structures should be inspected for defects using ultrasonic methods, the nuts should be inspected for tightness using a slug wrench and sledgehammer, and the pole-baseplate weld should be inspected visually using dye-penetrant enhancers, or ultrasonically, for cracks. The results of these inspections should be reviewed to determine whether additional field inspections are needed.

DISCLAIMER

The contents of this report reflect the views of the authors, who are responsible for the facts and the accuracy of the data presented herein. The contents do not necessarily reflect the official view or policies of the Federal Highway Administration or the Texas Department of Transportation. This report does not constitute a standard, specification, or regulation. This report is not intended for construction, bidding, or permit purposes. Ray W. James, P.E. 12430.

ACKNOWLEDGMENTS

Funding for this study was provided by the Texas Department of Transportation, cooperatively with the Federal Highway Administration and the Texas Transportation Institute, for which the researchers are appreciative. Special thanks is also due to the Project Director, Jim Yang, and to Karl Burkett and the many other technical advisors who assisted with different aspects of the study. Many TxDOT field personnel also assisted by sharing their knowledge and data. Special thanks are due to a few who worked closely to coordinate the placement of the field laboratory in Hempstead, including Mohammad Rafipour. Thanks are also offered to Louis Rychlik of the Materials and Test Field Office, Houston District, for sharing his files and anchor bolt experience with the researchers.

TABLE OF CONTENTS

LIST OF FIGURES

LIST OF TABLES

SUMMARY

Large-diameter anchor bolts, of bolt diameter 38 mm (1.5 in.) or greater, are commonly used to secure the bases of high-mast illumination poles (HMIP) and cantilever overhead sign structures (COSS) to drilled shaft foundation pedestals. Typically, a galvanized steel anchor bolt is cast in place in the reinforced concrete (RC) foundation, and a double-nut system, one above and one below the structural base plate, is used to plumb and secure the structure. No standards for developing any preload in the anchor are specified in TxDOT practice. The contractor is left to his own judgment with respect to how much to tighten the nut. Presently, it is common practice for the contractor to weld the nuts to the washers and the washers to the base plate after tightening, to prevent loosening. While this practice is probably effective, it prevents the inspection of nut tightness. Factors influencing nut loosening include anchor system compliance, preload, and thread pitch.

The loading environment for the structure is governed by four types of wind loads, as the structures are tall and often include a long cantilevered component subject to wind loading. Fatigue of the anchor bolts and nut loosening are two concerns.

The advantage of the double-nut system is the ease of construction. An additional advantage in the double-nut system is the preload induced in the anchor bolt in the region of the baseplate between the two nuts. This preload has a beneficial effect on the fatigue performance of the double-nut connection even though the portion of the bolt below the bottom nut is not preloaded in this system.

Recent COSS anchor bolt failures have emphasized these concerns. Michigan DOT, in reaction to these two failures, initiated a study of their practice in designing, specifying, inspecting, and tightening these anchor bolts. Their findings indicated that the cyclic loads caused by wind-induced vibration and vortex shedding were responsible for the fatigue failures in the bolts, leading to a catastrophic failure of the structure.

This study includes 1) a review of the literature addressing wind loading, fatigue, and tightening methods 2) a survey of practices by TxDOT and others responsible for tightening and maintaining large-diameter anchor bolts in COSS, HMIP and similar applications, 3) a study of

the stresses induced in the anchor bolts by tightening, 4) a study of the effectiveness of various tightening techniques, 5) laboratory fatigue tests of full-scale anchorages of both COSS and HMIP specimens, and 6) field studies of responses of both COSS and HMIP structures.

Results of the study are a series of fifteen conclusions regarding the desirability of preloading anchor bolts, the methods useful for achieving a preload, methods potentially useful for inspecting nuts for tightness in the field, general conclusions from laboratory testing, field performance of the two structure studied, and the significance of misaligned bolts. Also resulting is a recommended draft specification for tightening of large-diameter anchor bolts by the contractor at the time of installation.

INTRODUCTION AND PROBLEM STATEMENT

Large-diameter high strength anchor bolts are defined as bolts with diameters greater than or equal to 38 mm (1.5 in.) and yield strengths greater than 345 MPa (50 ksi) (Hasselwander, et al. 1974). Large-diameter anchor bolts are commonly used to secure the baseplates of cantilevered overhead sign structures (COSS) and high-mast illumination poles (HMIP) to drilled shaft foundation pedestals. Typically, galvanized steel anchor bolts are cast in place in the reinforced concrete foundation, and a double nut system, one above and one below the structural base plate, is used to secure the structure to the foundation. The double nut system is used primarily because of the ease with which the structure can be plumbed and secured.

Structures utilizing large-diameter anchor bolts are tall and often include a long cantilevered component. Vortex shedding from the wind loads is suspected to cause significant cyclic loading in the anchor bolts and has been a factor in recent failures in other states. The double nut system has been shown to improve the fatigue life of the anchor bolts when the top nut is tightened to produce a preload in the anchor bolt in the region between the top and bottom nuts (Fisher 1978). The preload moves the failure plane from a section beneath the top nut to a section beneath the bottom nut. The preload reduces the cyclic stress range induced in the bolt in this region between the two nuts. The portion of the bolt below the bottom nut is not preloaded in this system, however.

No standards for tightening the nuts or developing any preload in the anchor are specified in current Texas Department of Transportation (TxDOT) practice. The contractor is left to his own judgment to determine how much to tighten the nuts. Presently, it is common practice for the contractor to spot weld the nuts to the washers and the washers to the baseplate after tightening, to prevent loosening. While this practice is generally effective, it prevents future inspection of nut tightness.

Recent failures of four COSS structures have raised questions about the fatigue behavior of large-diameter anchor bolts. Two structures failed in Michigan, one in Georgia, and one in Texas. The Michigan failures were attributed to fatigue fracture of the anchor bolts caused by crosswind vibrations resulting from vortex shedding. Both the COSS and the HMIP structures

are susceptible to vortex shedding induced vibrations.

Background

The two failures in Michigan prompted the Michigan Department of Transportation (MDOT) to devise an action plan to resolve the problem in 1990. The action plan began with inspections of other COSS structures for cracked anchor bolts. These inspections resulted in the removal of seven damaged structures. Ongoing maintenance inspections were implemented. Next, MDOT began a metallurgical analysis of the failed anchor bolts. MDOT carried out tests at Lehigh University and devised recommendations for new designs, inspection procedures, and installation techniques (Culp, et al. 1990). It was found that the best way to overcome the fatigue problem was to preload the anchor bolts in the double nut configuration.

Michigan DOT also initiated a study of their practice in designing, specifying, inspecting, and tightening these anchor bolts (Ness and Till 1992). The findings indicated that the cyclic loads caused by wind-induced vibration and vortex shedding were responsible for the fatigue failures in the bolts, leading to a catastrophic failure of the structure. Their study resulted in lowering the allowable stress ranges allowed in the design of the bolts. The study also changed the way the erecting contractor develops bolt preloads and the way state maintenance forces inspect and correct nut tightness. Subsequent field inspections detected numerous loose anchor nuts thought to be a result of lax construction specifications, inadequate inspection, and careless construction practices, with nut loosening being a possible factor. These studies led MDOT to develop specifications for bolt preloads based on the "turn-of-the-nut" method (MDOT 1994).

Literature Review

Frank (1978) reported a study of fatigue tests of anchor bolts. The objective of the study was to determine the influence of several specifications and design parameters on the fatigue behavior of anchor bolts. The parameters that are of most interest to the present study are thread pitch, bolt diameter, grade of steel, stress range, and preload. Frank concluded

(a) the stress range was the most significant variable determining the fatigue life of an anchor bolt,

(b) the bolt diameter had no significant effect on the fatigue performance,

(c) low strength steels were found to have longer fatigue lives than high strength steels,

(d) preload in the double nut system increased the fatigue life, and

(e) thread pitch did not affect fatigue life, although future tests were recommended to confirm this last conclusion.

While this report includes excellent data concerning fatigue life, it did not address tightening procedures.

The Materials and Technology Division of the MDOT studied the static and fatigue strength of anchor bolts. Lower and Pearson (1987) concluded that (a) galvanizing reduced the fatigue life of anchor bolts, and (b) stainless steel bolts have much longer fatigue lives than galvanized bolts but are not cost effective. In another MDOT study (McCrum 1993), anchor bolts on two separate cantilevered sign structures were instrumented to measure anchor bolt stresses. This study found that the structure did not experience any loading that induced more than a 20 MPa (3 ksi) stress range in the anchor bolts for weeks to months at a time. McCrum (1993) reported,

> "When the conditions were right to produce significant loading, however, a fair number of cycles would usually occur in a relatively short period of time (i.e. several hundred to several thousand cycles/day). The most prevalent loading cycle pattern did not appear to be related to a shedding vortex produced by a relatively constant wind, but rather the result of a variation of wind conditions (speed and/or direction) that roughly corresponded to the structure's natural frequency (i.e. resonance). Peak load cycles were produced during relatively high variations in wind speed (i.e. 20-25 ksi load cycle corresponding to wind fluctuations from roughly 20 to 50 mph)."

MDOT developed specifications covering tightening procedures for COSS anchor bolts (MDOT 1994) applicable to all COSS anchor bolts installed in the field. The procedure for the

inspection of sign structures was also reviewed. These and a few other MDOT articles (Wong, et al. 1990; Ness and Till 1992; Till 1992) all resulted from the failures of COSS anchor bolts in January and February of 1990.

Fisher (1990) studied the failed bolts from one of the Michigan structures and estimated the stress range and number of cycles to fracture of the primary failure. Fisher determined that the bolt fracture grew while loaded with a stress range between 70 and 100 MPa (10 and 15 ksi) at a rate of 40,000 to 100,000 cycles per year over a period of ten years. The stress range was in agreement with the calculated vortex-shedding loading stress range. Fisher noted that the cyclic loading environment for these structures includes at least four distinct types of loadings or wind-induced motions: natural wind gusts, truck-induced wind gusts, galloping, and vortex shedding, and further research to measure wind loading due to the number of wind induced problems was recommended.

Other articles (McDonald, et al. 1995; Product Engineering 1977; Lockmann 1981; Siavelis and Hosteny 1984; Dann 1975; Maruyama and Nakagawa 1985; Bickford 1987) deal with various problems concerning anchor bolts. The need for preload, nut loosening, tightening methods, and effects of thread type on tightening are topics discussed in these articles. However, none of these studies specifically address large-diameter anchor bolts.

Although failures have not occurred in HMIPs, these structures have similar anchor bolt connections which see cyclic stresses from vortex shedding. Studies done at Texas Tech University evaluating current Texas Department of Transportation (TxDOT) wind loading design procedures show that the HMIPs located on the coast are subjected to higher wind load forces than previously assumed (McDonald 1995). HMIP anchor bolts were addressed in the present study.

Other factors which affect the fatigue behavior of anchor bolts include anchor bolt material and environmental effects. The most suitable steel for anchor bolts is ASTM A193 Grade B7. Nuts and washers should be ASTM A194 (Hasselwander 1974). This steel provides high levels of yield strength between 520 MPa (75 ksi) and 725 MPa (105 ksi) and has consistently uniform material properties. The bolt-nut-washer assembly is galvanized to prevent corrosion. It has been shown that galvanized anchor bolts have shorter fatigue lives than bolts

without galvanizing (Lower and Pearson 1987). This is primarily because galvanizing requires the molten zinc to be in the temperature range of heat treatment for steel, and this may diminish the steel mechanical properties. Also, the effects of freezing and thawing act to reduce the preload in a double nut configuration (Higgins and Klingner 1991).

An analysis of present methods of modeling wind induced cyclic loading applicable to cylindrical structures such as the HMIP, and supporting dynamic characteristics for the HMIP structure investigated in the present study is presented in Appendices A and B, respectively. Appendix A also includes the basis for potential improvements in present analytical methods.

OBJECTIVES OF THE STUDY

Open questions left from previous research include determination of how much preload, if any, is desirable in applications representative of TxDOT practice, whether snug tight or tightened nuts loosen under field loadings, and how best to tighten the nuts on the anchor bolt. Fisher (1990) also noted that more data was needed to understand the effects of wind-induced vibrations on structures. The objective of the present study is to develop standards for tightening procedures for large-diameter anchor bolts utilizing the double-nut system. Specifically, this study addresses the following three questions:

- How tight should the anchor bolt nuts be tightened?
- How can the desirable degree of tightness be obtained?
- Once the structure is in service, how can the nut tightness be confirmed?

Based on the findings of this study, a specification is developed to provide uniformity among TxDOT districts and to help ensure the continued good performance of large-diameter anchor bolts used to secure high mast lighting and overhead sign structures with the double-nut system.

CURRENT PRACTICES

Survey of Preferred Bolt Tightening Methods

Traffic Signal Office, Corpus Christi District, TxDOT (Turner and Stone 1994)

The Corpus Christi District Signal Office tightens large-diameter anchor bolts using knockerwrenches and sledgehammers. District personnel strike the knockerwrench with a sledgehammer until the nut ceases to turn. At this point, the pitch of the wrench hammer sound becomes much higher, and the knockhammer wrench starts to rebound significantly. Nuts are impact-tightened onto foundation base plates in an alternating pattern using this method. The District resorts to the use of a knockerwrench (as opposed to a cheater pipe on a large wrench) for large-diameter bolt tightening at bolt diameters of 38 mm to 44 mm (1.5 in. to 1.75 in.).

The knockerwrench is widely used in the petroleum industry. It is a 3.7 to 7.8 kg (8 to 17 lb) steel wrench that gives an approximately 0.36 to 0.42 m (1.2 to 1.4 ft) long lever arm for the sledgehammer impact. Table 1 shows some wrench data.

Table 1 Dimensions of knocker wrenches used in field.

Bolt diameter mm (in.)	Knocker-wrench mass kg (lb)	Overall length mm (in.)	Distance--℄ wrench end to ℄ knocker end mm (in.)	Angle-- knocker end to wrench end (deg)
60 (2-3/8)	18 (8.3)	366 (14.4)	74 (2.9)	3.6
70 (2-3/4)	20 (9.1)	357 (14.0)	71 (2.8)	2.9

The method used by the Corpus Christi District could be called a form of the turn-of-the-nut method; however, no measure is made of how much rotation is involved until the nut reaches its final position. The change in pitch of the tightening sound is thought to be independent of the effort of the person using the hammer.

East Nueces County Maintenance Office TxDOT (Bedolla 1994)

State maintenance personnel, in their annually scheduled Safety Lighting Contract inspection of bridges, sign support structures, cantilever sign support structures and luminaire foundations, provide for tightening of loose nuts and washers on large-diameter anchor bolts. If state forces find loose nuts and washers, they employ either large crescent wrenches with cheater pipes or a knockerwrench with sledgehammer, depending on the bolt size. This approach mirrors that of the Corpus Christi District Traffic Signal Office discussed above.

V. C. Huff, Inc. and Saxet Fabrication, Corpus Christi (Nava and Wheeler 1994)

These contractors follow the TxDOT Item 447 and Item 613 specification requirements to tighten large-diameter anchor bolts of 38 mm (1.5 in.) diameter and larger. This specification does not force them into the turn-of-the-nut method. Frank Nava (of V. C. Huff, Inc.) and Penty Wheeler (of Saxet Fabrication) expressed definite opinions concerning the turn-of-the-nut plus one-third tightening method. They consider that the knockerwrench tightening procedure used by the Corpus Christi District probably does approximate the turn-of-the-nut (snug tight plus one-third turn) tightening procedure. They noted that the largest bolt size governed by the turn-of-the-nut procedure in the TxDOT specifications is 38 mm (1.5 in.).

Traffic Signal Office, Houston District, TxDOT (Wong and Painter 1994)

The Houston District TxDOT requires its contractors and State Forces to use the turn-of-the-nut tightening method as described in TxDOT Specifications Item 447 "Structural Bolting." Top nuts are turned to a wrench tight condition using an open end wrench and a six-foot cheater pipe. Nuts are turned an additional two-thirds turn or 240° after wrench snug tight. The Houston District then requires contractors to come back a week later and recheck the bolts for tightness with a wrench and a 1.8m (6 ft) cheater pipe to guard against relaxation loosening from the relaxation forces from hot-dip galvanized surfaces.

The Houston District personnel expressed that their contractors may not be providing adequate wrenches to accomplish proper tightening in some cases. This is especially true for the 92 mm (3.625 in.) nuts required to fit the 57 mm (2.25 in.) anchor bolts used on many high mast lighting installations around the District. Contractors are currently fabricating a square wrench to handle the large hex nuts and are employing a 1.5 m to 1.8 m (5 ft to 6 ft) cheater pipe with this wrench. Concerning overall contractor practices in the Houston District, contractors are not using calibrated or special torque wrenches, and they are not using knockerwrenches.

TxDOT Design Division Personnel (Burkett and Yang 1994)

Design Division personnel indicated that TxDOT needed a simple procedure for tightening large-diameter anchor bolts, many of which were 38 mm (1.5 in.) in diameter or larger in overhead sign supports and high mast lighting installations in the field. The bolt tightening procedure should be easily implemented in the field. It should also avoid expensive equipment such as calibrated torque wrenches. Finally, it would be most desirable if bolt strain, both longitudinal and radial, could be determined. This strain measurement could possibly be done by calibrated washers, extensometers or other adaptable indicating devices.

King Ranch Gas Plant, Exxon Corporation (Meyers 1995)

Bolted installations at the Exxon King Ranch Gas Plant are single nut systems. Exxon blocks and shims up their foundation mounted equipment, grouts to the bottom of bearing bases and flanges and tightens down top nuts on washers onto the top the equipment bearing and base plates to secure the equipment to the foundation. Exxon employs three methods for tightening of anchor bolts in their single nut systems. These include (Turner and Stone 1994) wrenches with cheater pipes, (Bedolla 1994) knockerwrenches with sledgehammers and (Nava and Wheeler 1994) calibrated torque wrenches. Knockerwrenches are the least used methods. These tend to be used only for those inaccessible installations where the other two methods cannot be successfully used. Exxon employs either 3.5 kg (8 lb) or 8.7 kg (20 lb) sledgehammers to impact knockerwrenches on nuts. This hammer size selection is dependent on the ability of the person using the hammer to swing it effectively.

Wrenches with cheater pipes are often used. Open-end wrenches are used on bolts of up to 25 mm (1 in.) in diameter, while closed end wrenches are used for larger size bolts. Cheater pipe lengths used with the above wrenches may range from 1 m (3 ft) to as long as 3.7m (12 ft), with six people operating, for tightening 57 mm (2.25 in.) anchor bolts.

Torque wrenches are the tightening method of preference at the King Ranch Gas Plant. They employ a torque wrench obtained from Nelms-Shineberg Tool in Corpus Christi, Texas. Exxon company policy calls for them to use the torque wrench according to the manufacturer's specifications. Approximately 99 percent of the Gas Plant's bolt tightening is accompanied with this wrench. The bolt tightening done by the Gas Plant personnel has two major objectives. The first is to achieve an anchor nut sufficiently tightened on the bolt so that it does not loosen under the effects of vibration and heat encountered in the service of their reciprocating engines. An accompanying second objective is to not stress bolts so as to cause excessive yielding.

Central and South West Services (Polasek 1994)

Central and South West Services uses the turn-of-the-nut method to tighten the top nuts on their anchor bolted structural pole towers for their 69, 138 and 345 kVA power transmission lines. This method is outlined in the American Institute of Steel Construction steel manual, "Specifications for Structural Joints Using ASTM A325 or A490 Bolts," Section 8, page 5-273 (AISC 1989). Other than this AISC specification, Central and South West have no written procedure. Polasek indicated that it is common practice in the power industry to use the turn-of-the-nut method. Central and South West Services appears to be completely satisfied with the results of this method.

Thomas & Betts, Memphis, Tennessee (Hinkle 1995)

This design firm that serves the electric power industry calls for nuts on large-diameter anchor bolts, typically 57 mm (2.25 in.) diameter, to be tightened to a "wrench snug" condition. After this, the nuts are turned an additional one-sixth turn or 60° of rotation to complete the tightening. These bolts experience 99 to 100 percent of their structural loading in tension.

Survey of Preferred Large-Diameter Anchor Bolt Materials, Construction and Special Practices

Anchor Bolt, Nut, and Washer Steel Material

V. C. Huff, Inc. and Saxet Fabrication Contractor (Nava and Wheeler 1994) noted that they typically furnish ASTM A325 grade high strength anchor bolts on TxDOT projects for the Corpus Christi District. Alloy steel anchor bolts when used are ASTM A193 Grade B7 material

with ASTM A194-2H nuts and ASTM A436 washers.

Central & South West Services (Polasek 1994) requires number 18 or 57.2 mm (2.25 in.) jumbo rebar with cut threads for its installation anchor bolts. These bolts conform to ASTM A615, Grade 75. The top 600 mm (2 ft), including threads, are hot-dip galvanized.

The King Ranch Gas Plant (Meyers 1995), Exxon Corporation uses a common black bolt ASTM B7 for their anchor bolts. The Gas Plant does not galvanize its bolts, as most service of its bolts is indoors to anchor reciprocating engines. The Gas Plant has used stainless steel with bolts up to 32 mm (1.25 in.) diameter, but feel that stainless steel for larger diameter bolts is too expensive.

Thomas & Betts (Hinkle 1995) specifies anchor bolts for the power industry. The anchor bolts they design for are typically 57 mm (2.25 inch) diameter, standard threads, and come with oversize nuts because of the galvanizing. The anchor bolts typically specified are made of 75 ksi yield strength steel. Thomas and Betts personnel feel that anchor bolts should either consist of mild steel and/or meet a certain Charpy Impact Test requirement. This requirement should be 1.2 N-m/cm^3 (15ft-lb/ in^3) at -30° C (-20° F).

Anchor Bolt Threading, Galvanizing, Lubrication, and Washer Use

Corpus Christi District, TxDOT (Turner and Stone 1994). The Corpus Christi District (Signal Office) requires galvanizing on the top 0.6 m (2 ft) of their 2.4-m (8-ft) long anchor bolts that go into their high mast luminaire foundations. They use a stick treatment to patch deep scratches in galvanized surfaces. The Corpus Christi District appears to be happy with galvanized treated bolts, nuts and washers.

The Corpus Christi District uses no special surface treatments or special thread coatings prior to nut tightening. They feel that oil for better lubrication of thread surfaces would tend to be unsafe. True, this would allow the galvanized nut to be wrenched onto the bolt tighter, but it would also provide increased liability of the nut to loosen against lessened friction.

East Nueces County Maintenance Office, TxDOT (Bedolla 1994). Loose bottom and top nuts on double-nut anchor bolt installations have been a continual problem for this TxDOT Maintenance Office. Maintenance personnel attribute this problem to poor or no inspection being accomplished on these installations at the time of construction. Interestingly, of eight anchor bolted installations observed on January 16, 1996, in the company of Mr. Bedolla, the author observed four installations whose anchor bolts had no washers at the bottom and top nuts. No detrimental performance, however, appeared to be attributable to these installations.

The Nueces County Maintenance Office has also had trouble with top nuts coming loose on low to medium height luminaire poles located on concrete median barriers. Here the problem has been lock washers failing in fatigue, because the top nuts were not tightened down sufficiently at the finish of installation. When the lock washers failed, the top nuts loosened and the poles listed. Bedolla stated a dislike for the use of both regular washers and lock washers. He preferred a procedure calling for tightening nuts directly onto base plates.

V. C. Huff, (Contractor) and Saxet Fabrication (Contractor), Corpus Christi, Texas (Nava and Wheeler 1994). These contractors believe that washers serve the important function of spreading the load and making it easier to wrench nuts into place during bolt tightening. In their opinion, spot welding of top nuts to washers and then washers to base plates would probably not be necessary if nuts were tightened with knockerwrenches. These contractors believed that lubrication of the top nut and protruding bolt threads (above the base plate) could probably be employed as a tensioning advantage. Since all large-diameter anchor bolts are Unified National Coarse (UNC) threads, Frank Nava and Penty Wheeler believed that, if lubrication were used, the thread-lubrication situation would reduce thread galling and still prohibit the backing off of nuts due to the lubrication. They consider that the pipe thread coat allowed by the TxDOT specifications would serve the same purpose as the beeswax proposed by the Michigan Department of Transportation.

Traffic Signal Office, Houston District, TxDOT (Wong and Painter 1994). The Houston District prefers the double nutted anchor bolt installations with a washer under each nut. Nuts are tack welded to washers, which in turn are tack welded to base plates. Concerning washers, the Houston District personnel do not feel the need for them if the base plate bolt holes are not too large in relation to the nut. The nuts used in the Houston District are required to have washer faces, which are believed to work well in this situation. The Houston District personnel believes that proper lubricants on the threads of top nuts and on protruding bolts are acceptable, but improper lubricants can cause thread galling.

TxDOT Design Division Personnel (Burkett and Yang 1994). These personnel expressed concern over practices of lubrication of the top nut and protruding bolt threads prior to bolt tightening. They feel that in some instances tightening nuts on bolts in this lubricated condition might lead to overstressing of the anchor bolt in the region of the base plate.

King Ranch Gas Plant, Exxon Corporation (Meyers 1995). Because all of their installations are indoors, the King Ranch Gas Plant does not use galvanizing on any of their anchor bolts. The Exxon Gas Plant personnel do not want to have galvanizing in their stressful situations of intense heat and vibration. Since these are high temperature operations, any galvanizing might flake off. Other potential problems here would include the locking or seizing up of nuts on bolts in service. Threads on the Gas Plant anchor bolts are the coarse threads of pitch 3-4 mm (7 or 8 threads per inch). Exxon does not use lock washers or other special devices such as locking pins. Exxon does not tack weld washers at the King Ranch Gas Plant.

The King Ranch Gas Plant has several important requirements for washers and their single-nutted, grout- padded installations. First, washers should be steel and acceptably flat. Secondly, the King Ranch Gas Plant places considerable importance on the use of washers in an effort to get an "honest torque." Washers, therefore, help overcome wrenching friction and thus achieve more net torque in running the nut down on the anchor bolt and compressing the base

plate. Thus, washers are credited with the beneficial effects of increasing tension in the anchor bolt, evening out torque on the bolt and preventing the scoring of the base plate by the faying surface of the turning nut. Concerning anchor bolt thread preparation, the King Ranch Gas Plant first achieves a good brushing and cleaning of the anchor bolt's threaded surfaces. They then lubricate the threads of nuts prior to bolt tightening.

Central and South West Services (Polasek 1994). Central and South West Services tack welds nuts to washers and washers to base plates after tightening the top nuts. Blemishes in galvanizing on anchor bolts, nuts and washers are touched up with a coat of zinc-rich galvanizing compound, such as CRC. Polasek sees no need to call for a lubricant to be used on top nut and anchor bolt threads to increase base plate bearing pressure for the same tightening torque.

Thomas & Betts, Memphis, Tennessee (Hinkle 1995). Typical anchor bolts are made from jumbo reinforcing steel and have cut threads. Hinkle saw no need to go the extra expense of obtaining anchor bolts with rolled threads, although rolled threads would avoid the inclusion of microscopic failure surfaces that occur in the cutting of threads during manufacture. Typically, the bolts that Thomas & Betts specify are hot-dip galvanized for the top 300 mm (12 in.) to 600 mm (24 in.). Tack welding of top nuts and washers is accomplished by some industry members to ensure that top nuts and washers do not loosen. Other industry members employ an additional one-half thickness nut on top of the anchor nut to serve as a jam or locking nut and dispense with tack welding.

Anchor Bolt Failure Experience

The Corpus Christi District has never experienced bolt failures from bolt fatigue cracking. They have experienced an instance or two when top nuts became loose on luminaire pole foundations. The Houston District has never encountered an event where bolts failed due to loose top nuts causing subsequent bolt fatigue failure. They did have one cantilever sign support structure fall onto the Southwest Freeway due to snapped bolts. Two factors contributed to this failure. First, anchor bolts had been cold worked after concreting to straighten them out. Second, no reinforcing cage had been placed around the anchor bolt assembly to hold concrete around the bolts.

V. C. Huff, Inc. and Saxet Fabrication indicated no experience with anchor bolt failures caused from fatigue failure due to top nuts becoming loose on the bolts. The King Ranch Gas Plant has had anchor bolts crack and/or break. They believe that loose nuts plus vibration and heat have been the primary causative factors here. The loose nuts on their reciprocating engine anchor bolts may be due in part to vibration and thermal expansion; however, Exxon personnel feel that failure to properly torque the nut is the real cause of nut loosening. Central and South West Services have experienced no problems with nut loosening in service. They have had no problems with bolts cracking or failing in service. Thomas & Betts personnel indicated no encounters with anchor bolt failures due to bolt fatigue resulting from loose nuts.

Special Agency Situations

Traffic Signal Office, Houston District, TxDOT (Turner and Stone 1994)

The Traffic Signal Office personnel expressed concern that a major oversight existed in the TxDOT specifications concerning large-diameter anchor bolt tightening. This problem stems from the galvanizing of threads and faying surfaces on bolts, nuts and washers. The problem is

that the tightened galvanized surfaces creep or relax after first tightening within probably one week's time. This relaxation creates a state of looseness in the bolt, nut and washer system.

The solution should be that the specifications require these galvanized nuts to be retightened as needed a week after first tightening. After this retightening, then tack welding of washers to nuts and base plates would be allowed to take place.

King Ranch Gas Plant, Exxon Corporation (Meyers 1995)

Cadmium plated bolts have caused significant failure problems at the King Ranch Gas Plant. Such special plated bolts have consistently failed in service and are no longer allowed for use in the plant.

FIELD STUDY--HMIP AT TAMU RIVERSIDE CAMPUS NEAR BRYAN, TEXAS

Stress range histograms for three anchor bolt axial bridges and two pole bending bridges were collected on an instrumented HMIP at the Texas A&M University Riverside Campus. This HMIP structure, shown in Figure 1, was used in a previous TxDOT sponsored project to study the illumination properties of different fixtures and lighting arrangements (Walton and Rowan 1969). The test HMIP structure is 53 300 mm (175 ft) tall and is composed of six linearly tapered, octagonal cross-sectioned segments. The flat-to-flat diameter varies from 910 mm (36 in.) at the base to 200 mm (7.75 in.) at the top. The wall thickness of the six segments are 14 mm (9/16 in.), 14 mm (9/16 in.), 13 mm (1/2 in.), 11 mm (7/16 in.), 10 mm (3/8 in.), and 8 mm (5/16 in.), respectively from bottom to top. The base of the HMIP structure seen in Figure 2 has twelve 57 mm (2.25 in.) anchor bolts. The anchor bolts have a thread pitch of 3.2 mm (8 threads/in.), and the nuts are tack welded to the baseplate. (See Appendix A for a detail drawing of the HMIP bottom segment and base plate.)

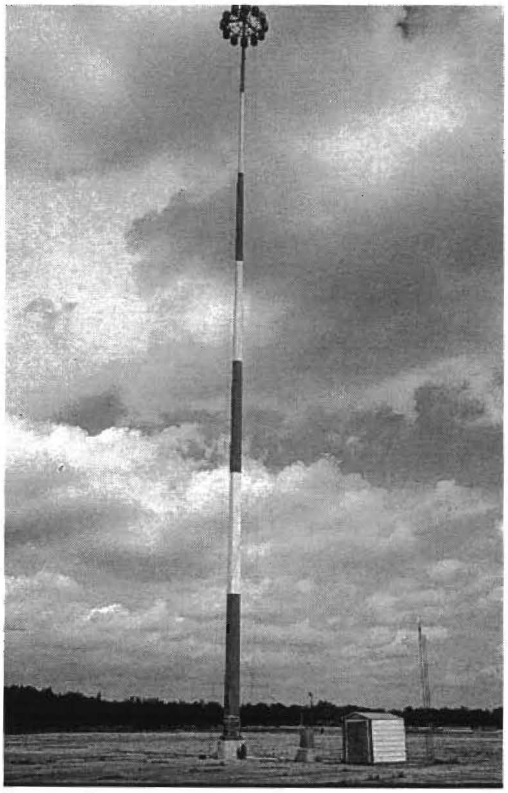

FIGURE 1 Test HMIP structure at Riverside Campus, Texas A&M University.

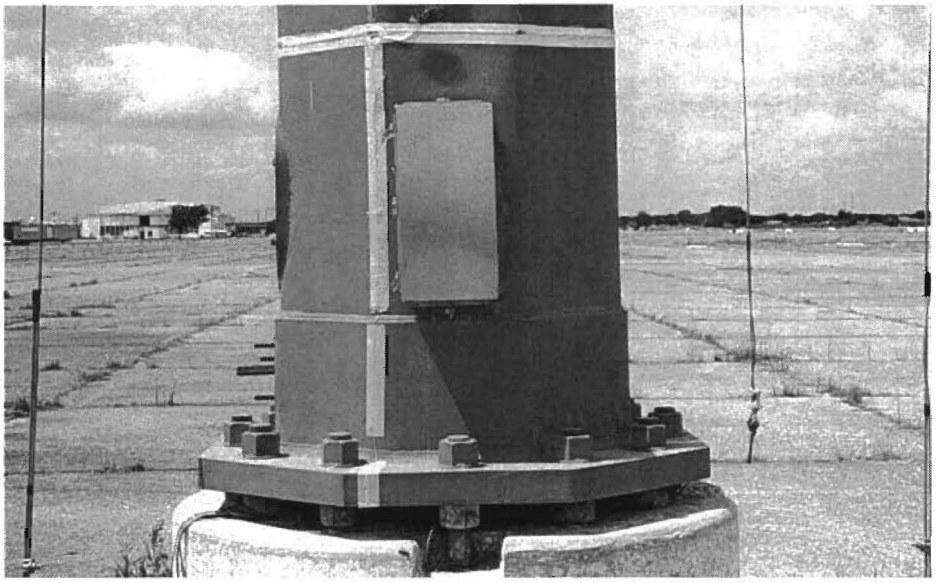

FIGURE 2 Base of HMIP Structure.

The histograms were collected by instrumentation of the north, south, and west anchor bolts with strain gages. Figure 3 is a photograph of the strain gage installation. Strain gages were also attached to the pole to measure bending stresses in the North-South and East-West directions. A lightning strike that damaged some of the signal conditioners disrupted data collection. A subsequent calibration error in the recorded histograms was discovered after data collection. This error results in an overestimation of the stress ranges from 4% to 8% for that part of the data acquired after the lightning strike. Since the error provides conservative results, the stress range histograms have not been adjusted to account for the gage factor error.

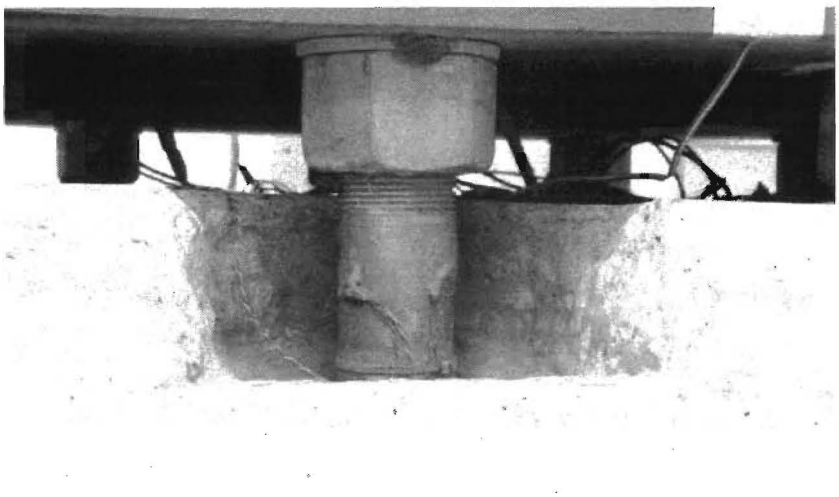

FIGURE 3 Strain gage attached to south bolt of HMIP structure.

The simulated lighting assembly seen at the top of the HMIP in Figure 1 was constructed of twelve 610 mm (24 in.) deep, 210 liter (55 gallon) capacity, steel drum sections. A 430 mm x 310 mm x 13 mm (17 in. × 12 in. × 1/2 in.) steel plate was added to the base of each barrel to simulate the weight of each light. The lighting assembly was added to simulate mass, gravity loads from the weight of the lights, and aerodynamic properties of the lights.

The data was collected using the ASTM rainflow cycle counting algorithm (ASTM E1049-85). This algorithm counts the number of peak to peak stress cycles at a given stress range. The stress ranges were divided into 0.7 MPa (100 psi) increments over the range from 0 MPa to 68 MPa (0 psi to 9900 psi). Stress range histogram data was collected at the test structure for 0.3 year from September 1995 to January 1996. High wind events and storms did occur during this testing period, but since data was not collected during the spring, many of the thunderstorms which occur during the year were not accounted for. Theoretically, large amplitude vortex shedding vibrations occur at wind speeds up to 12 m/s (27 mph) for the test HMIP and smaller vortex shedding vibrations occur at wind speed up to 89 m/s (200 mph). The maximum wind speed measured during the data collection was 16 m/s (35 mph). The test HMIP is designed for a maximum wind speed of 45 m/s (100 mph). Because these high wind events, such as thunderstorms, do not cause significant vortex shedding responses in the pole, the 0.3 year data is a good representation for an average year extrapolation and the resulting fatigue life values are valid. The stress range histograms for the north, south, and west anchor bolts can be

seen in Figure 4 through Figure 6.

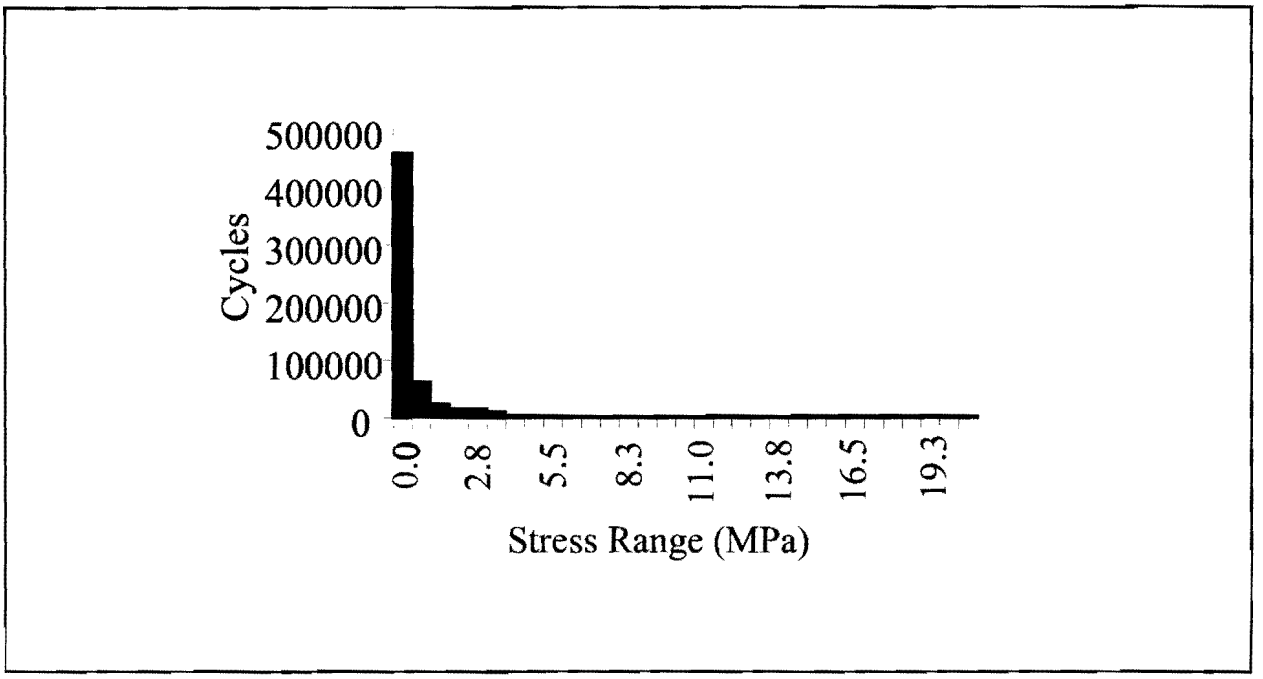

FIGURE 4 Stress range histogram for north bolt.

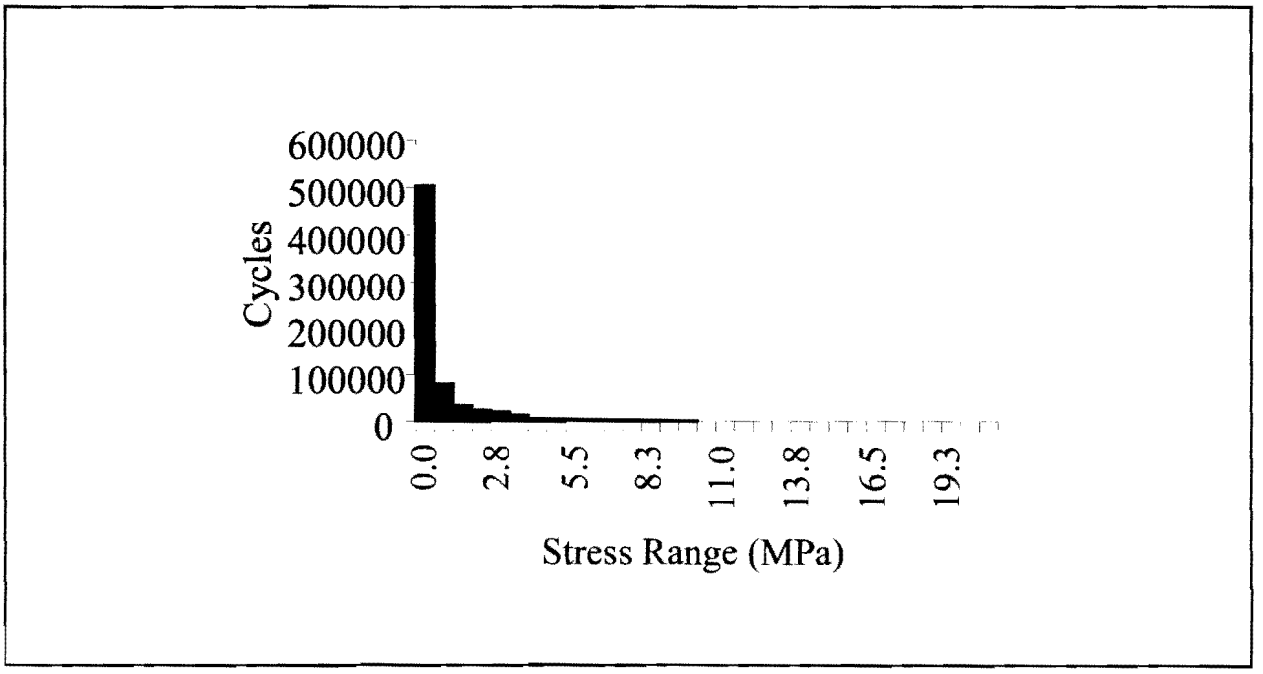

FIGURE 5 Stress range histogram for south bolt.

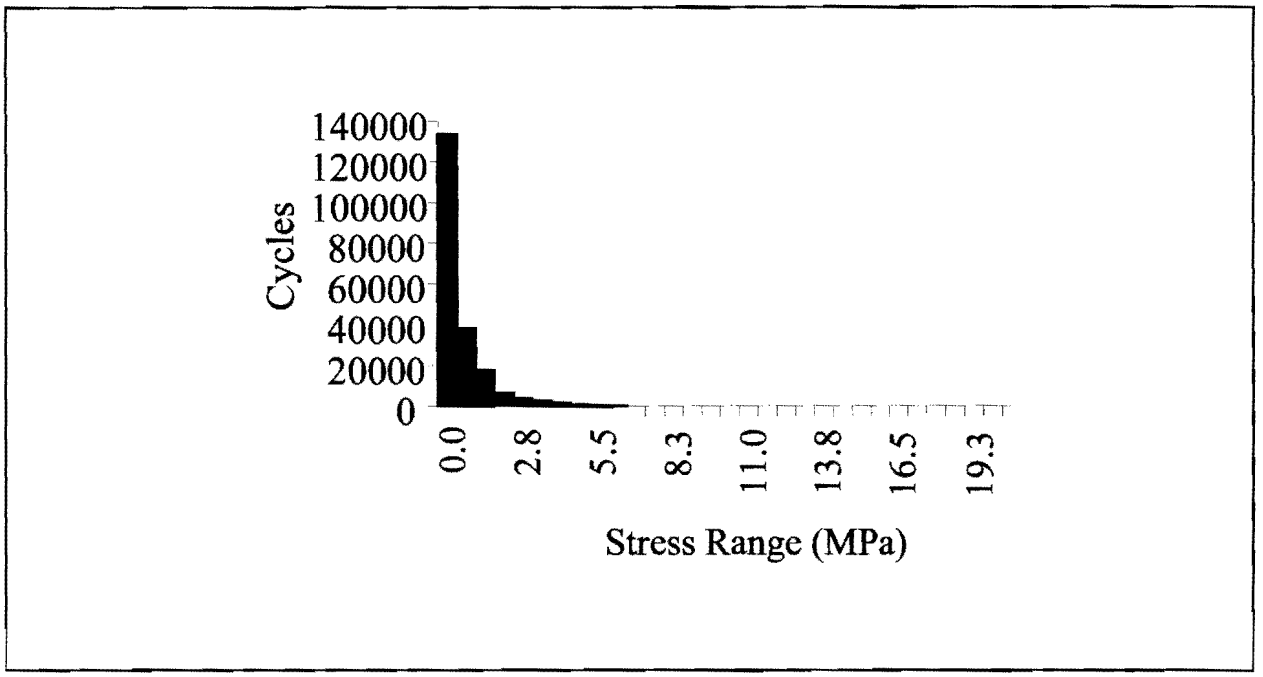

FIGURE 6 Stress range histogram for west bolt.

These histograms were analyzed to estimate the cumulative fatigue damage for the instrumented HMIP structure using a linear fatigue damage approach and calculating an effective stress range. The linear fatigue damage approach uses the Palmgren-Miner linear damage rule (Miner 1945, South 1994):

$$D = \sum_{i=1}^{N_i} \frac{n_{sri}}{N_{sri}} ,$$

where:

D = damage fraction for time period data is collected,

N_i = number of discrete stress ranges considered,

n_{sri} = applied stress cycles for stress range i in a given time period,

N_{sri} = $C(S_r)^m$ = number of available cycles for stress range i,

C = fatigue strength coefficient = 8.22×10^{27} (5.38×10^{19})(South 1994),

S_r = stress range, MPa (ksi), and

m = fatigue strength exponent = -9.76 (South 1994).

The fatigue strength coefficient and exponent given above are handbook values for anchor bolt materials and assume no bolt preload. The damage fraction, D, is equal to one when failure occurs. Essentially, when the number of applied cycles is equal to the number of available cycles, the fatigue life of the material is exhausted. In general, the fatigue life of a material is dependent on the mean stress level. A lower mean stress results in a higher fatigue life. The mean stress level in HMIP anchor bolts is compressive below the bottom nut, because the weight of the pole puts the bolts into compression. This compressive mean stress in the bolts is approximately 2.1 MPa (300 psi). Because the mean stress is compressive, the full stress cycle is not always tensile. It is the tensile portion of the stress range which causes fatigue damage. The expected fatigue life can be determined by the relationship:

$$L = \frac{1}{D'},$$

where:

L = expected fatigue life in years, and

D' = the damage fraction for a representative year.

For the stress range histogram data presented in Figure 4 through Figure 6, the estimated fatigue lives for the anchor bolts based on the linear fatigue damage approach are summarized in Table 2. Current AASHTO fatigue design methods relate detail connections such as anchor bolts to established design categories (Keating and Fisher 1986). Using the linear fatigue damage approach with AASHTO detail category coefficients on the critical north bolt results in the fatigue lives presented in Table 3.

Table 2 Summary of anchor bolt fatigue lives from linear fatigue damage approach

Anchor Bolt	Estimated Fatigue Life (years)	Conclusion
North	1.16×10^{8}	Infinite Life
South	2.12×10^{12}	Infinite Life
West	6.73×10^{8}	Infinite Life

Table 3 Bolt fatigue lives from linear fatigue damage approach (AASHTO Coefficients)

North Anchor Bolt	Estimated Fatigue Life (yr)	Conclusion
Category C	5313	Infinite Life
Category D	2609	Infinite Life
Category E	1281	Infinite Life

The pole bending stress range histogram data can be used to estimate the fatigue life of the pole-to-baseplate weld detail. Fatigue strength coefficient and exponent values used to estimate the fatigue life of the pole-to-baseplate weld detail are found in the American Welding Society Code (AWS 1995) and are given by C = 7.02×10^{10} (1.00×10^{8}), and m = - 3.393. A similar approach for this data shows that the fatigue life for the pole in north-south bending is 1280 yr and in east-west bending is 3710 yr. Even though these results can also be interpreted as infinite life, it is interesting to note that the welded pole-to-baseplate connection is critical compared to the anchor bolts. The pole-to-baseplate welded connection is classified as AASHTO Category E′. Using the coefficients from the Category E′ design curve, a fatigue life of 4930 yr is obtained. This is a longer fatigue life than that calculated using AWS coefficients. However, the AWS coefficients have never been updated to the current AASHTO fatigue design curves, which are based on the study by Keating and Fisher.

Effective Stress Range Approach

The effective stress range approach calculates an effective stress range, $S_{r\text{-}eff}$, based on a root mean cube method as:

$$S_{r\text{-}eff} = \left(\sum \varphi_i S_{ri}^3\right)^{1/3} ,$$

where:

$S_{r\text{-}eff}$ = effective stress range, MPa (ksi),

φ_i = frequency of occurrence of stress range S_{ri}, and

S_{ri} = stress range of interval i, MPa (ksi).

The effective stress ranges for the data shown in Figures 4 through 6 and the stress range histograms for north-south and east-west pole bending can be seen in Table 4. It can be seen from Figures 4 through 6 that the majority of the stress cycles seen during the testing period are below 6.9 MPa (1000 psi). These stress cycles do not begin to significantly contribute to the fatigue behavior of the bolts until near the end of their fatigue lives. If all stress ranges seen in Figure 4 through 6 below 6.9 MPa (1000 psi) are neglected when calculating the effective stress range, a better approximation of the effective stress range which actually damages the bolts is obtained. Table 5 summarizes the modified effective stress ranges.

Table 4 Summary of effective stress ranges

Histogram Data	Effective Stress Range, MPa (ksi)
North Bolt	5.2 (0.75)
South Bolt	2.6 (0.37)
West Bolt	5.1 (0.74)
North-South Pole	2.3 (0.34)
East-West Pole	1.6 (0.23)

Table 5 Modified summary of effective stress ranges

Histogram Data	Effective Stress Range MPa (ksi)
North Bolt	24 (3.4)
South Bolt	9.3 (1.4)
West Bolt	29 (4.2)
North-South Pole	9.3 (1.4)

Current AASHTO fatigue design procedures involve the use of design curves. Some of these curves are shown in Figure 7. These curves relate the stress range to the number of cycles to failure on logarithmic plots known as S-N curves. The design curves are decomposed into a series of design categories, A through E′. The design categories serve to describe the varying fatigue behavior of different structural details including stress concentration effects. Typically, these design curves are used for the design of welded connections but are also used for other design details, such as bolt details. The effective stress range is plotted versus number of cycles on these S-N curves, and the fatigue life is determined as the number of cycles to failure. This value is found by determining the number of cycles to failure at the point where the effective stress range intersects the S-N curve for the appropriate category of detail.

Previous research (Frank 1978) indicates that a double nut configuration in the snug tight position gives fatigue behavior similar to AASHTO Category E. Determination of fatigue lives for the different effective stress ranges shown previously can be accomplished by plotting these ranges against the AASHTO detail categories.

The horizontal straight line portion of the AASHTO detail category S-N curves represents the endurance limit, defined as the stress at which failure will not occur even for an infinite number of cycles. Essentially, the anchor bolts show infinite life. Theoretically, however, the bolts do not have infinite life, even though the effective stress ranges fall below the endurance limit of detail Category E′. For a detail to have infinite life, the maximum stress seen in a variable amplitude loading history must also fall below the endurance limit. The stress range histograms of HMIP anchor bolts studied indicates maximum stresses greater than the 31 MPa (4.5 ksi) endurance limit of the Category E detail. An estimate of the fatigue life can be determined based on Category E′, because the critical effective stress range of 29 MPa (4.2 ksi) seen in the west bolt is greater than the endurance limit of 18 MPa (2.6 ksi) from the Category E′ curve. Using this critical effective stress range, an expected fatigue life of 5.1 million cycles is obtained for the Category E′ detail.

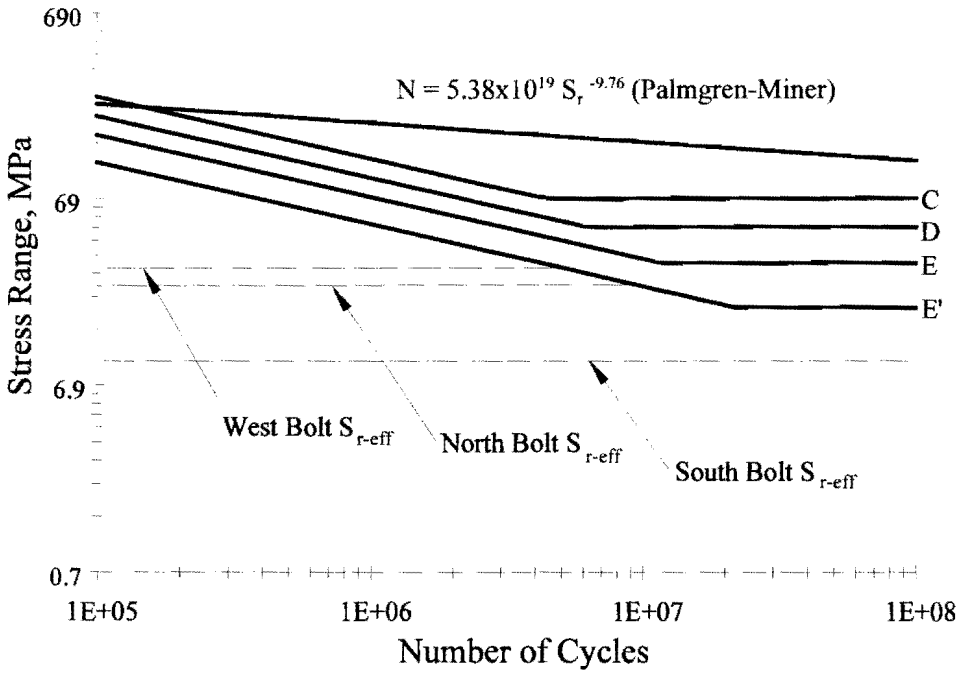

FIGURE 7 Effective stress ranges on AASHTO Categories.

FIELD STUDY--COSS ON US 290 AT HEMPSTEAD, TEXAS

Site Description

A field study was conducted on a TXDOT COSS structure located near Hempstead, Texas. Data collected from this structure established expected stress ranges near the base of the pole structure and provided evidence of the dynamic susceptibility to wind-induced response, such as vortex shedding and galloping phenomena. The structure, depicted in Figure 8, is located adjacent to the west lane at station 529+50 on Texas Highway 290 bypass around Hempstead, Texas. Strain gage bridges installed 762 mm (30 in.) above the tower base recorded wind inducted stresses in the circular tower. Principal base reactions were extracted from these stresses and statically equivalent stress ranges determined for a critical base anchor bolt.

FIGURE 8 Photograph of COSS field study structure near Hempstead, Texas.

The COSS tower is nominally 8.2 m (27 ft) tall with a 10.7 m (35 ft) cantilevered span supporting a single 3.8 m (12.5 ft) wide by 3 m (10 ft) tall highway sign at the end of the span. The cantilevered span is a standard TxDOT 1.4 m (4.5 ft) by 1.4 m (4.5 ft) truss structure. The structure tower is a single 762 mm (30 in.) OD circular pole with a wall thickness of 10.3 mm (0.406 in.). A 1040 mm (41 in.) by 51 mm (2.00 in.) thick circular baseplate supports the tower (see Appendix A). The tower is attached to the foundation by eight symmetrically spaced 57 mm (2.25 in.) double-nutted anchor bolts as seen in Figure 9. The anchor bolt threads are 8 UN, and the anchor bolt nuts and washers were not tack welded in place.

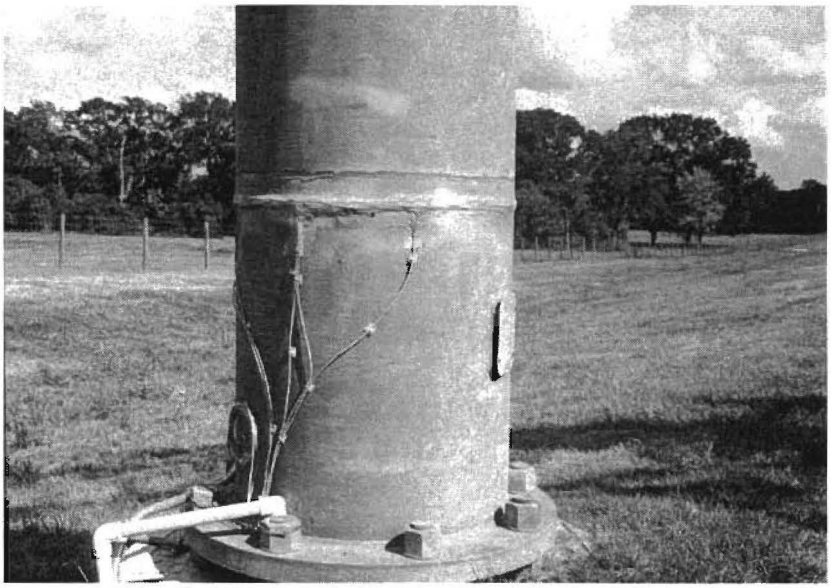

FIGURE 9 Fully instrumented and weatherproofed pole base of COSS field structure near Hempstead, Texas.

Instrumentation and Data Collection

Six strain gage bridges were mounted 762 mm (30 in.) above the top surface of the tower base. These bridges were designed to monitor torsion, axial force, shear in two directions, and bending moments parallel and perpendicular to the overhanging structure. In addition, wind speed and direction were monitored at the site. Photographs of the installation are shown in Figures 9 and 10.

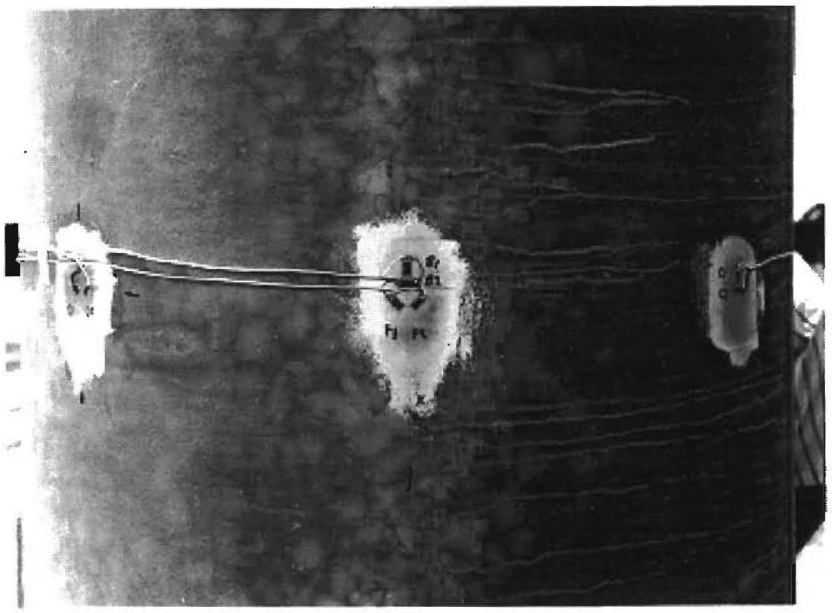

FIGURE 10 Installation of strain gage bridges on COSS field structure near Hempstead, Texas.

The data was collected using the ASTM rainflow cycle counting algorithm (ASTM E1049-85). This algorithm counts the number of peak-to-peak stress cycles at a given stress range. The stress ranges were divided into 0.7 MPa (100 psi) increments and ranged from 0 MPa to 68 MPa (0 psi to 9900 psi). Stress range histogram data was collected at the test structure for 3.5 months from July 15, 1996 to November 1, 1996. Theft of the anemometer prevented collection of wind speed and direction data during the last month of the data acquisition period. Winds during the study period were predominantly from the south as shown in Figure 11. Wind direction was affected by vehicular traffic. Gusts from large vehicles tended to rotate the anemometer in a random manner after passage of the vehicle. This effect was more apparent in directional response than in wind speed response, however. Figure 12 depicts the distribution of wind speeds recorded during a major portion of the study period. Wind speeds were typically in the 4-7 m/s (10-15 mi/hr) range. A small number of high speed events occurred during the study period, including one gust 20 m/s (46 mi/hr), but the large majority of wind speeds were less than 13 m/s (30 mi/hr).

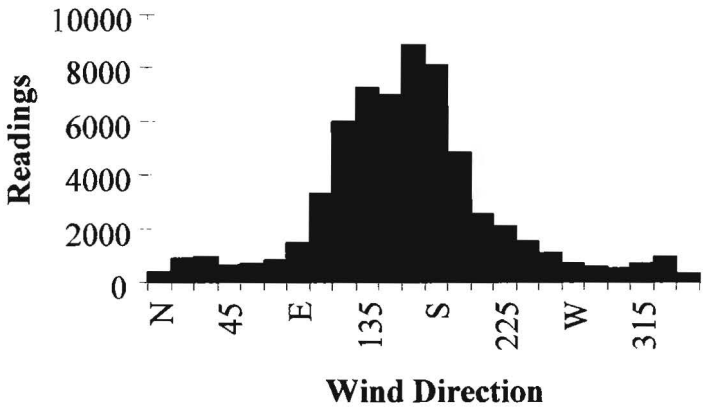

FIGURE 11 Distribution of wind direction COSS near Hempstead, Texas (period July 15 to Sept 23).

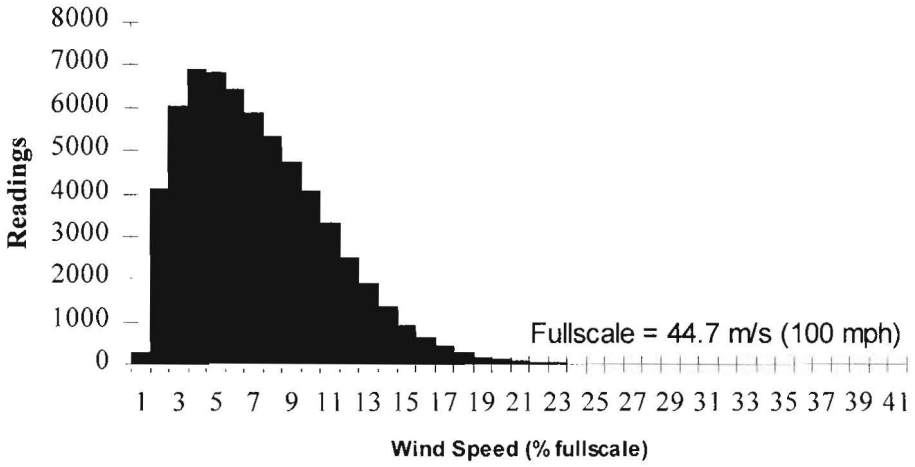

FIGURE 12 Distribution of wind speed near COSS structure, Hempstead, Texas (Period July 15 to Sept. 23).

Pole Stresses

Six strain gage bridges attached to the COSS tower and positioned as seen in Figure 13 were monitored to determine the six principal forces and moments in the tower 762 mm (30 in.) above the tower baseplate. Stress histograms associated with these principal forces and moments are presented in Figure 14 through 19.

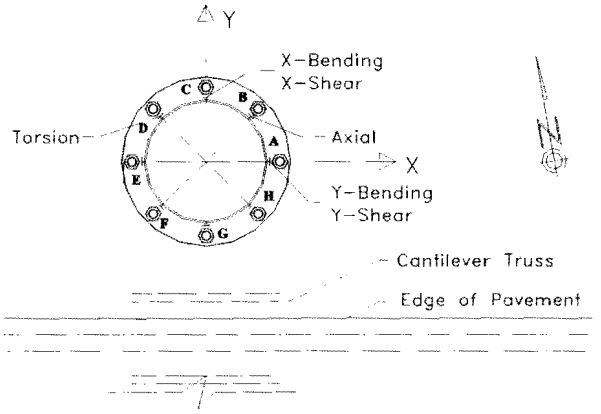

FIGURE 13 Position of strain gage bridges on COSS field specimen near Hempstead, Texas.

A review of the stress histograms indicates that wind induced stresses in the COSS tower are very low. Almost all recorded stress levels are between 0 and 2.1 MPa (0 and 300 psi). Isolated

Table 6 Total stress histogram bin counts for COSS field specimen near Hempstead, Texas

Order	Stress	Total Count
1	Y-Bending	199,200
2	Torsion	126,409
3	X-Bending	118,500
4	Axial	95,900
5	Y-Shear	57,600

readings (1 or 2 counts) at higher stress levels were found in the recorded data, but the vast majority of readings were in the first two 0.69 MPa (100 psi) bins. The most active channels based on the number of total counts are tabulated in Table 6.

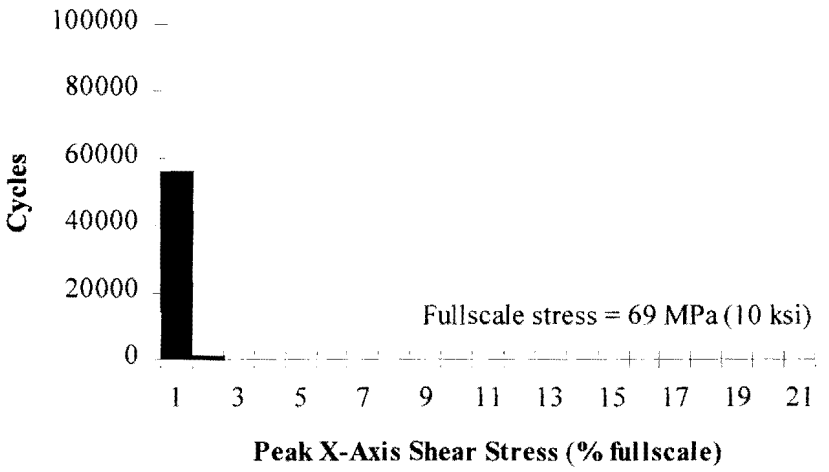

FIGURE 14 Stress histogram of peak shear stress parallel to X-axis - COSS field specimen Hempstead, Texas.

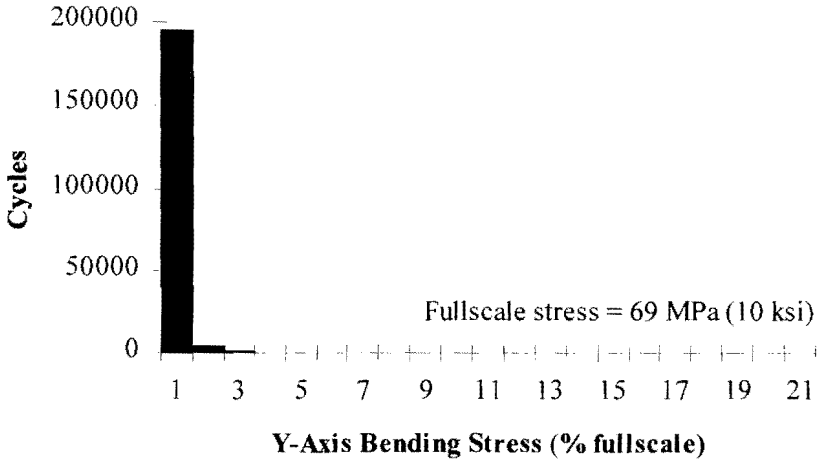

FIGURE 15 Stress histogram of bending stress about Y-axis - COSS field specimen Hempstead, Texas.

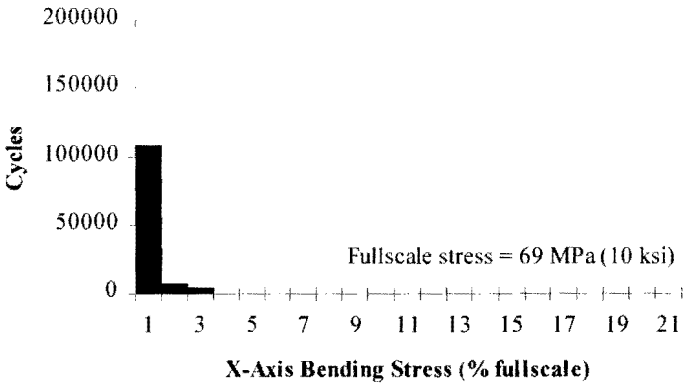

FIGURE 16 Stress histogram of peak shear stress parallel to X-axis - COSS field specimen Hempstead, Texas.

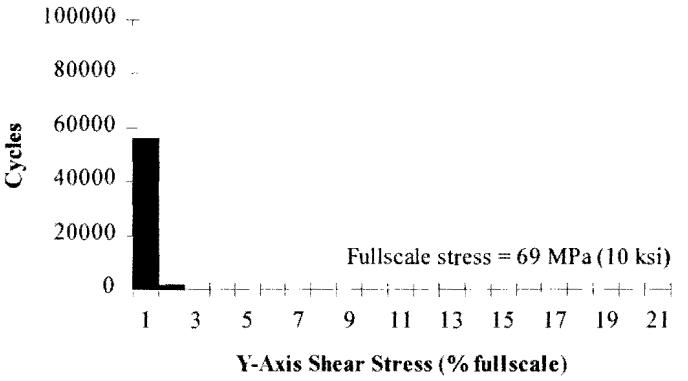

FIGURE 17 Stress histogram of peak shear stress parallel to Y-axis - COSS field specimen Hempstead, Texas.

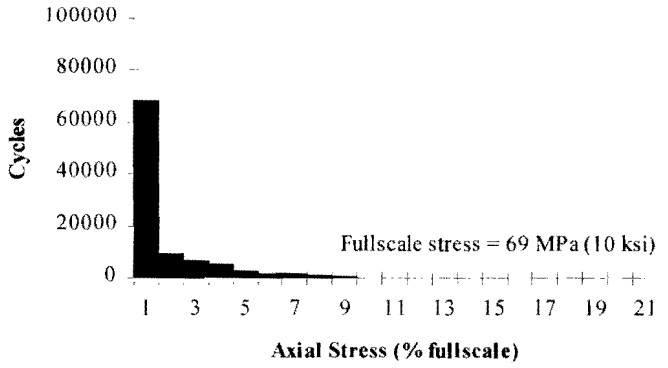

FIGURE 18 Stress histogram of axial stress in COSS field specimen near Hempstead, Texas.

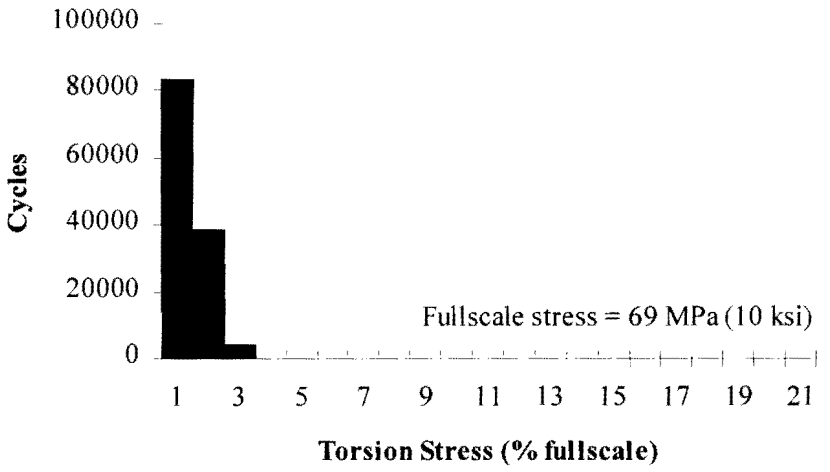

The maximum wind speed recorded during the data collection period was 21 m/s (46 mph). Wind direction was predominantly from the south and in a range of 4-7 m/s (10 to 15 mph). A larger number of high stress bin counts, in the 5.5 MPa (800 psi) range, was noted in the axial stress histogram, even though total count for axial stresses was relatively low. Shear stress was insignificant both in amplitude and total count.

Wind induced vibrations in the tower resulting from vortex shedding and galloping were not noted in time traces of the test data. Gusting and changes in wind direction were noted in response data during passage of large vehicles. Several traces were recorded to quantify the magnitude of stresses induced by these events. It was expected that the air turbulence of passing vehicles would excite the tower structure, which was confirmed by observation. The resulting traces were quite complex and the stress levels relatively low. Several of these traces are presented below to document this phenomena. The background response of these time histories is attributed to wind gusts exciting the structure between passing vehicles. Shear traces are not presented here. The measured stress levels were extremely low, on the order of 7 Pa (10 psi).

Vehicular Induced Pole Stresses

Figures 20 through 23 depict four time histories of a large van passing under the cantilevered sign. The leading edge of the cab passes the COSS structure starting at approximately 2 seconds. Y-axis bending (in the plane of the overhead sign) and torsion bridges respond almost immediately. This response is probably due to air accelerated by the drag of the vehicle impacting the overhead sign. Figures 21 and 22 show the response of the X-axis bending perpendicular to the plane of the sign) and axial force to passage of the vehicle. Both traces show a delayed response of two to three seconds. The axial trace exhibits a significant number of sharp stress peaks. All time histories exhibit the response of a lightly damped freely vibrating structure slowly returning to a steady-state condition after passage of the vehicle. The first mode frequency of the COSS structure is approximately 2.4 Hz. Higher modes are also present in the data. These time histories correspond with the stress histograms discussed earlier and support both the order of activity found in the histograms and the magnitude of stress levels found in these histograms. It appears that vehicular traffic may be responsible for much of the low stress response depicted in the stress histograms.

The Y-axis bending stresses had the highest number of counts, followed by torsion. The responses are closely correlated. The axial and X-bending traces are also correlated. The peaks in the axial trace may be the cause of the large number of high stress cycles in the axial histogram.

Bolt Stresses

A static analysis of the base/anchor bolt connection indicates that the maximum longitudinal bolt stress is 1.4 times greater than the bending stress in the tower for the same applied moment. The longitudinal stress in the anchor bolts is 1.1 times greater then axial stress in the tower. Prior studies have indicated that the highest stressed bolt in the pattern and the one most likely to fail is the bolt farthest from the pavement edge, bolt C in Figure 13. This is due to the bending

moment created by the cantilever sign structure dead load and vertical oscillations of the cantilever structure. The dynamic stresses from vehicular traffic are highest about the Y-axis. The highest stressed bolts due to this bending moment are bolts A and E in Figure 13. X-axis bending due to vehicular traffic tends to add to the stress levels on bolt C. Galloping would also tend to cause vertical oscillation of the cantilever structure, resulting in high stresses in bolts C and G. A conservative estimate of the stress histogram for the highest stressed bolt is presented in Figure 24. This histogram is simply the sum of the X-axis, Y-axis, and axial stress histograms. The stresses between the individual histograms are not time correlated; in fact, the time histories just presented indicate that the actual structure dynamic response history is quite complicated, at least for vehicular induced stresses.

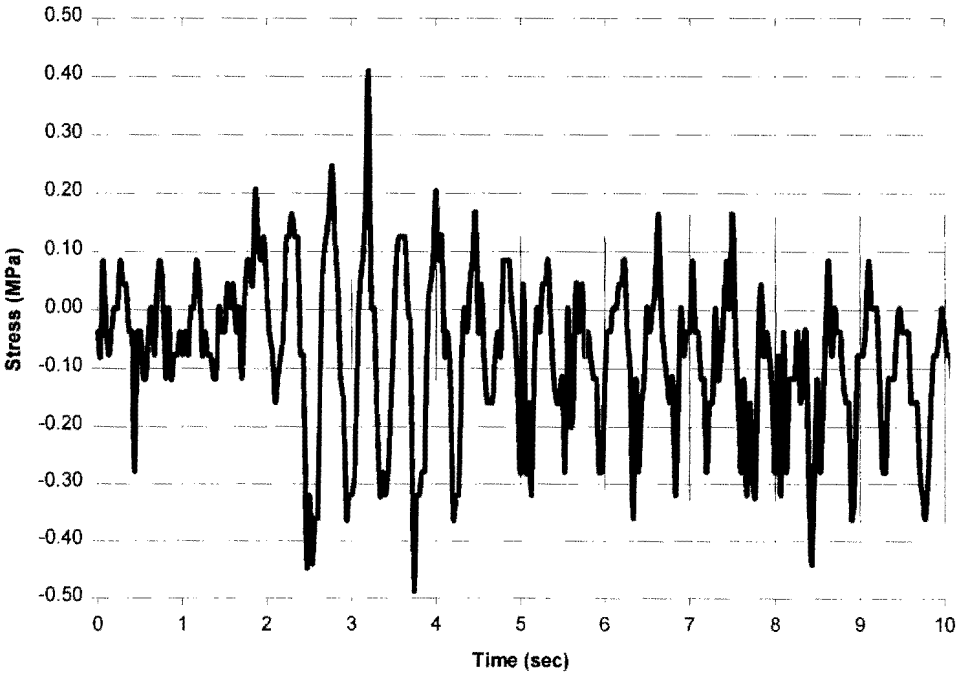

FIGURE 20 Y-axis bending stress of van trailer passing COSS structure near Hempstead, Texas.

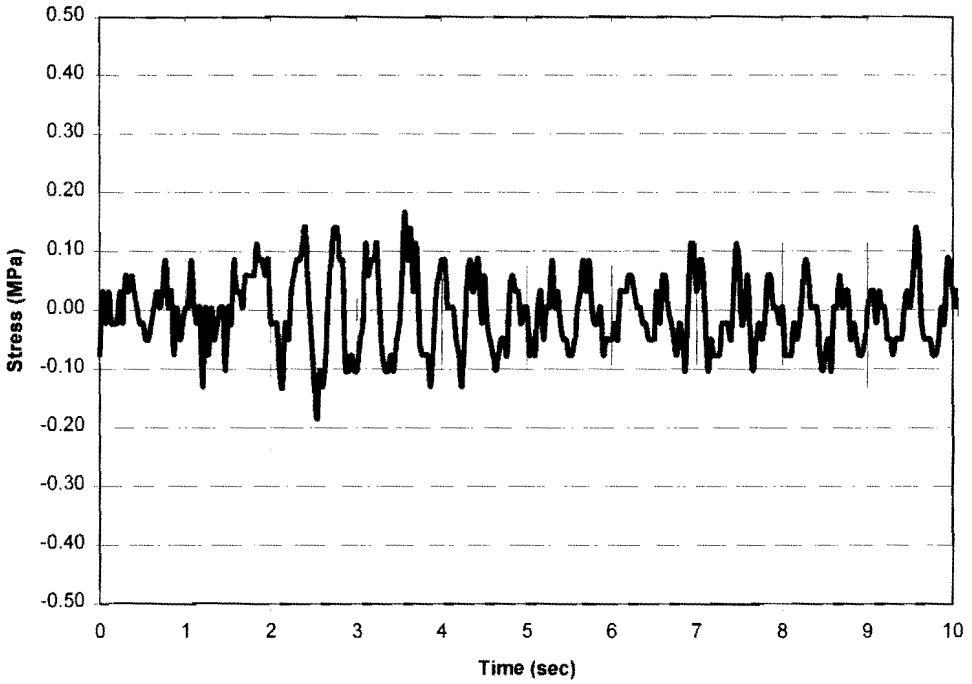

FIGURE 21 Torsional stress response to passage of a van trailer past COSS field specimen near Hempstead, Texas.

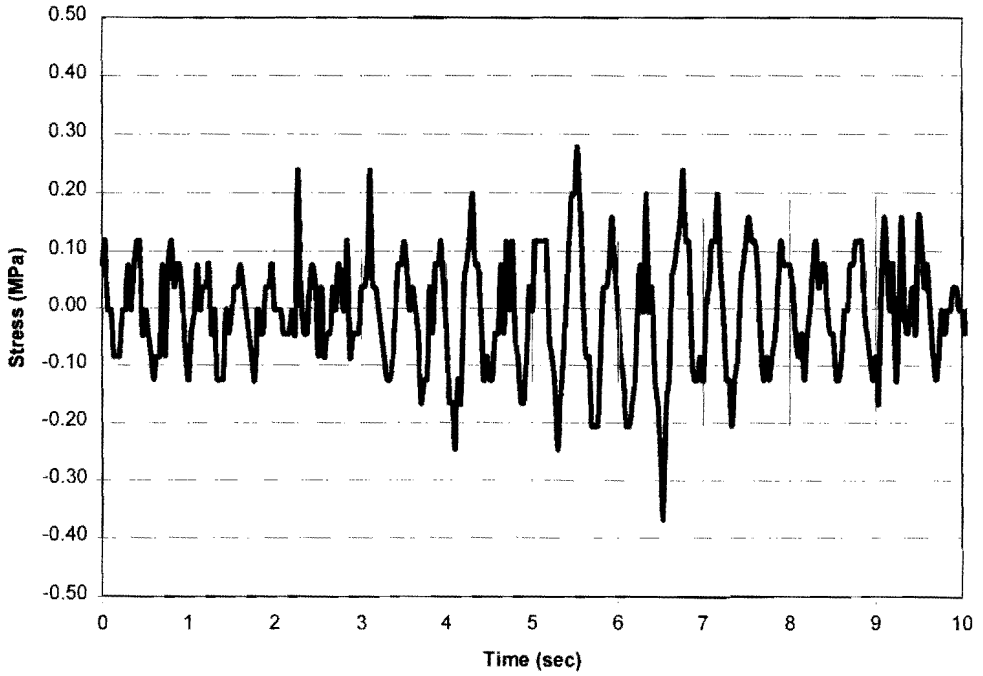

FIGURE 22 X-axis bending stress response to a van trailer passing COSS field specimen near Hempstead, Texas.

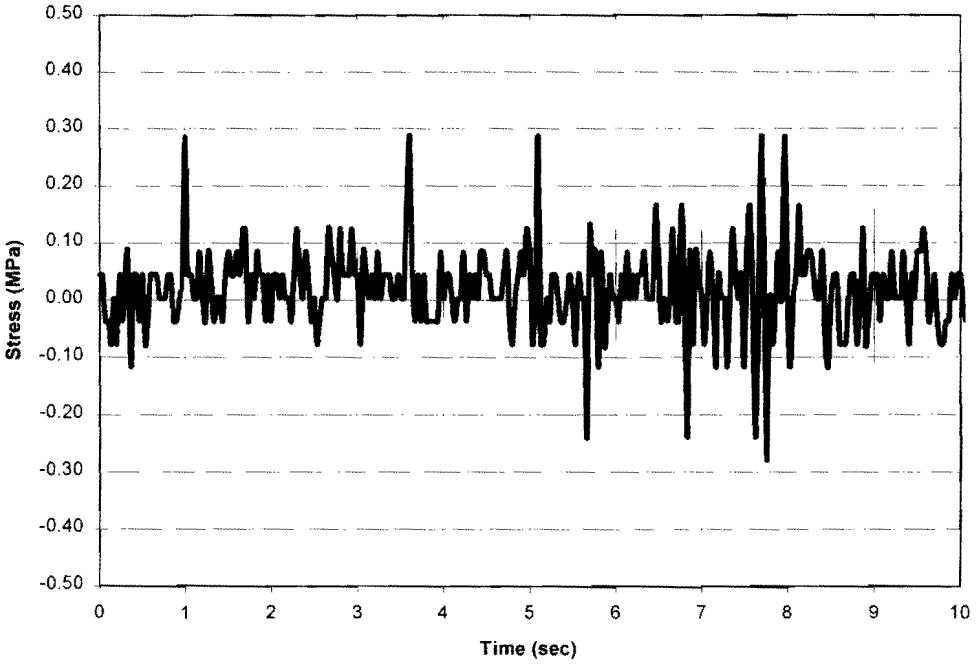

FIGURE 23 Axial stress response to passage of a van trailer past COSS field specimen near Hempstead, Texas.

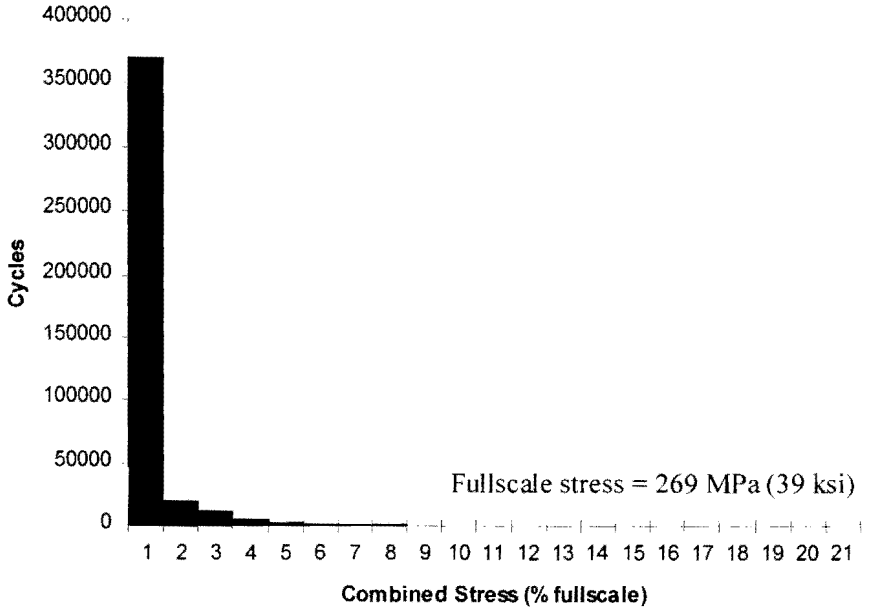

FIGURE 24 Composite stress in critical bolt of COSS structure near Hempstead, Texas.

ANALYTICAL AND NUMERICAL STUDIES

Previous research has shown that double nut anchor bolt connections that are preloaded by tightening to one-third turn past snug tight exhibit longer fatigue lives than similar snug tight connections (Frank 1978). This study was performed on anchor bolts with diameters ranging from 35 mm to 51 mm (1.375 in. to 2 in.) and with thread pitches of 5.6 mm and 3.2 mm (4.5 and 8 threads per inch). Fatigue failures of snug tight connections typically occur in the bolt in the region just below the top nut, identified as Location 1 in Figure 25. On the other hand, when the anchor bolt is given a preload, the locations of failure shift to Location 2, as shown in Figure 25 (Frank 1978). This shift in failure location occurs because the preload reduces the stress range between the nuts.

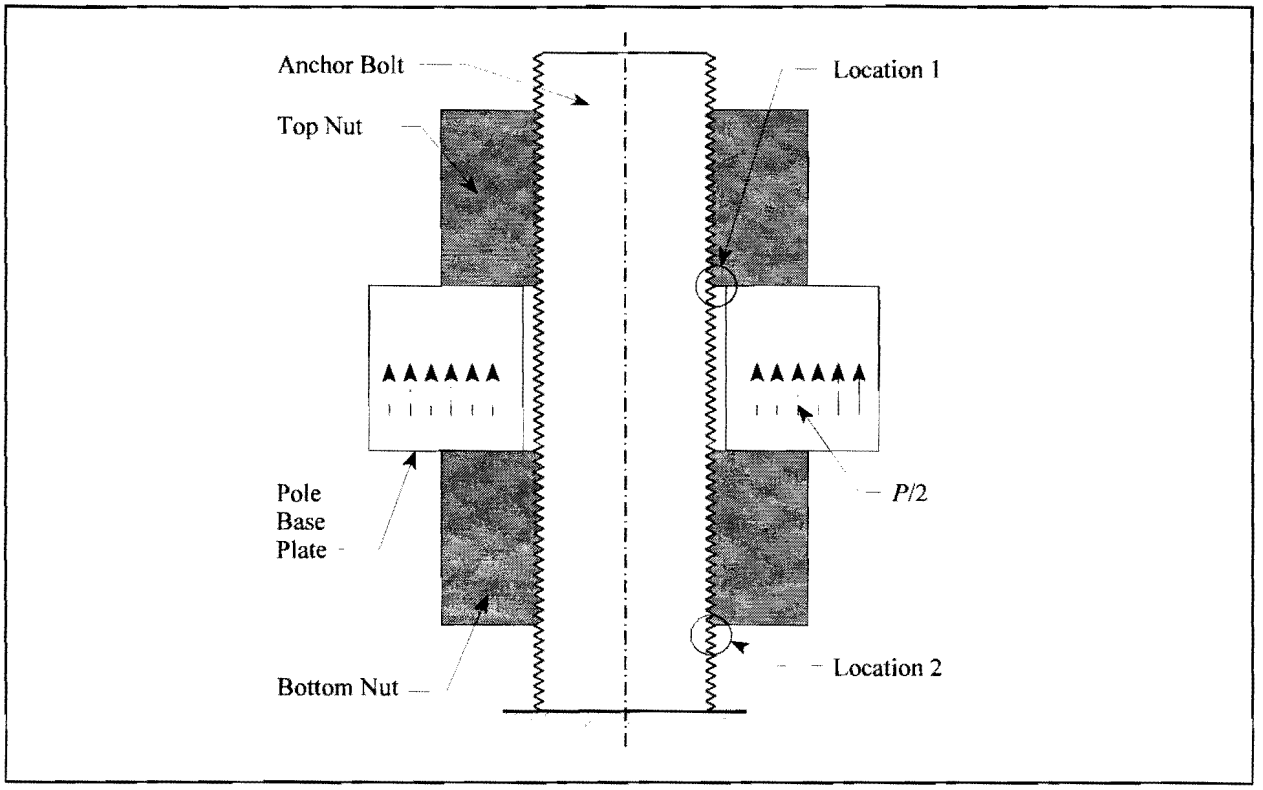

FIGURE 25 Location of fatigue failure initiation in anchor bolts.

A linear elastic finite element study of the double nut anchor bolt connection is presented in order to explain this shift in the location of failure and to investigate why preloaded

connections perform more favorably with regards to fatigue for large diameter anchor bolts. The finite element analysis is useful for comparative purposes only and is not meant to accurately predict thread root stresses. In addition, the effect of bolt misalignment is investigated to determine if higher than normal stress concentrations develop for both snug tight and preloaded conditions.

Finite Element Modeling of a Snug Tight Connection

The finite element mesh of a snug tight double nut anchor bolt is represented in Figure 26. For the purposes of this modeling, snug tight is defined as zero preload. The model is based on two-dimensional plane strain behavior and was generated to run on the ABAQUS finite element software (Hibbitt, Karlson, and Sorenson 1995). The model incorporates 196 6-node quadratic triangular plane strain elements for the nut and bolt threads, 2726 8-node biquadratic square plane strain elements, 18 6-node contact elements, 136 4-node contact elements, 4 2-node truss elements, and 8014 nodes.

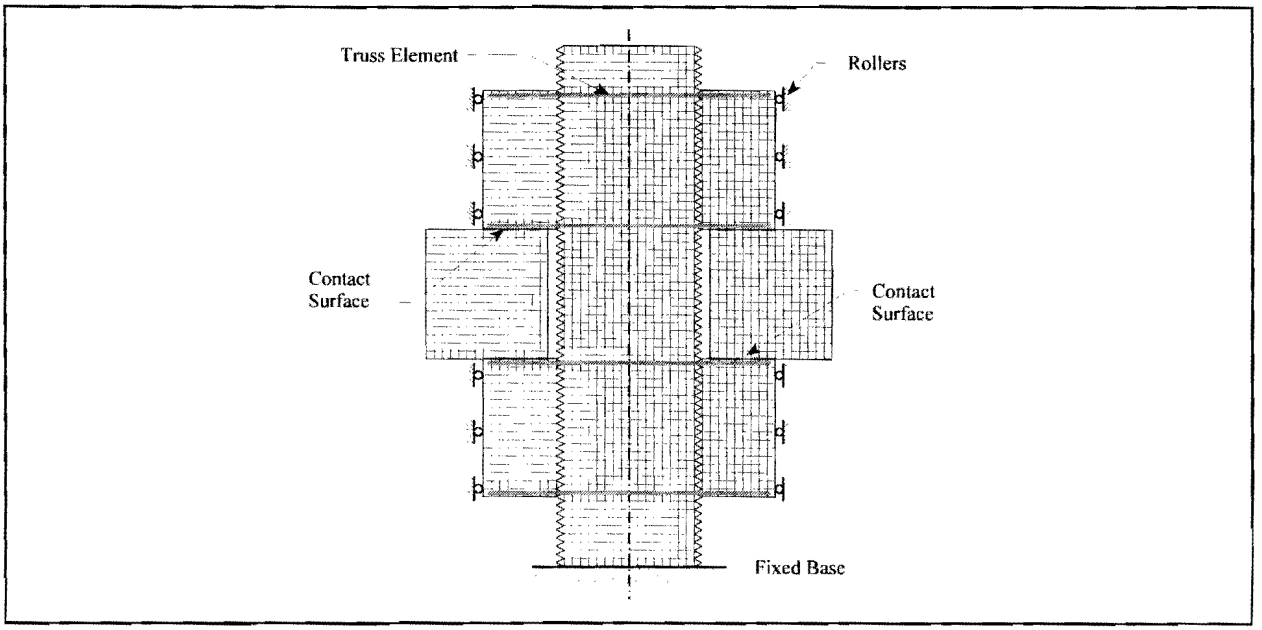

FIGURE 26 Snug tight finite element mesh.

The model boundary conditions have vertical element distributed loads imposed upward on the centerline of the plate, as shown in Figure 27. Boundary conditions of this model also include the contact surfaces shown in Figure 26. The elements in the plate are not connected directly to the elements in the bottom nut because the nuts are snug tight and the plate and nuts do not act as a continuous unit; therefore, contact elements are used here. Contact elements are not used at the bottom of the bottom nut because loading is always in the vertical direction. Contact elements also exist in between the bolt and nut threads. The base of the model is fixed in the horizontal and vertical directions. The edges of the nuts are fixed against lateral translation. These boundary conditions are used in conjunction with the truss elements attached to the nuts to prevent rigid body motion of the four nut sections. The contact element modeling between the threads can be seen in Figure 27.

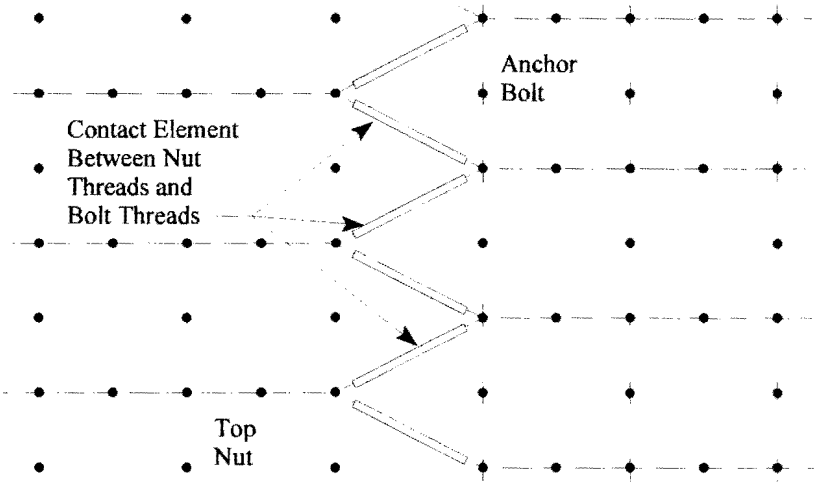

FIGURE 27 Nodal connectivity at the threads.

The axial stresses due to this loading are most important with regard to fatigue and can be seen in Figure 29. The other horizontal and shear stresses are not significant for fatigue. The relative intensity of the axial stresses are shown in Figure 28 along with the coordinate system used to define the stresses. For this coordinate system, the axial stresses are denoted σ_{yy}.

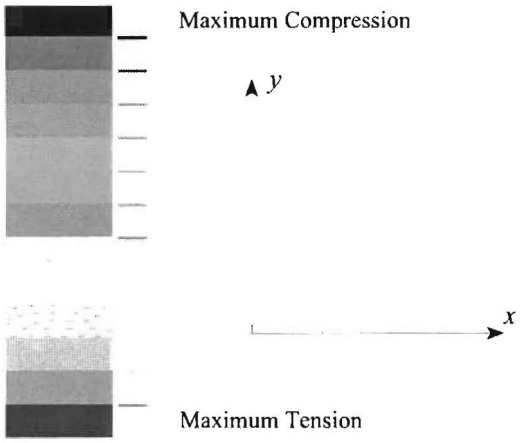

FIGURE 28 Stress intensity and coordinate system for FEM results.

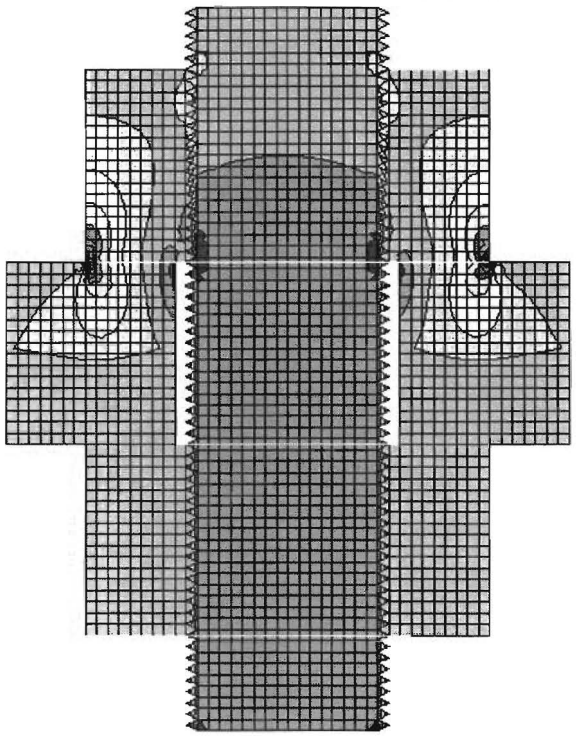

FIGURE 29 σ_{yy}, Longitudinal normal stresses in snug tight bolt.

It can be seen that the location of the maximum axial stress is at the thread just beneath the top nut, denoted Location 1 in Figure 25. The variation of axial stress, σ_{yy}, normalized with respect to the average or nominal axial stress, $\sigma_{nominal}$, with position along the length of the bolt can be seen in Figure 30. The solid line represents the axial stress at the centerline of the bolt, and the dashed line represents the axial stress at the bolt thread root.

Figure 29 shows a localized increase in stress at the first fully engaged thread root near the bottom of the top nut. The localized stress is 1.4 times the nominal axial stress in the bolt. This stress concentration value is in the range of expected values (Peterson 1974). Note that the axial stresses approach zero at the end of the bolt, since loading of the bolt is through the base plate.

The failure location due to fatigue will occur at Location 1 because the fatigue crack in the bolt will tend to initiate from the location of maximum local tensile stress and propagate from the location of maximum stress range. The maximum stress range occurs at the same location as the maximum local tensile stress. The normalized stress range was evaluated with S_{max} = 207 MPa (30 ksi), S_{min} = 103 MPa (15 ksi) giving a stress range, S_r = 103 MPa (15 ksi). Figure 31 shows the stress range, S_r, at the bolt thread root normalized with respect to the nominal stress, $\sigma_{nominal}$. Therefore, according to the finite element model, any fatigue failures due to axial loading at snug tight conditions will occur at Location 1.

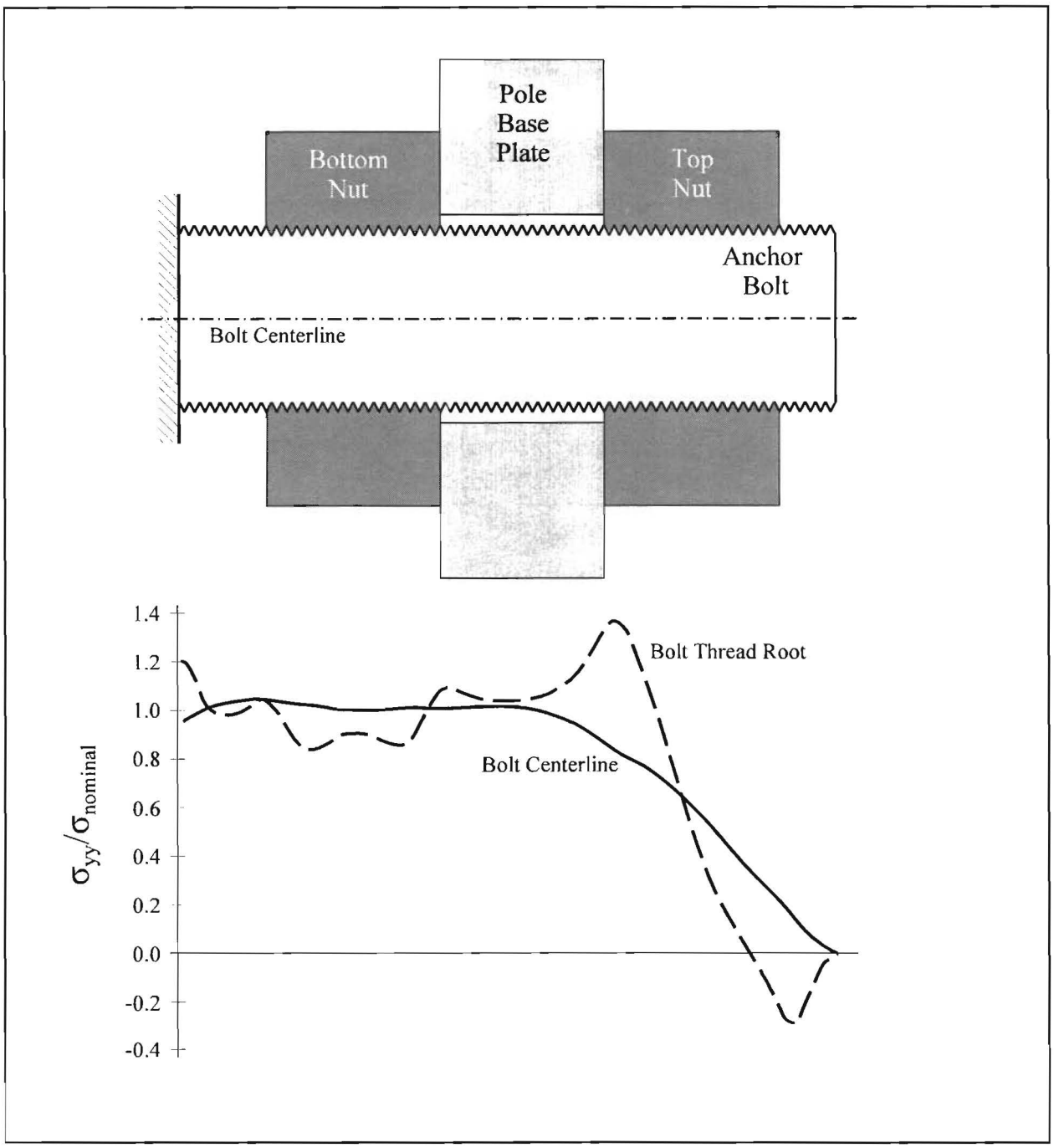

FIGURE 30 Variation of normalized axial stress with position in snug tight bolt.

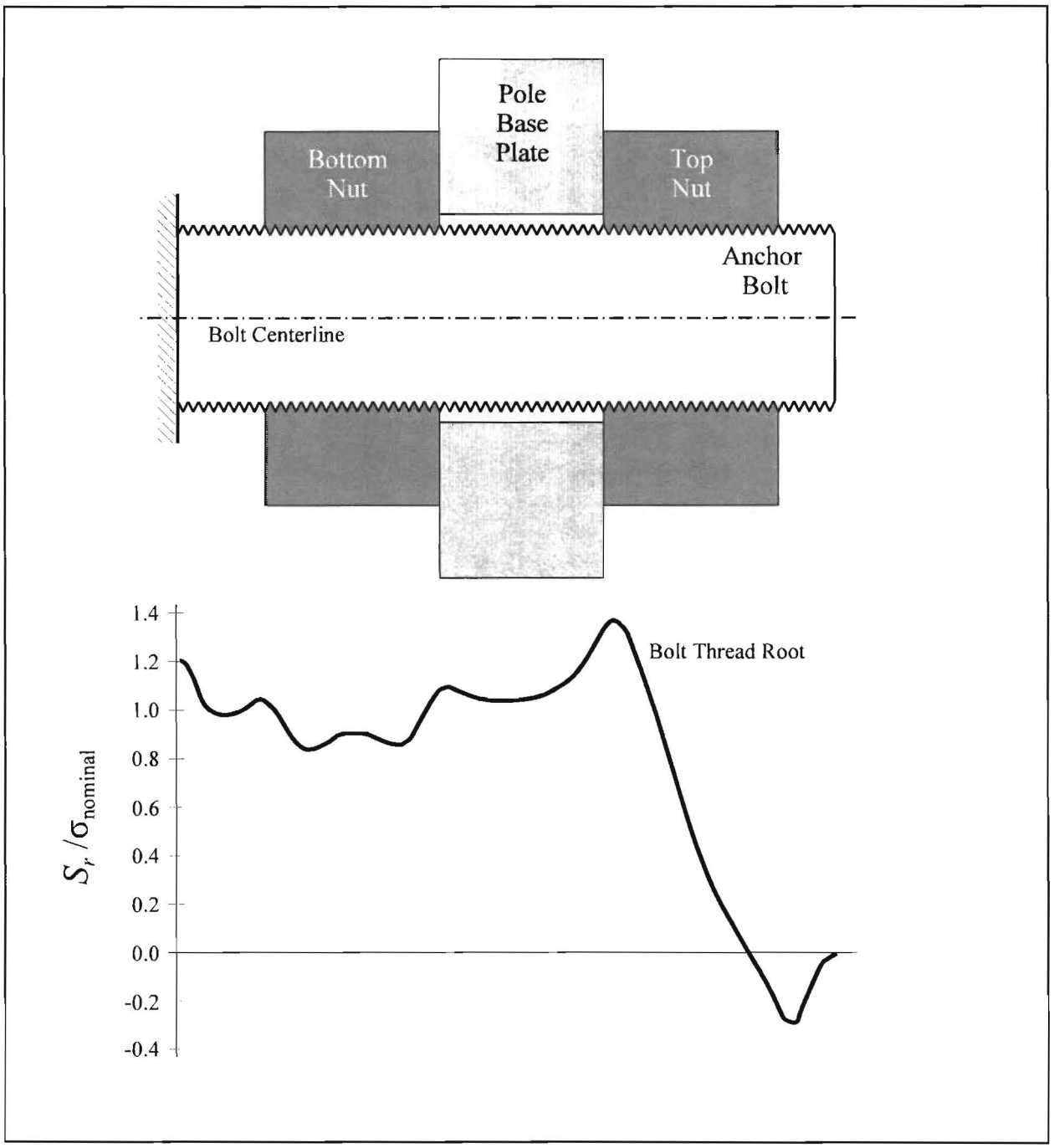

FIGURE 31 Variation of normalized axial stress range with position in snug tight bolt.

Finite Element Modeling of a Preloaded Connection

The finite element mesh of a preloaded double nut anchor bolt is also represented in Figure 26. The preloaded finite element model assumes a preload level equal to 70% of the maximum yield stress of the material. Again, the contact elements in between the threads are used, as seen in Figure 27. These contact elements allow the preload to draw the nuts together and relieve the stresses in the threads in the presence of a vertical load applied to the plate. The preload is imposed by subjecting the elements making up the bolt to an initial state of stress. This is accomplished by giving the specified elements initial stress boundary conditions. This preload stress in the bolt varies from a maximum of 480 MPa (70 ksi) in the middle of plate to zero at the top of the top nut and the bottom of the bottom nut. Figure 32 shows the axial stresses induced by the preload. Using these new boundary conditions, a vertical load is applied to the plate. Figure 33 shows the axial stresses due to this loading.

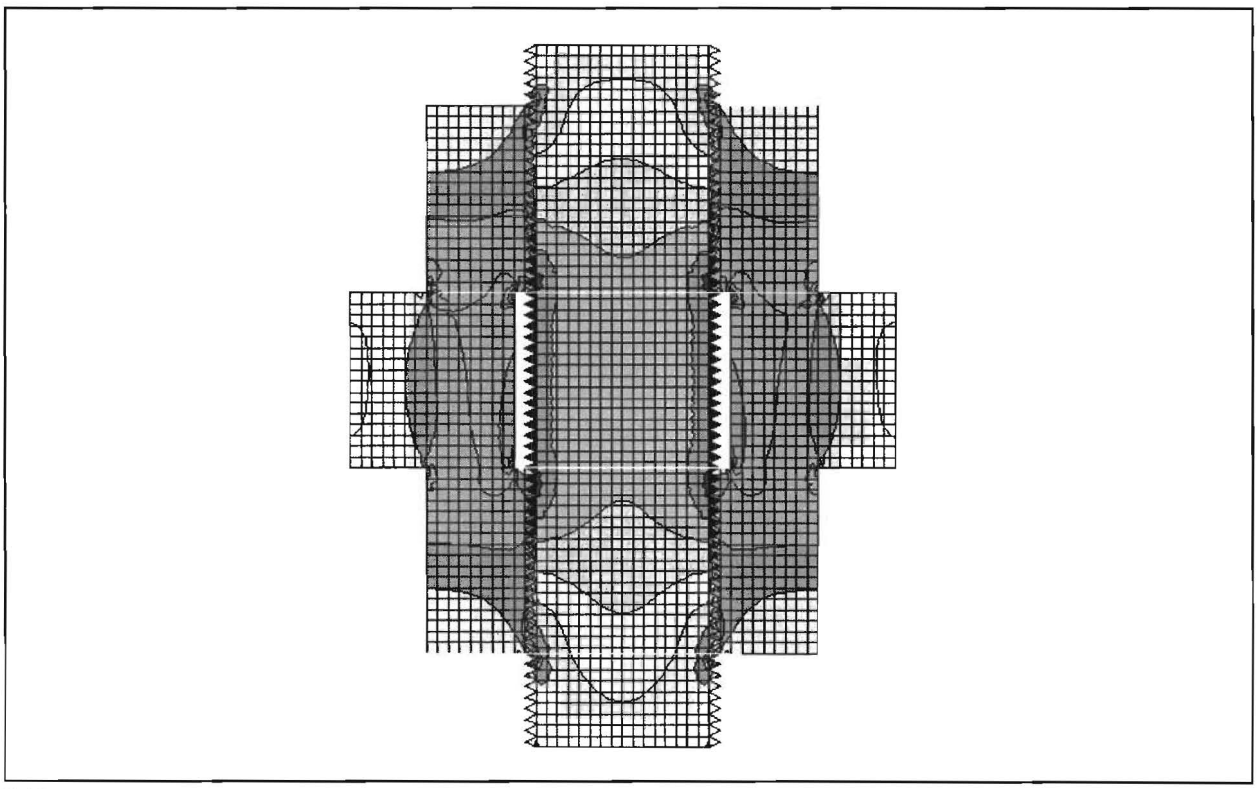

FIGURE 32 σ_{yy} stresses on preloaded bolt (no externally applied load).

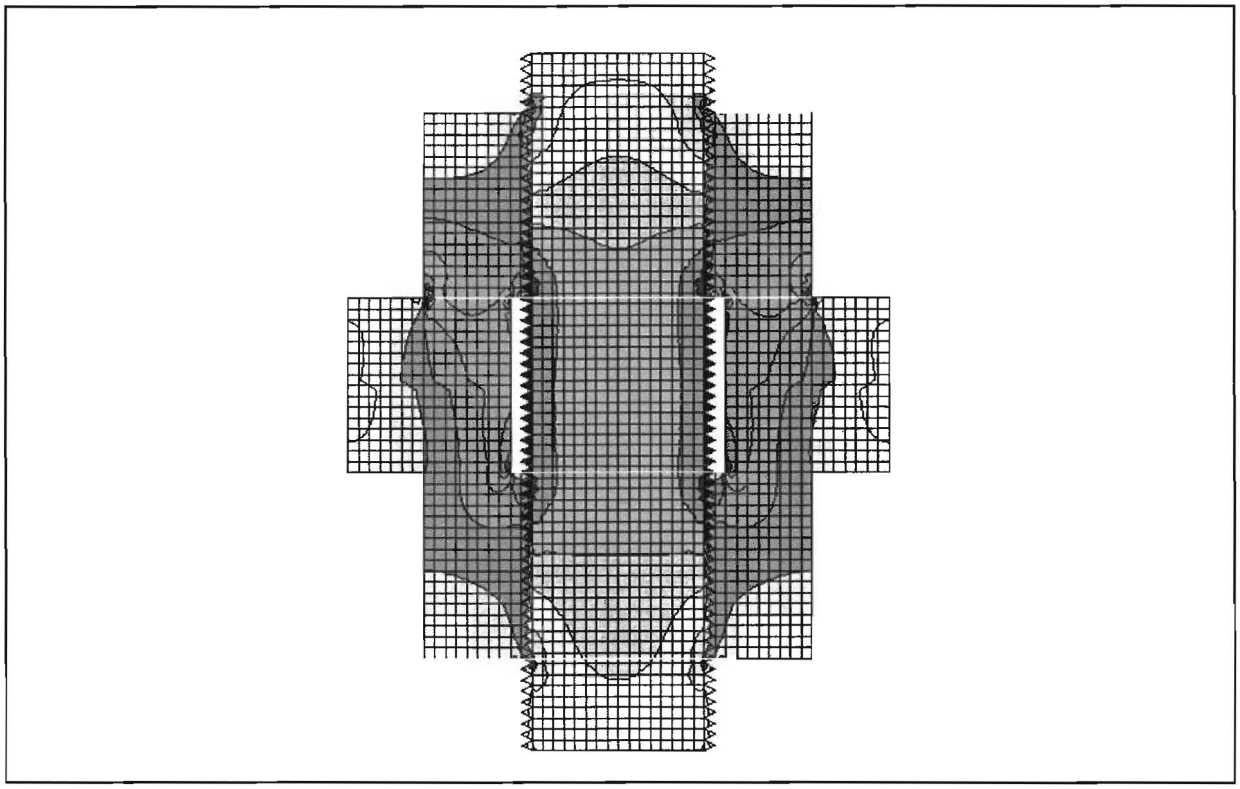

FIGURE 33 σ_{yy} stresses in preloaded bolt with externally applied load.

A stress concentration can now be seen in Location 2. The variation of axial stress, σ_{yy}, normalized with respect to the average or nominal axial stress, $\sigma_{nominal}$, with position along the length of the bolt can be seen in Figure 34 for the anchor bolt connection with a 480 MPa (70 ksi) preload. Again, the solid line represents the axial stress at the centerline of the bolt, and the dashed line represents the axial stress at the bolt thread root.

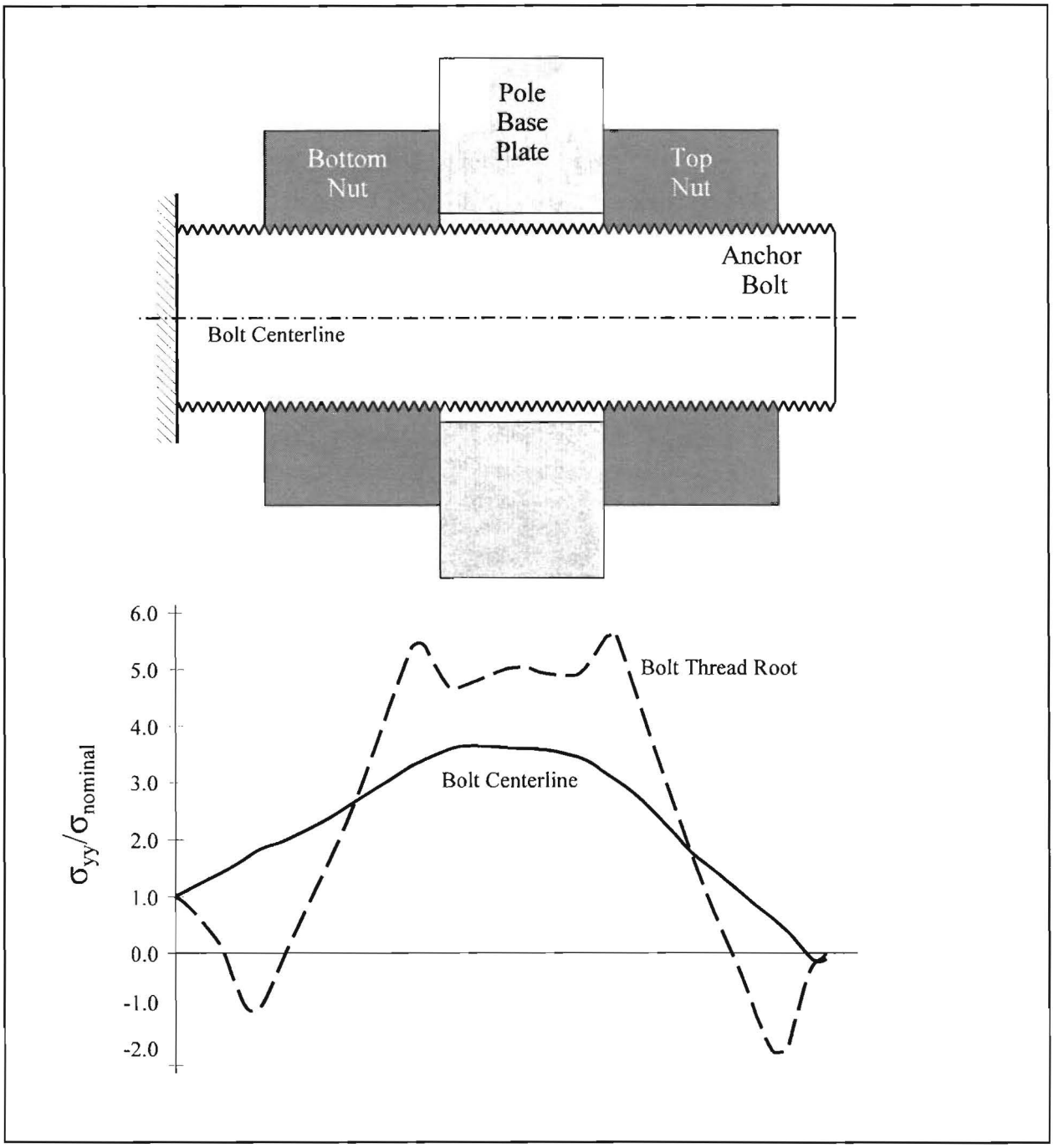

FIGURE 34 Variation of axial stress with position for preloaded bolt.

The location of maximum axial tensile stress is at the top and bottom nut to plate intersection. This localized increase in stress corresponds to a stress concentration factor of approximately 2.4. Why does the addition of the preload to the connection force the mode of failure from Location 1 to Location 2? The failure location due to fatigue is caused primarily by

the stress range, S_r, and not necessarily by the maximum axial stress. The variation of axial stress range with position at the bolt thread root can be seen in Figure 35. This figure shows the stress range, S_r, normalized with respect to the nominal stress, $\sigma_{nominal}$, for a preload of 480 MPa (70 ksi) with S_{max} = 210 MPa (30 ksi) and S_{min} = 100 MPa (15 ksi) giving a stress range of S_r = 100 MPa (15 ksi). As seen in Figure 34, the addition of the preload puts the thread roots at Location 2 into compression. Because of this, the full stress range seen from the loading conditions is not tensile. Figure 35 shows both the axial stress range and the axial tensile stress range. The location of the maximum axial stress range is Location 2, which explains why the mode of failure shifts to this region.

Further analysis with varying loading conditions and varying preload conditions showed that when the nominal preload stress in between the plate is two times greater than the maximum axial stress seen for a given stress range, the reduction in tensile stress range is 40%. This amount of preload forces the thread roots into compression so that the full stress range is not tensile near Location 2. On the other hand, when the nominal preload stress in between the plate is one-third to two times greater than the maximum axial stress seen in a stress range, the reduction in tensile stress range is 25% to 40%. Under these preload conditions, the thread roots are no longer in compression, but the maximum tensile stress range in Location 2 is still lower than that seen in the snug tight model at Location 1. For a preload stress less than one-third of the maximum axial stress seen in a given stress range, the mode of failure shifts back to Location 1, and there is reduction in maximum axial stress range from 25% to 0% when there is no preload.

This explains the fatigue benefit seen in preloaded double nut anchor bolt connections. These lower stress ranges increase the fatigue life of the bolts 2.3 to 4.6 times. This result is consistent with previous research (Frank 1978) that states preloaded double nut connections show a fatigue life three times that of a single nut connection. Also, laboratory fatigue testing in the present study on preloaded double nut connections has shown a similar reduction in stress range.

Previous research has indicated that the fatigue behavior of large diameter anchor bolts is not highly dependent on parameters such as thread spacing or method of thread forming.

Because of this, these numerical studies do not address directly these parameters.

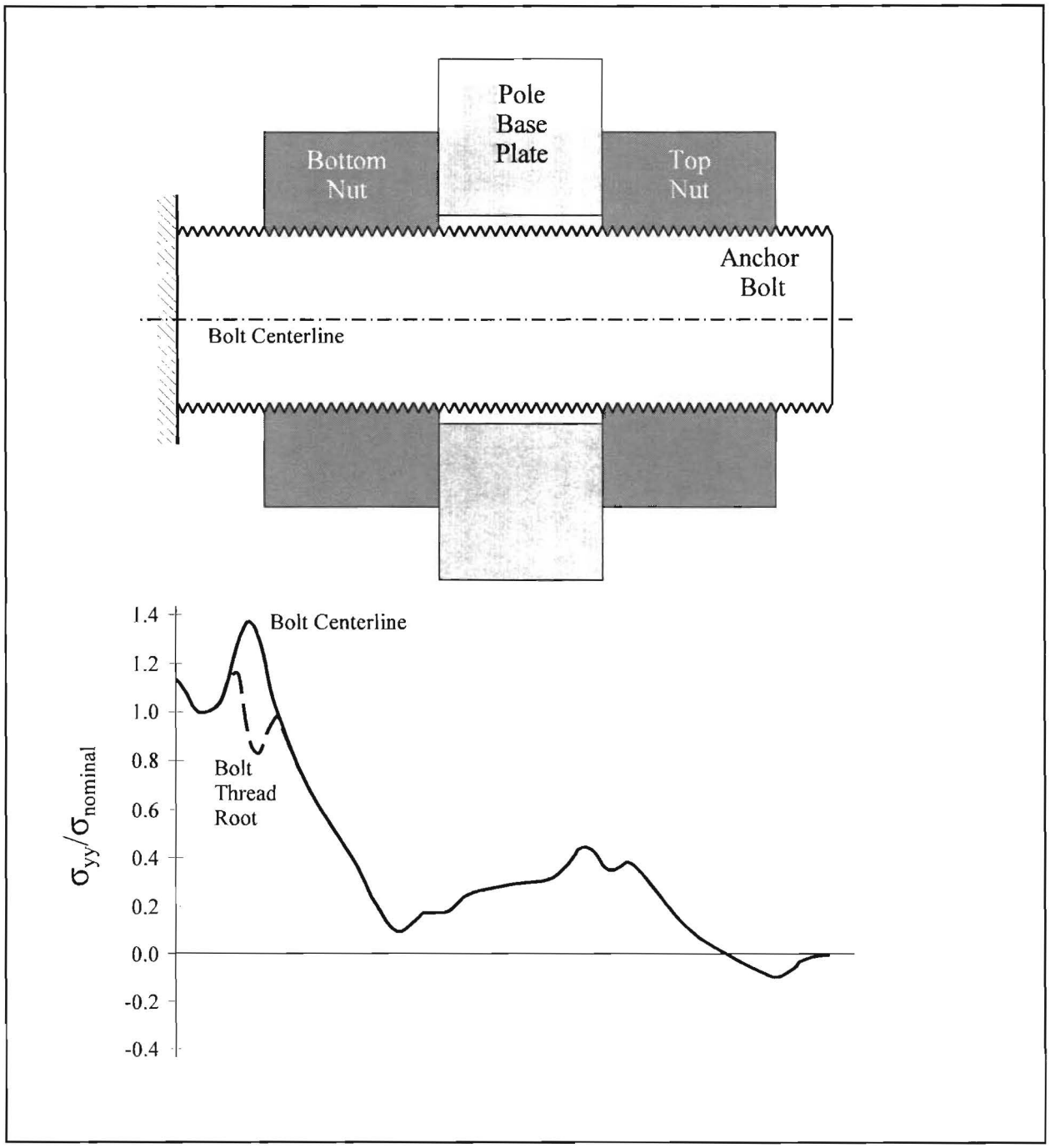

FIGURE 35 Variation of axial tensile stress range for preloaded bolt.

Misalignment of anchor bolts is a factor in their response to static and cyclic loadings. Misalignment can take two forms: misalignment (deviation from vertical) of the group of anchor bolts or misalignment of individual bolts in the pattern from the other bolts. This latter type of misalignment is mitigated by the use of top and bottom templates to maintain relative alignment of the bolts during construction. Based on experience in constructing laboratory specimens, proper installation of these templates is an effective technique to prevent relative misalignment. One mode of relative misalignment which is theoretically possible is the torsional rotation of the top template relative to the bottom template, but the clamping action of the double nuts on the templates effectively prevents this mode. The misalignment of the group of bolts is the most likely type of misalignment to be a problem in the field. To study the effects of anchor bolt misalignment, the finite element model was employed, simulating the effect of misalignment by a concentration of the bearing pressure between nuts and baseplate near the outside edge of the nut. It is not possible to say exactly what degree of misalignment is approximated by this model; the results of this portion of the study are only qualitative.

Finite Element Modeling of a Misaligned Snug Tight Connection

Many problems with anchor bolts failing in fatigue can be attributed to higher stress concentrations in the threads caused by improper installation. Some failures have been attributed to misaligned anchor bolts being hammered into alignment, which can cause cracking at or just below the top surface of the concrete shaft. In fact, when a bolt template is not used during installation, it is extremely difficult to align the anchor bolts properly. This misalignment tends to worsen the stress conditions in the bolt because of the localization of load transfer. The following finite element analysis models this condition.

The finite element mesh of a misaligned double nut anchor bolt is represented in Figure 36. The model uses the same mesh used in previous models, except that boundary conditions are modified so that only a small portion of the nut and plate are in contact at the contact surfaces. The contact surfaces are modeled using connectivity between the nuts and the plate in these

small regions. Using these new boundary conditions, a vertical load is applied to the plate. The axial stresses due to this loading can be seen in Figure 37.

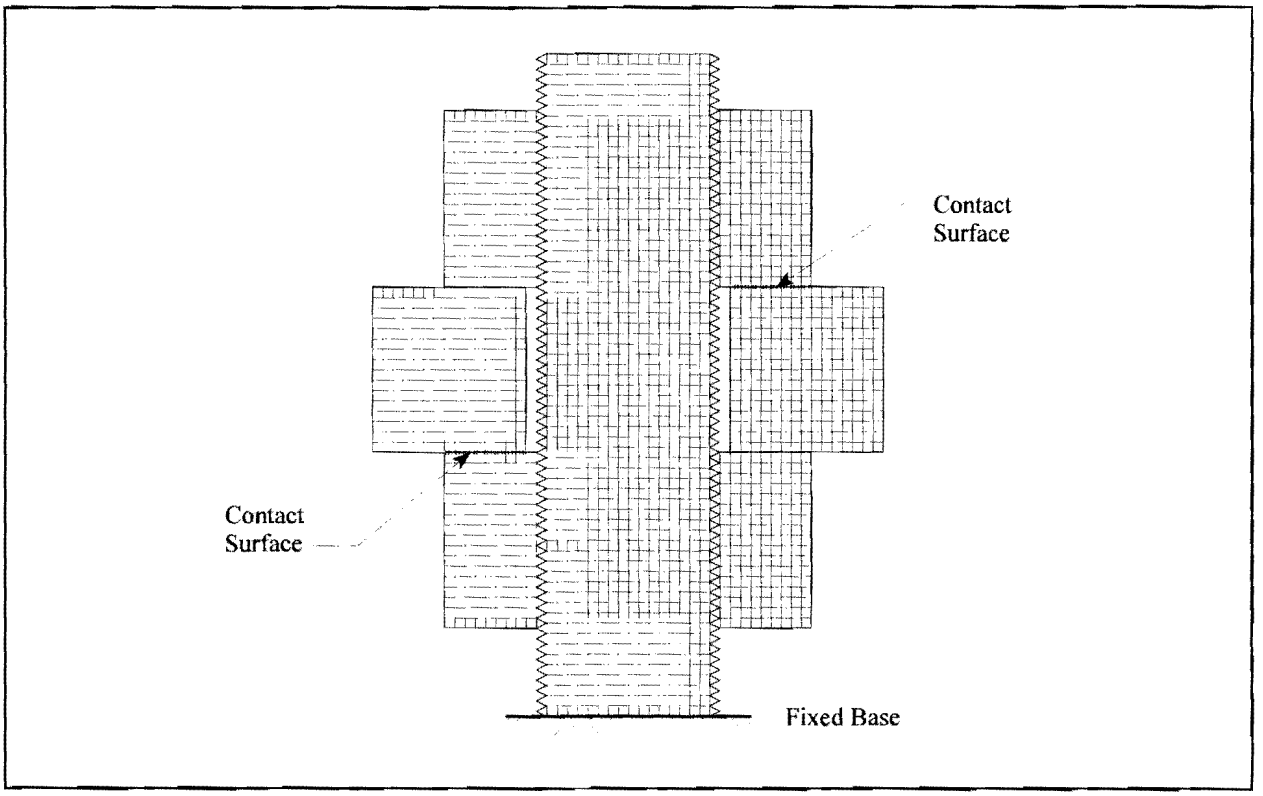

FIGURE 36 Finite element mesh for misaligned anchor bolt study.

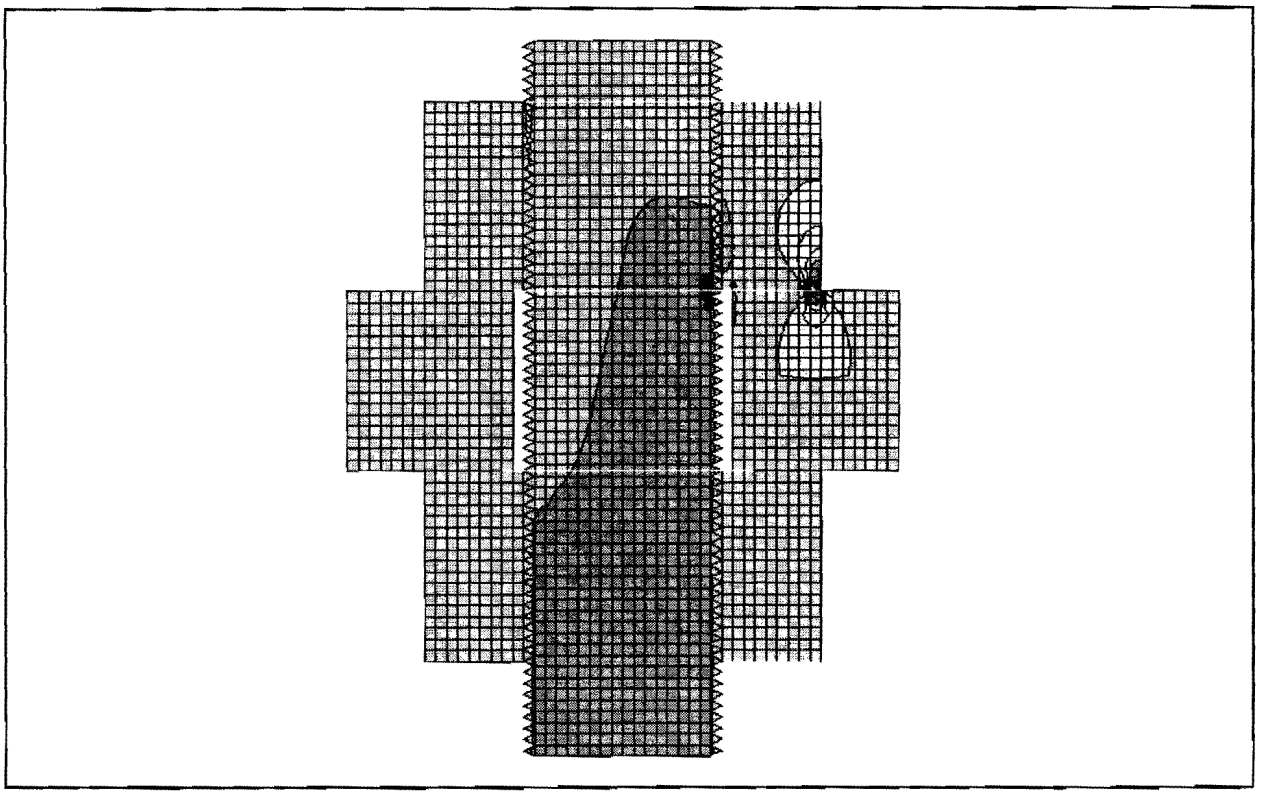

FIGURE 37 σ_{yy} stresses on misaligned snug tight bolt.

It can be seen that the location of the maximum tensile stress is Location 1. The variation of axial stress, σ_{yy}, normalized with respect to the average or nominal axial stress, $\sigma_{nominal}$, with position along the length of the bolt can be seen in Figure 38. Figure 39 shows the stress range, S_r, at the bolt thread root normalized with respect to the nominal stress, $\sigma_{nominal}$. The normalized stress range for the aligned bolt is shown for comparison.

The misalignment of a bolt upon installation concentrates the load transfer to one side of the bolt and increases the stress seen in that region. This localized increase in stress will result in a lower fatigue life. The misalignment results in stress concentration factors near 3, higher than the value of 1.4 seen in the snug tight connection. The maximum tensile stresses seen in the misaligned finite element anchor bolt model are 215% greater than those seen in the snug tight anchor bolt model resulting in 215% higher stress ranges. This indicates that a misaligned anchor bolt can exhibit a reduced fatigue life, therefore special care must be taken to ensure proper anchor bolt alignment at the time of installation.

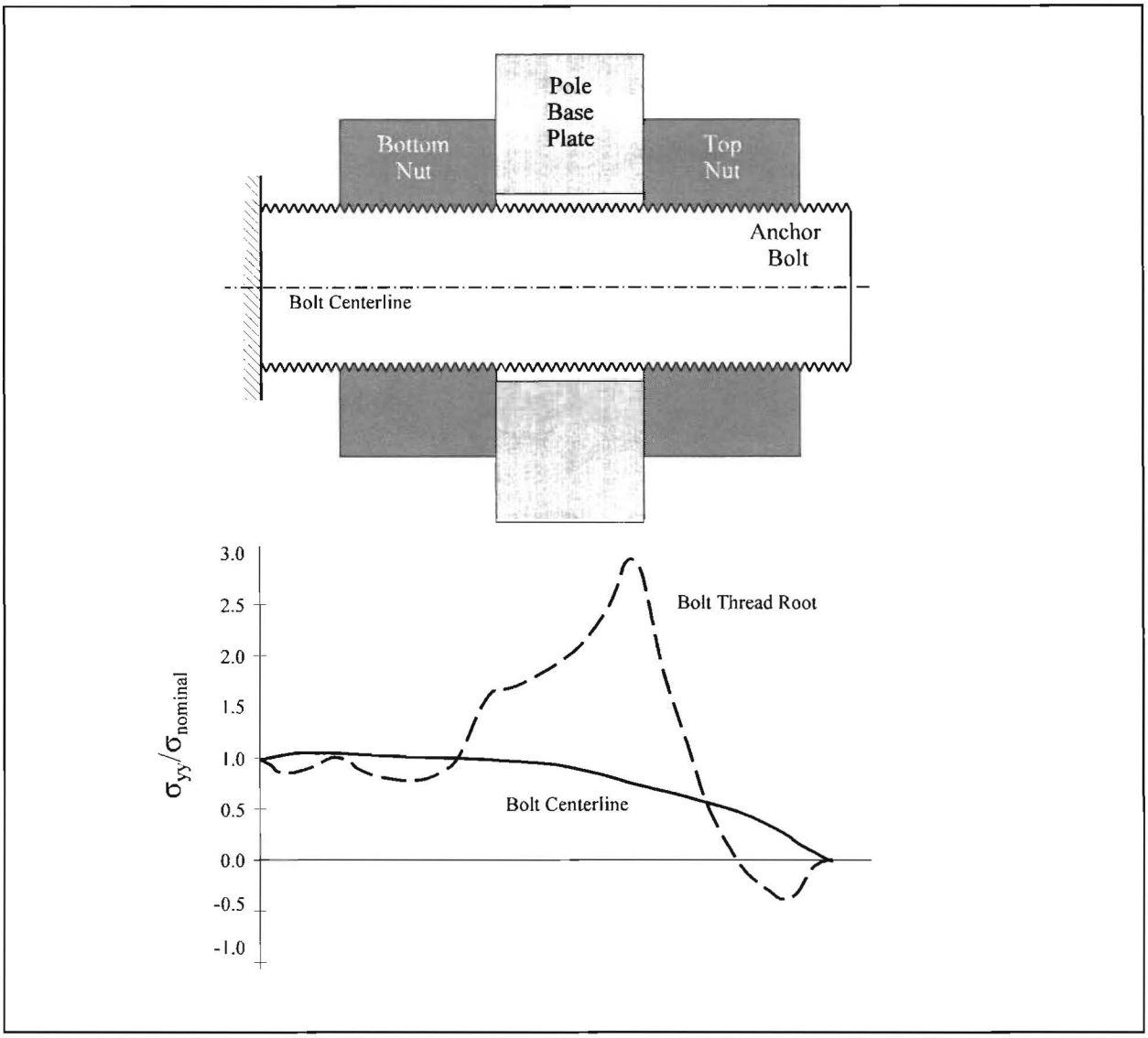

FIGURE 38 Variation of axial stress with position for misaligned snug tight bolt.

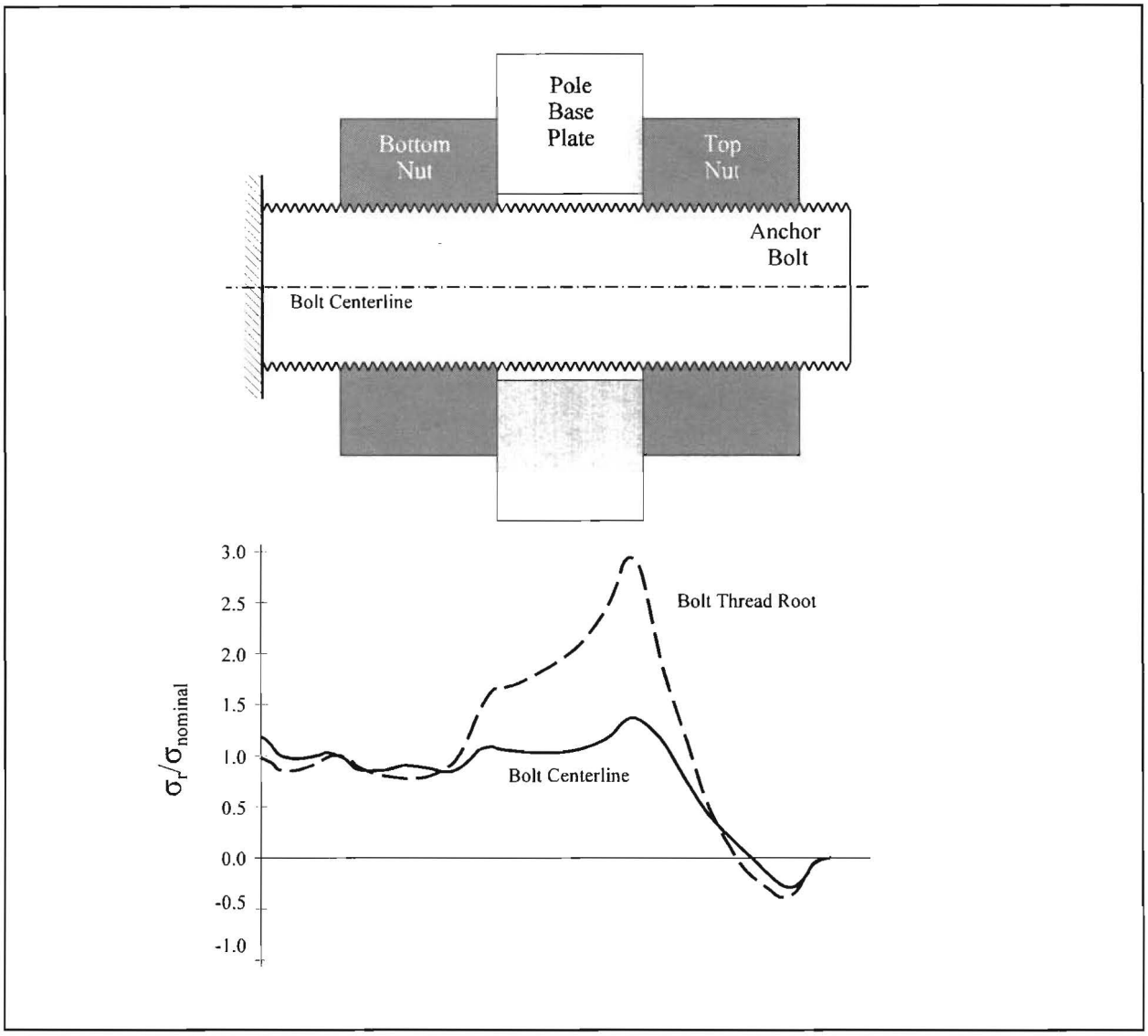

FIGURE 39 Variation of axial stress range with position for misaligned snug tight bolt.

Finite Element Modeling of a Misaligned Preloaded Connection

The addition of a preload to the misaligned finite element mesh seen in Figure 36 does not have the same beneficial fatigue effects as seen previously for the aligned case. Addition of a 70 ksi (482.6 MPa) preload to the misaligned finite element mesh still results in high axial stresses at Location 1, which can be seen in Figure 40.

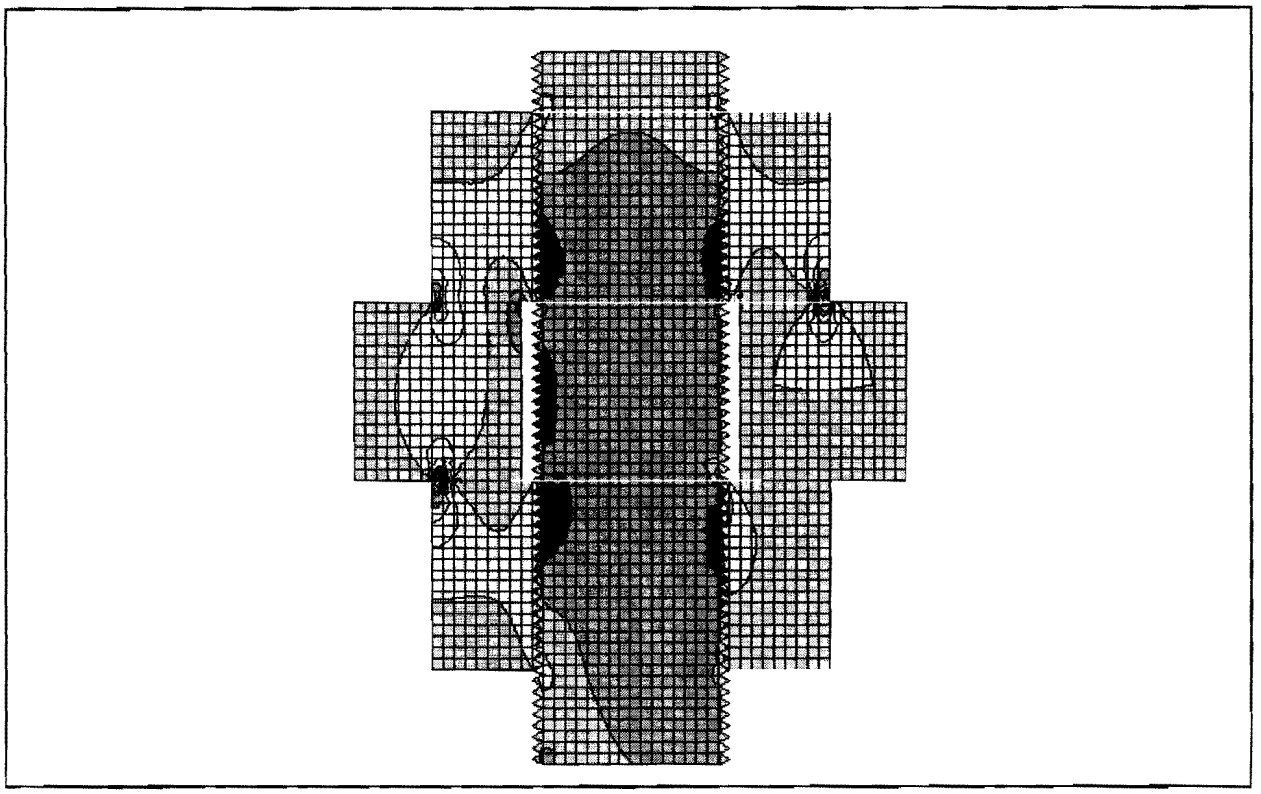

FIGURE 40 σ_{yy} Stresses on misaligned preloaded bolt.

Figure 41 shows the variation of axial stress, σ_{yy}, normalized with respect to the average or nominal axial stress, $\sigma_{nominal}$, with position along the length of the bolt for a 480 MPa (70 ksi) preload. Figure 42 shows the stress range, S_r, at the bolt thread root normalized with respect to the nominal stress, $\sigma_{nominal}$, for the same 480 MPa (70 ksi) preload.

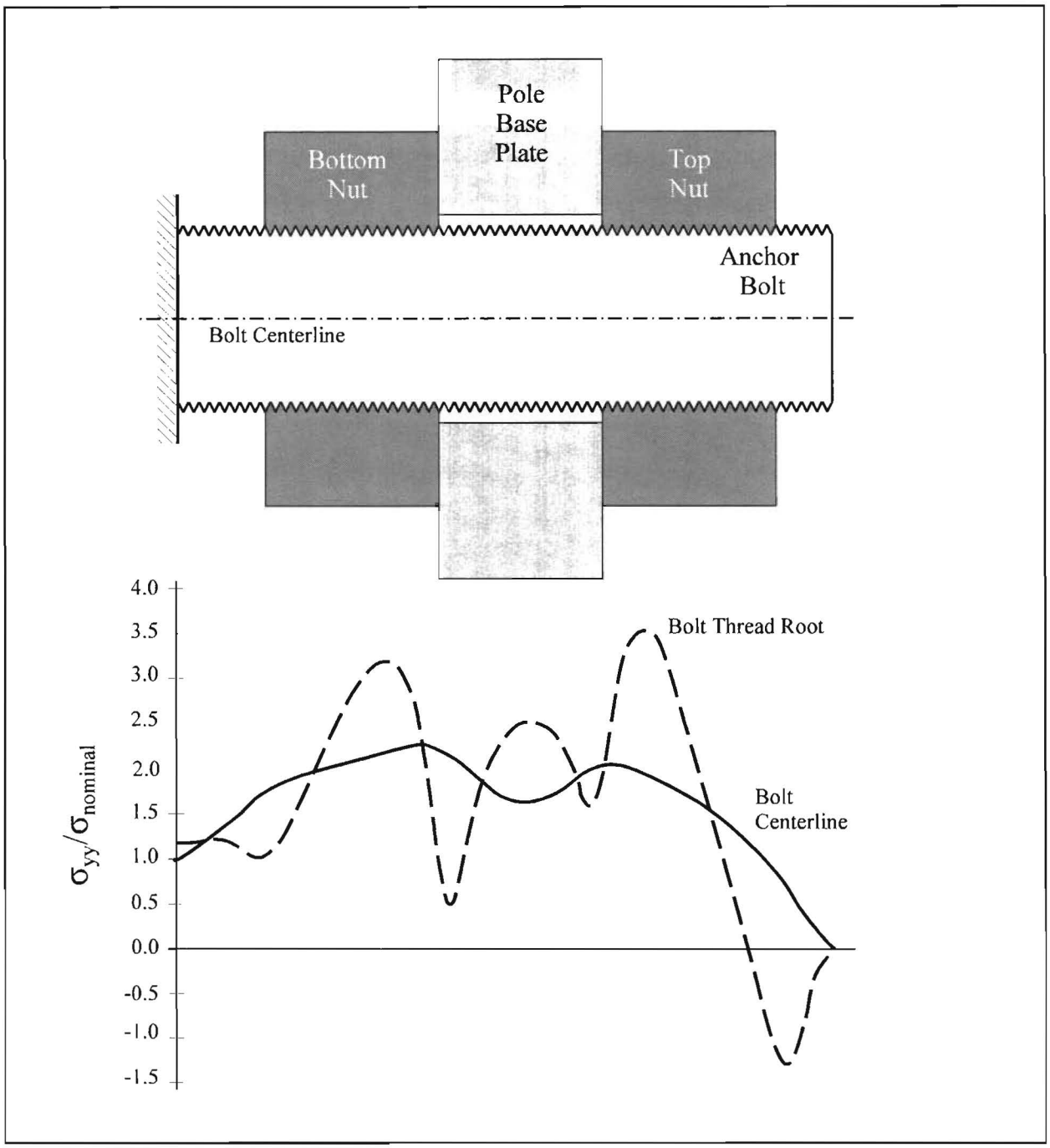

FIGURE 41 Variation of axial stress with position for misaligned preloaded bolt.

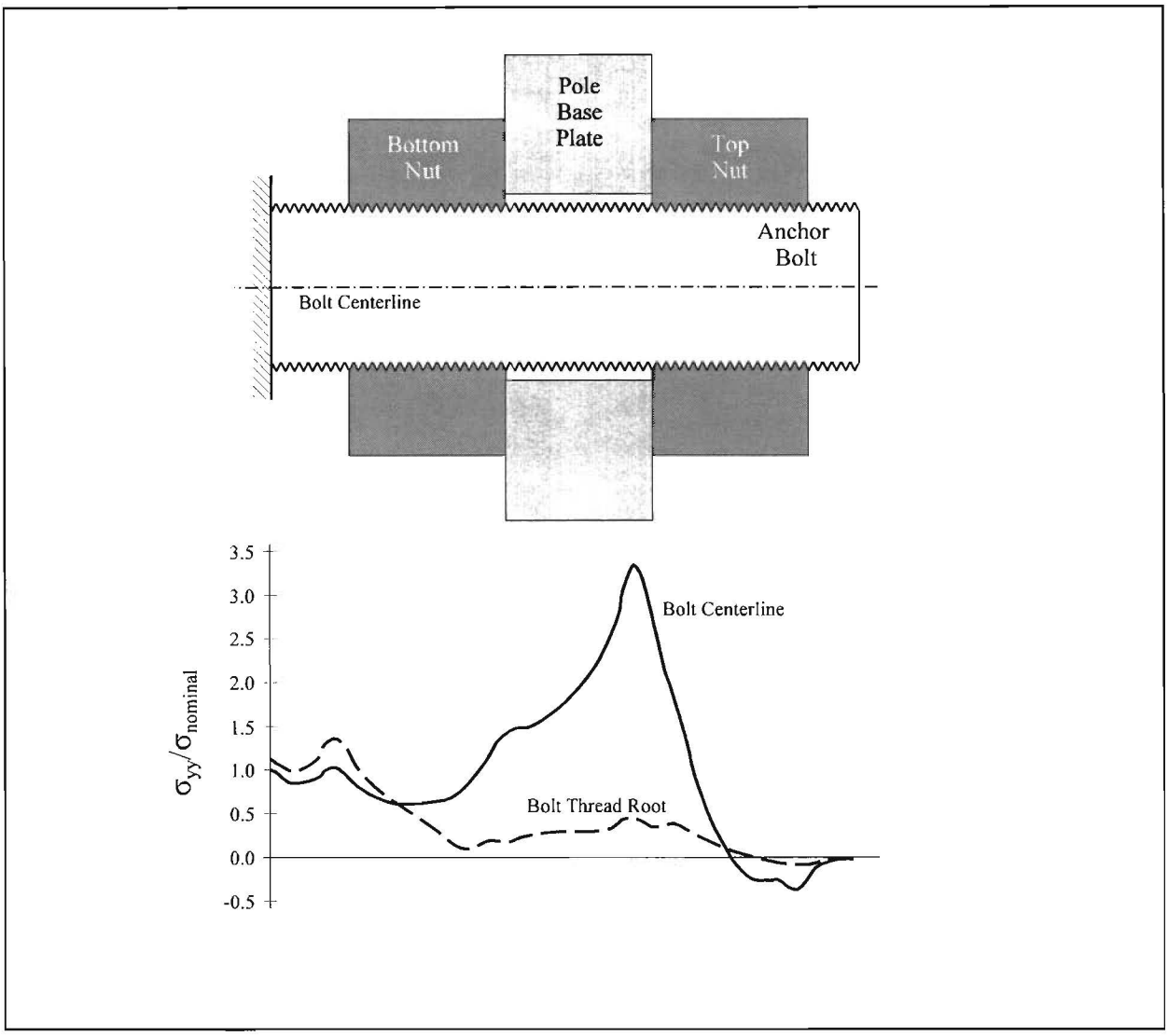

FIGURE 42 Variation of axial stress range with position for misaligned preloaded bolt.

The effect of the preload on the misaligned bolt increases the stress concentration factor at Location 1 up to 3.4 from the value of 1.2 in the snug tight case. The stress range seen in the preloaded misaligned bolt in Figure 42, however, is similar to that seen in the snug tight misaligned bolt in Figure 39 both in location and magnitude. This indicates that the increased fatigue life benefits of the preload double nut connection are lost when the bolts are improperly installed. In fact, the preloaded misaligned connections can experience shorter fatigue lives than the snug tight bolt. Because of the higher stress ranges seen in misaligned double nut anchor bolt connections, it is important that the bolts be installed in alignment.

LABORATORY STUDIES--COSS SPECIMENS

Experiment Design

From review of the failures in Michigan and Georgia, TxDOT cantilever overhead sign structure (COSS) designs, and previous research, the testing variables were established. The test variables were to be thread pitch, including both 4 1/2 UNC and 8 UN thread pitch, as used in TxDOT designs, and nut tightness. All anchor bolts were to be grade 105 steel, f_y = 724 MPa (105 ksi), a commonly used steel for such anchor bolts. Previous research indicated that some tightening procedures used in the field can produce a preload stress of up to 480 MPa (70 ksi) preload stress. To evaluate such tightening procedures, the higher strength bolts were selected. The tightening tests were performed on these specimens to establish the relationship between thread pitch and the preloads induced for different degrees of tightness. Even though grade 55 anchor bolts are also used, previous research indicated that the steel strength does not have a significant effect on the fatigue life at low stress ranges (Frank 1978). The tests in this study were all planned for grade 105 bolts. However, the 8 UN anchor bolts tested are grade 55 steel, f_y = 380 MPa (55 ksi), due to an error by the supplier that was not discovered until the bolts were tested. Because of this error, the 8 UN bolt specimens could not be preloaded to the same stress level as the 4 1/2 UNC bolt specimens.

The 51 mm (2 in.) diameter was selected as a representative anchor bolt size because of the frequent application of bolts of that size and because that was the diameter of the bolts that failed in the COSS base in Michigan. The bolt diameter is not considered a test variable since it is not expected to affect the fatigue life (Frank 1978), and tightening procedures can be adjusted theoretically for different bolt diameters.

The fatigue test stress range was chosen after study of expected service loads and fatigue category classification. Previous research (Frank 1978) indicates this bolt detail can be classified between AASHTO Category E and Category C, depending upon the nut tightness. Under current specifications, AASHTO Category C details can be used for connections that experience more than two million cycles of stress ranges of 70 MPa (10 ksi) (AASHTO 1985).

Specimen Design

Two COSS specimens were designed using standard TxDOT COSS plans (COSSF Drawings, Sheets 1-3, 7/83). The section of the specimen containing the anchor bolts was designed according to TxDOT standards. The COSS portion of the specimen was a single 600 mm (24 in.) OD circular pole with a wall thickness of 12.5 mm (0.50 in.). An 876 mm (34.5 in.) by 51 mm (2.00 in.) thick circular baseplate supports the pole (see Appendix A). The pole was attached to the concrete foundation by eight symmetrically spaced 57 mm (2.25 in.) double-nutted anchor bolts. The bottom portion of the specimens was designed to be secured to the testing lab floor. The specimens were designed so that they could be rotated about the longitudinal axis, to allow for two different loading configurations. After the first test on a specimen was completed, the specimen was rotated 90 degrees about the longitudinal axis. This rotation allowed for the testing of the anchor bolts that were on the neutral axis during the first test. The specimens were designed to be statically and dynamically loaded to determine the effects of bolt preload and the fatigue life of the different anchor bolts.

Specimen Construction

The specimens were constructed according to the TxDOT COSS design standards. Class A concrete for each specimen was placed in two lifts. First, the square base was poured. Once the concrete had cured to design strength, the circular cylindrical top section, simulating the top of the drilled shaft, including the anchor bolts, was placed. The threads of the anchor bolts were covered during the placement of the concrete to protect them and to keep them clean. The type and strength of the concrete were specified by the TxDOT COSS plans. Cylinder tests verified the concrete strength. Figure 43 shows a completed specimen.

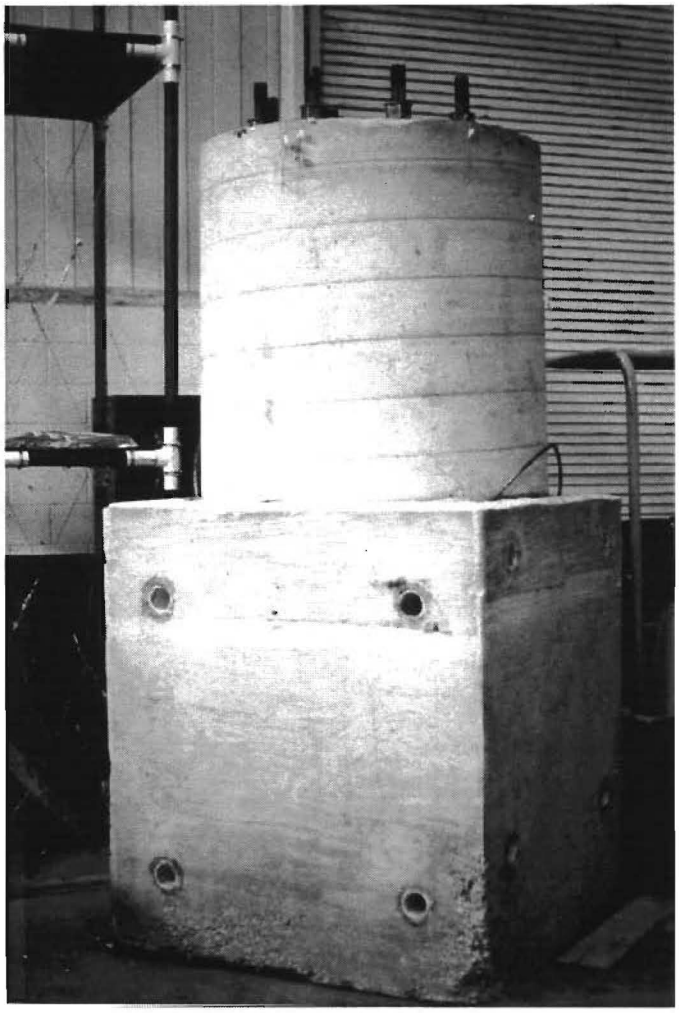

FIGURE 43 Photograph of test specimen.

Loading Configuration

When a specimen was ready for testing, it was placed on its side and secured to the lab strong floor with 64 mm (2.5 in.) diameter threaded rods, as indicated in Figure 44. The bars passed through the holes in the base of the specimen and were secured with nuts and washers. The pole section was then installed using the overhead crane. Once the pole was in place and the anchor

bolt nuts were tightened to their desired tightness, a 250 kN (55 kip) capacity hydraulic ram was connected to the COSS pole using a steel clamping device. Figure 45 shows the loading configuration.

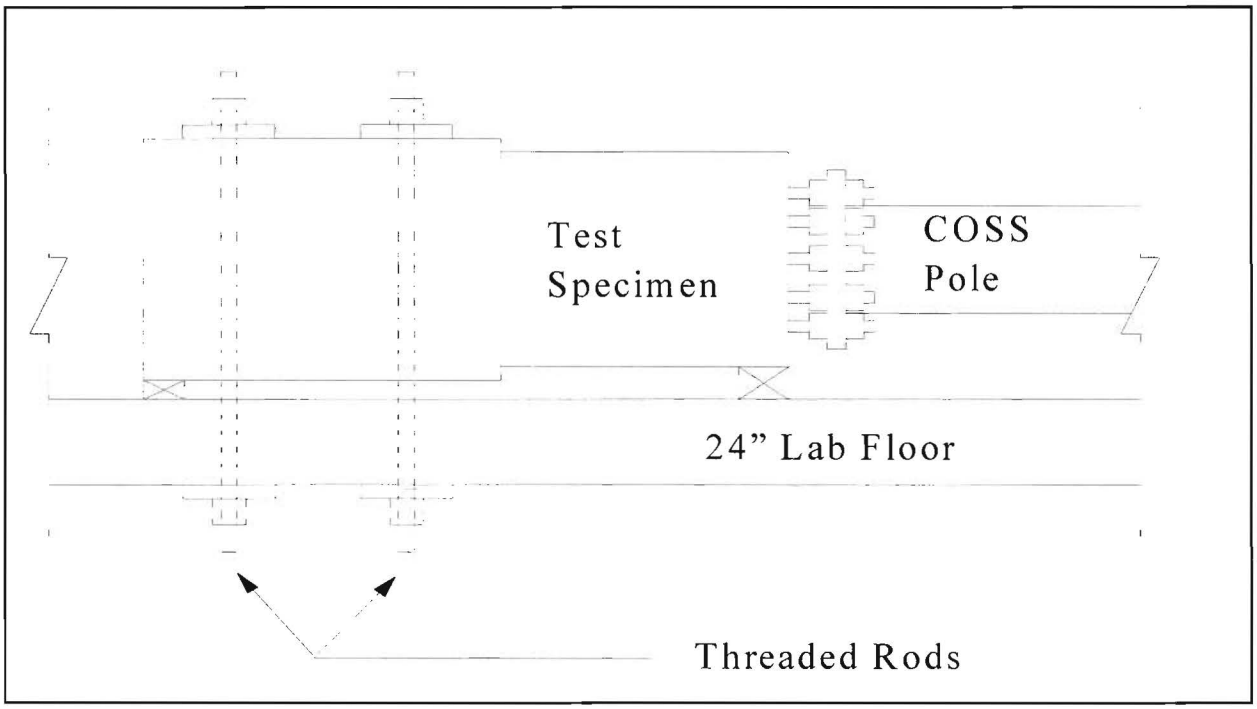

FIGURE 44 Test specimen configuration.

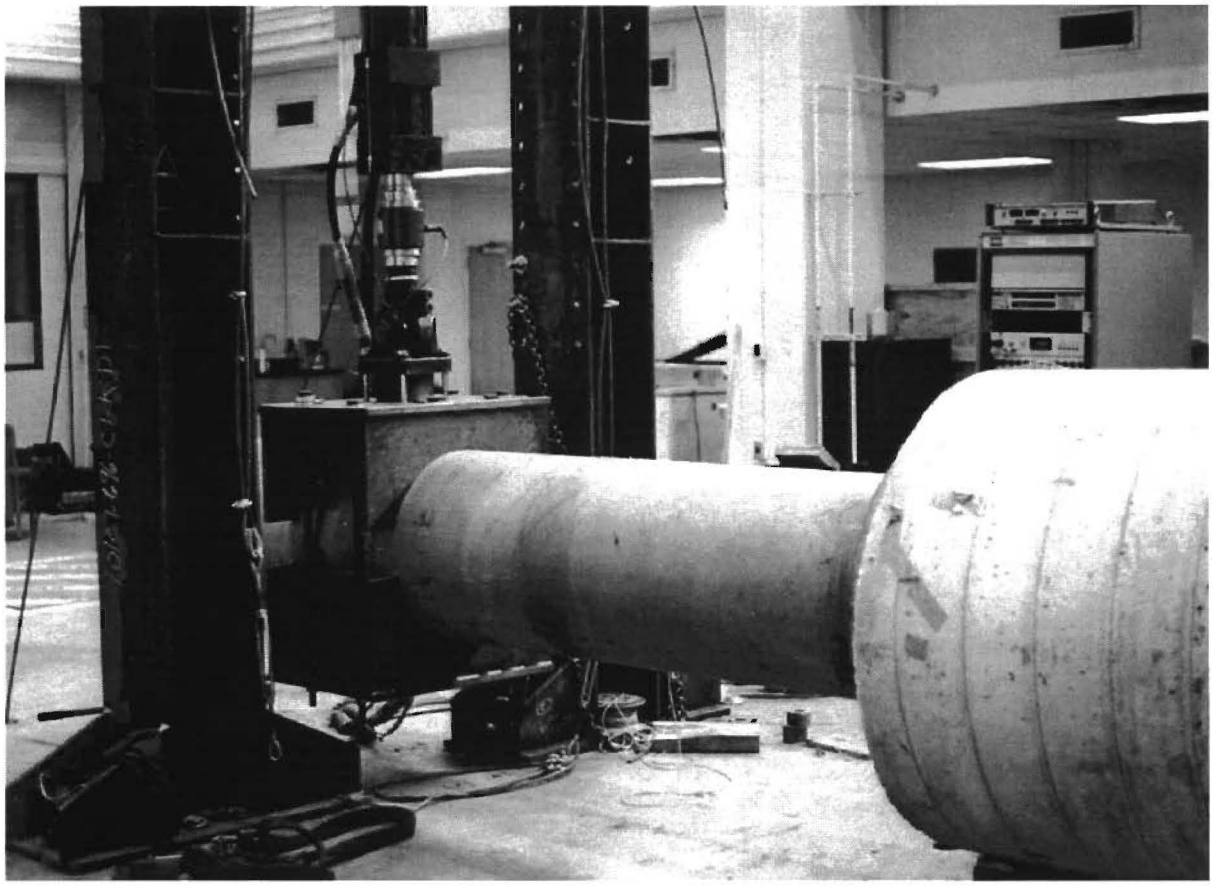

FIGURE 45 Photograph of fatigue loading apparatus.

Instrumentation

For each specimen, selected anchor bolts were instrumented with strain gages in different sections of the bolt. For the first test of the first specimen, the bolts were arranged and labeled as shown in Figure 46. Longitudinal keyways were milled on opposite sides of the bolt for the placement of strain gages, allowing the leads to pass beneath the nuts. Figure 47 shows the location, size, and orientation of the keyways on the bolts.

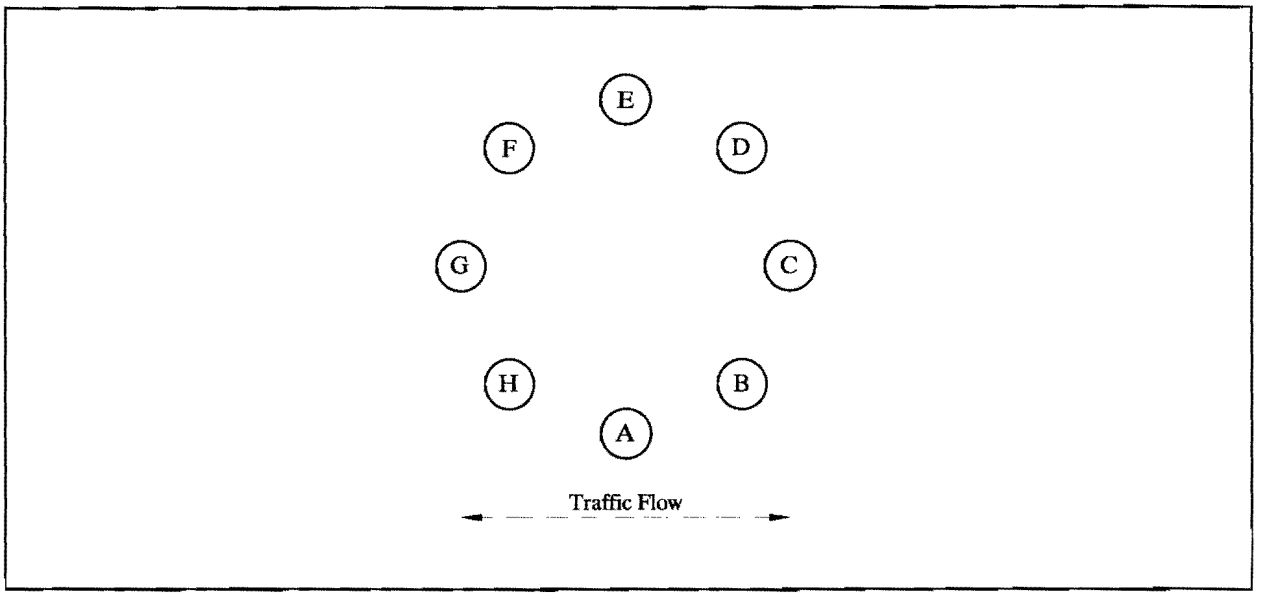

FIGURE 46 Anchor bolt pattern and nomenclature (8-bolt pattern).

Bolts A, C, E, and G were instrumented with ten gages each. The first four gages were located in the region covered by the top nut, the next four gages were placed in the region of the base plate, between the nuts, and the last two gages were located in the region covered by the leveling nut. With two gages at each station monitored separately, both tension and bending stresses could be measured. The location of the gages is shown in Figures 48 and 49. The gages are in pairs, on opposite sides of the bolt. Bolts B, D, F, and H were instrumented with two single, unpaired strain gages. One gage was located in the region covered by the top nut, and the second gage was located in the middle of the base plate. These gages were placed on the same side of the bolt to determine the tension stresses in the bolt in these two regions, assuming there are no bending strains at the gage locations. Because the gages were installed on only one side of the bolt, bending stresses in the bolt could not be measured for these bolts.

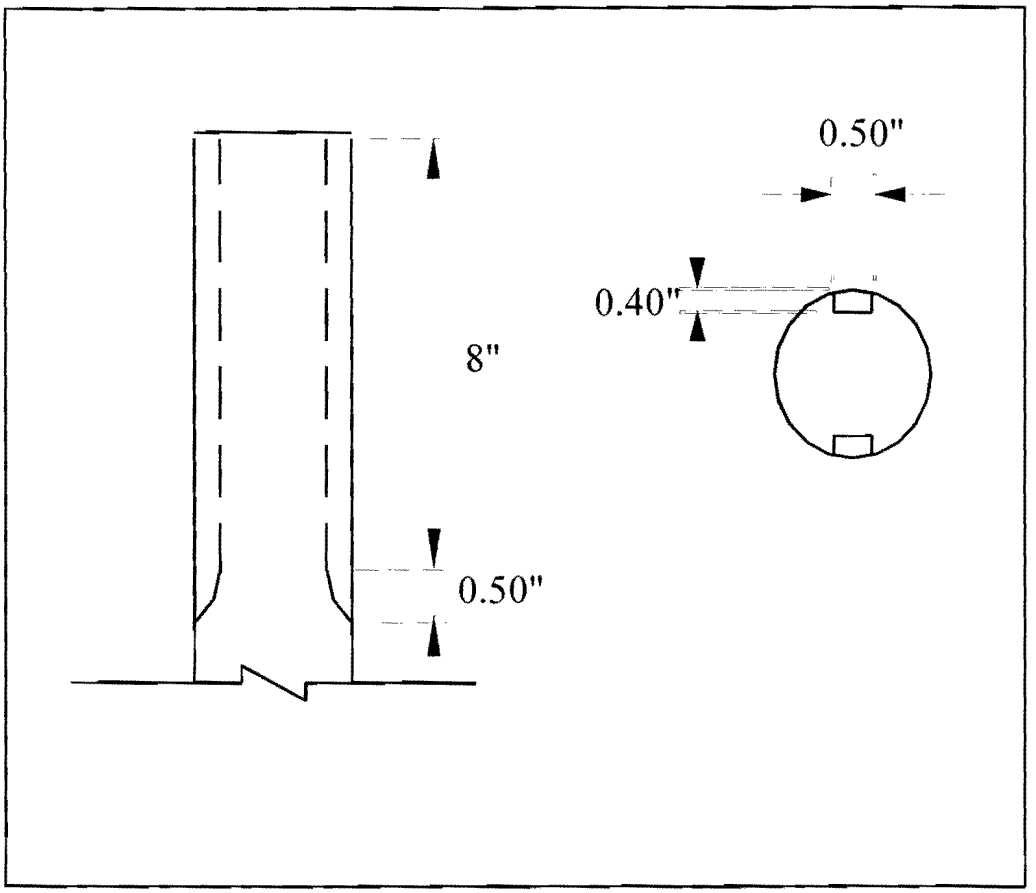

FIGURE 47 Bolt milling for strain gage instrumentation.

To determine the torque needed to tighten the nuts to a specified tightness, a load cell was connected from the overhead crane and the 3 m (10 ft) cheater pipe. Figure 49 shows this set up. This system was also used to find the torque needed to loosen the nuts after certain tests.

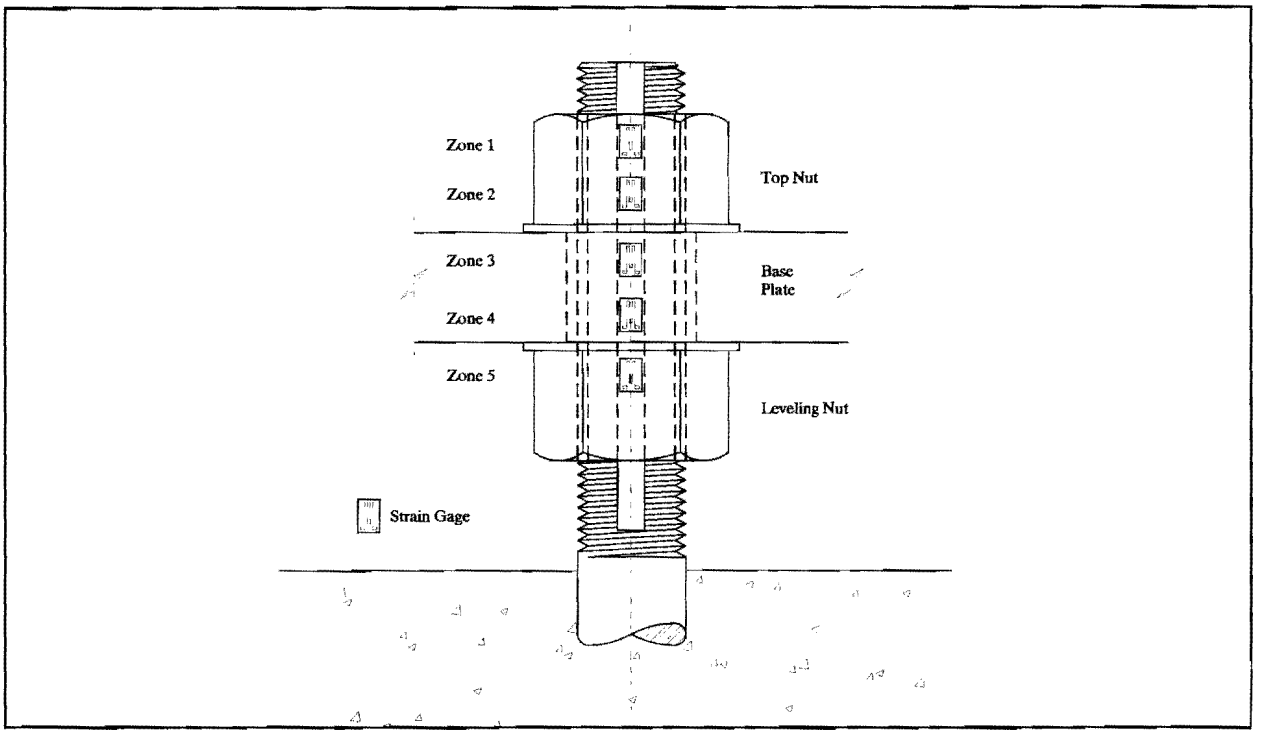

FIGURE 48 Location of strain gages on bolts A, C, E, and G.

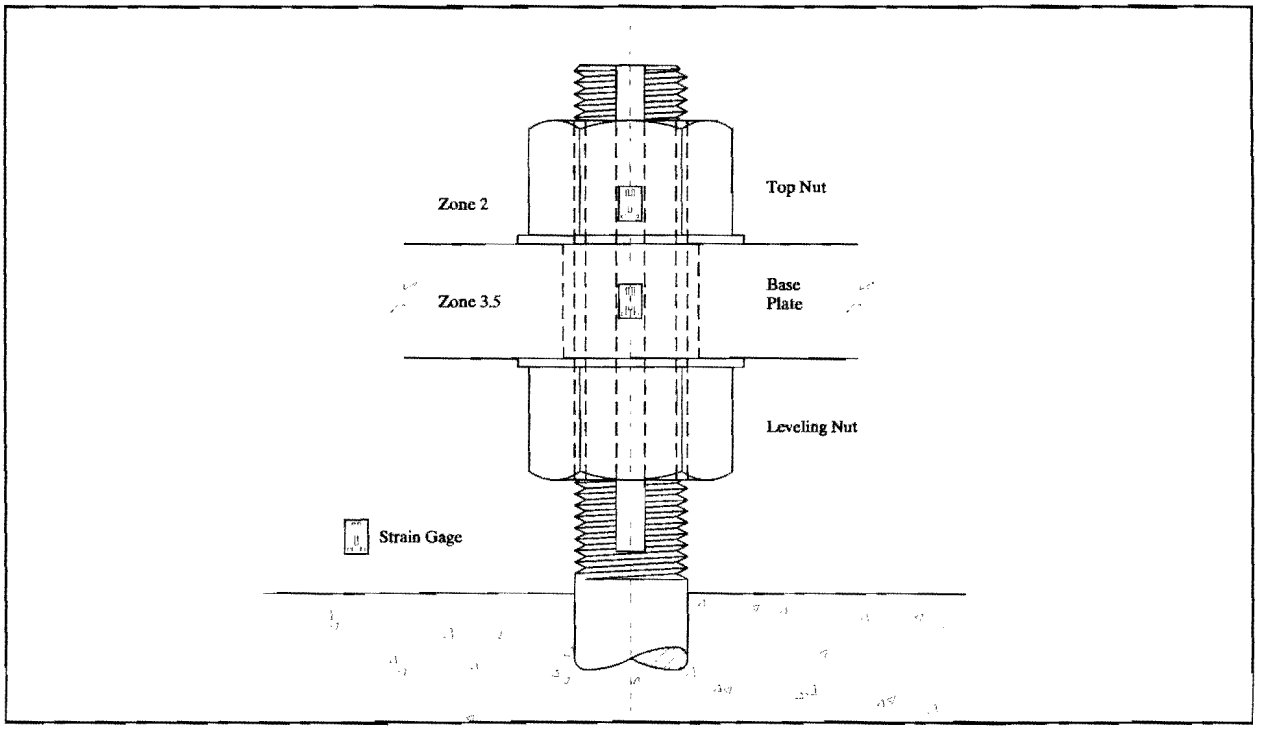

FIGURE 49 Location of strain gages on bolts B, D, F, and H.

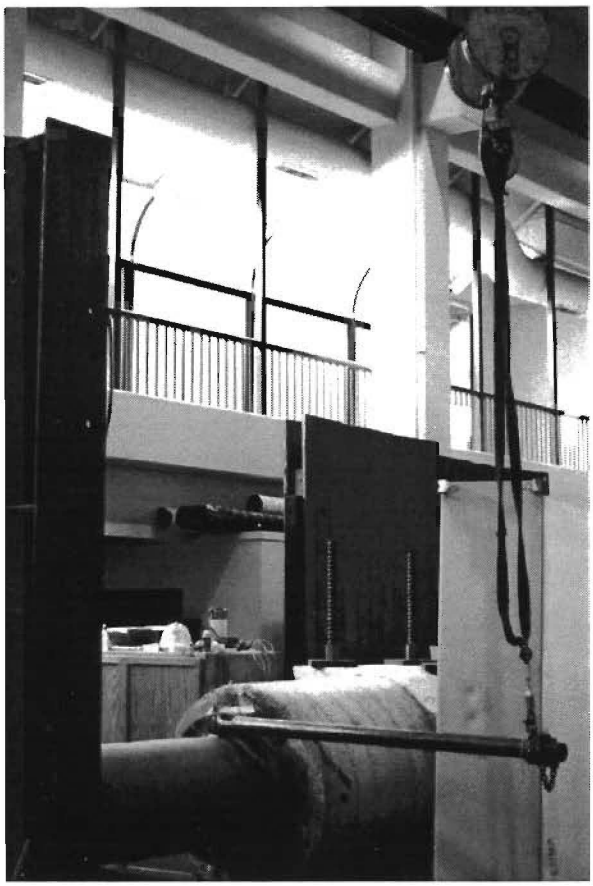

FIGURE 50 Photograph illustrating apparatus for measuring tightening torque.

Laboratory Studies Procedures

Three types of tests were completed on each specimen: tightening, static loading, and fatigue loading. The objective of the tightening tests was to determine the amount of preload induced between the nuts for different levels of tightness and the torque needed to obtain these different levels of tightness. The goal of the static load tests was to determine the relationship between the column base moments and the anchor bolt stresses. Lastly, the objective of the fatigue tests was to determine the fatigue life of the bolts at different levels of tightness.

Tightening Studies

Two methods of nut tightening were used in the tightening tests: static tightening with a wrench and a 3 m (10 ft) cheater pipe handle and impact tightening using a 7 kg (16 lb) sledgehammer with a knocker wrench. Both methods were adequate to tighten both the 4 1/2 UNC bolts and the 8 UN bolts to 60 degrees (one-sixth turn) past snug tight.

The same tightening procedure was followed with both tightening methods. This procedure involved first aligning or plumbing the sign pole and tightening each bolt in a prescribed sequence. The sequence of nut tightening was determined from the orientation of the pole. The bolt opposite the cantilever arm was tightened first. The remaining bolts were then tightened in the sequence shown in Figure 51. During each tightening test, the strains induced in the bolts were recorded, and the preload stresses calculated. This data was used to determine the relationship between bolt stresses and the amount of nut rotation.

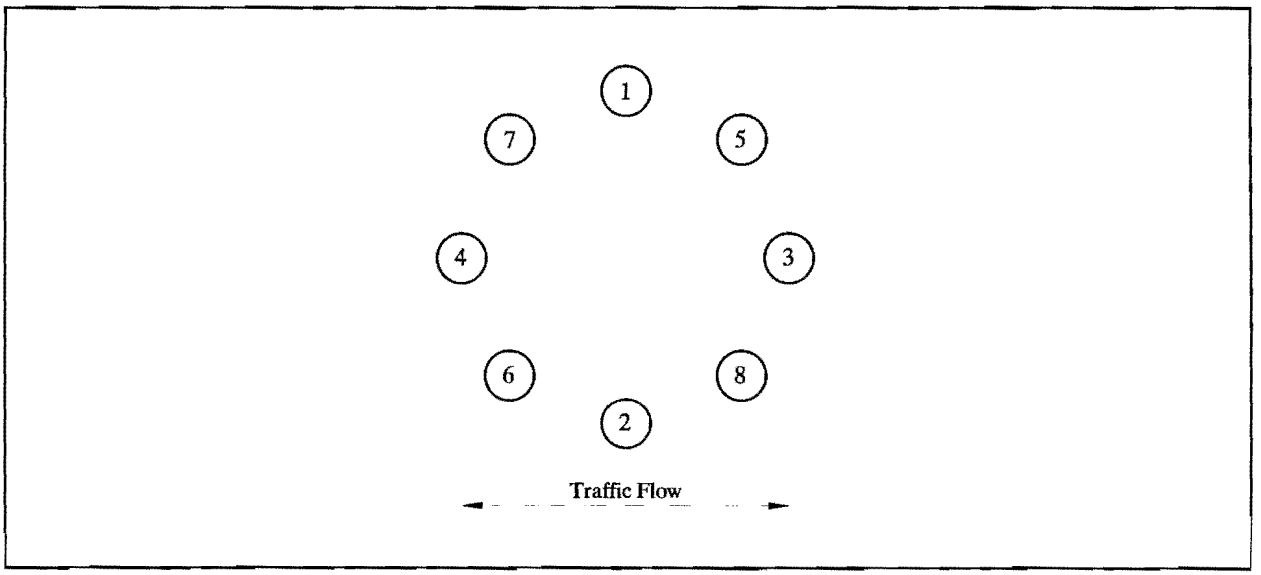

FIGURE 51 Nut tightening sequence.

Snug Tight

Snug tight is defined in structural bolting applications as "...the tightness that exists when all plies are in firm contact" (RCSC 1988), a definition which is adopted in the present study. A snug tight condition in structural bolting applications can usually be obtained by the full effort of a person using a wrench, if the force is applied as close to the end of the wrench as possible. The full effort must be used until the nut stops rotating. In the present study of large-diameter bolts, it was noted that this level of tightening effort did not always bring the entire nut into full contact with the washer. However, the washer was always observed to be in full contact with the base plate. The contact developed between the nut and the washer for a given tightening effort depends on the size of the bolt, the friction in the system and the alignment of the bolt to the base plate. The alignment of the anchor bolts in the present study is controlled using templates at the top and bottom of the bolts during construction. This system still allows some slight misalignment due to the oversized holes in the template and due to potential rotation of one template with respect to the other. This misalignment was determined to be insignificant when attempts to assemble the anchor bolts into the template with intentional misalignment were unsuccessful. When the anchor bolts were installed normally, the preload induced in the bolts at a snug tight condition was consistent from bolt to bolt, so the misalignment effects appeared to be negligible.

To develop the snug tight condition in the anchor bolts, three leveling (bottom) nuts were first adjusted to plumb the baseplate and structure. Then all the bottom nuts were turned up to contact the baseplate and each top nut was turned down to contact the baseplate. Then, beginning with the Bolt E, the leveling nut was first tightened to snug tight, followed by the top nut. Following the tightening sequence described above, the leveling nut on the second bolt was tightened to snug tight followed by the top nut, and so on in sequence. This procedure was followed until all leveling and top nuts were tightened to a snug tight condition. Once all of the nuts were snug tight, each top nut was removed, one at a time in the same order as tightened, and thoroughly lubricated with beeswax. After the nut was lubricated, it was retightened to a snug tight condition. This process was repeated until all nuts were lubricated and snug tight.

Impact Tightening with Knocker Wrench

A knocker or slug wrench is a heavy duty steel box-end wrench with a large striking surface near the end of the handle. A 7 kg (16 lb) sledgehammer was used to strike the knocker wrench. Approximately 16 blows of the sledgehammer typically were required to turn the nut 60 degrees (one-sixth turn) past snug tight. For approximately the last 6 blows, the nut rotation was very slight, nearing refusal. This method of tightening is demonstrated in Figure 52.

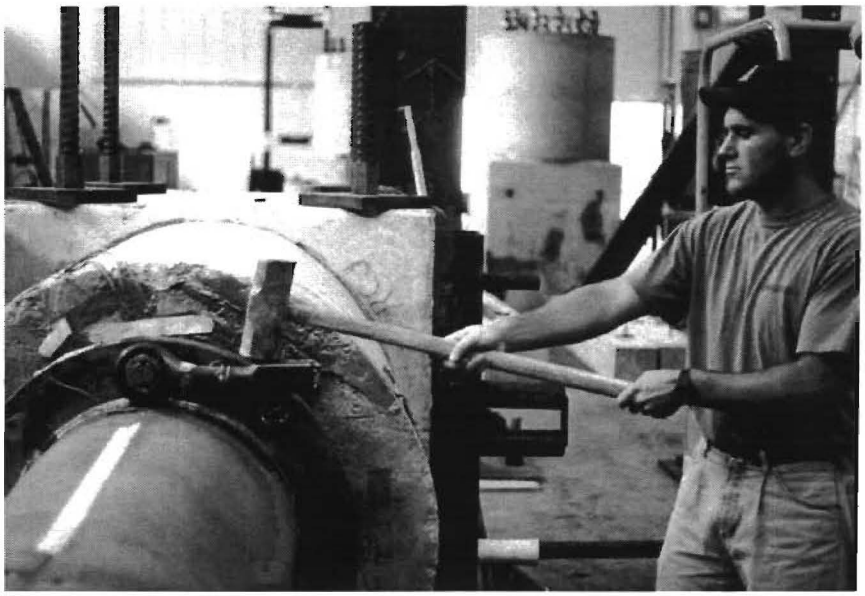

FIGURE 52 Photograph showing tightening with knocker wrench and sledgehammer.

Due to the constraints in the laboratory, bolt tightening was accomplished with the specimen in a horizontal orientation; therefore, the knocker wrench was swung through an arc in a vertical plane, turning the wrench about a horizontal axis, tightening some nuts on a downward swing and others on an upward swing. While this orientation is different than in the field, nut tightening was easily accomplished. Field tightening by turning the nuts through a vertical axis is not significantly different and is probably accomplished more easily. The advantage of impact tightening is obvious in either case; one person can tighten the nuts effectively in either instance. The only constraint of this method of tightening is the space needed to swing the sledge hammer. Nearby obstructions in the field could prevent application of this technique.

Static Tightening with Wrench and Cheater Pipe

Another method of tightening a nut past snug tight is to use a cheater pipe, which perhaps is the most commonly used method in the field. In this study, a 3 m (10 ft) steel pipe was used with a box wrench. The pipe is fitted over the end of the wrench and force is applied statically at the end of the cheater pipe. While this method of tightening is effective, it takes more than one person, or a significantly longer cheater pipe, to tighten the nuts in some cases. The horizontal orientation of the specimen made this method of tightening easier in the laboratory, where the cheater pipe was turned using the overhead crane. The overhead crane applied the necessary vertical force, but in most cases, more force was required than two or three people could apply horizontally in the field, due to limited traction.

Static Loading Tests

The objective of the static tests was to determine the relationship between the column base moment and the stresses in the anchor bolts, as a function of nut tightness. At several degrees of tightness, applied pole base moments and induced bolt stresses were computed from recorded anchor bolt strains. The static tests were also used to determine the nominal bending stresses induced at the welded connection from the pole to the base plate using a strain gage placed close to the weld.

Cyclic Loading Tests

The objective of the fatigue tests was to determine the equivalent AASHTO fatigue category classification of the bolt detail for each amount of nut tightness. The effect of nut tightness on fatigue life of the 4 1/2 UNC bolts was evaluated in fatigue tests at two degrees of tightness: snug tight and 60 degrees past snug tight. The results of these fatigue tests are discussed later.

Results of Tightening Studies

Tightening tests were performed on two COSS specimens to determine relations between nut rotation and preload and between torque and preload and to evaluate different tightening techniques. Two tightening techniques were studied: use of a long cheater pipe and use of a slug or knocker wrench. The method of tightening used in most of the tests was the 3 m (10 ft) cheater pipe. Because of the orientation of the specimen, the tightening tests were performed more easily with the cheater pipe and overhead crane. However, in the field, the best way for one person to tighten the nuts beyond snug tight is the use of a knocker wrench and a sledgehammer.

4 1/2 UNC Bolts

Preload Induced in Snug Tight Condition As the nuts were tightened to snug tight, the strains induced in the bolts were measured. After the completion of all the snug tight tests, the average axial stress in each of the five zones was recorded. Table 7 shows the results of the snug tight tests on the 4 1/2 UNC bolts. The snug tight condition induced a preload tensile stress of more than 35 MPa (5 ksi) in the region between the leveling nut and the top nut. The tension stress induced in the snug tight condition was consistent for the different bolts tested. However, the bending stress induced was not as consistent. Reasons for this variation are the tolerances allowed for bolt and nut fit and alignment of bolt to base plate. While the bolts were carefully aligned with a top template, and plumbed vertically, the hole tolerance in the top template allows for a slight misalignment of approximately 2 mm (1/16 in.). Figure 53 shows the stress distribution in the bolt caused by the snug tight condition.

Table 7 Stresses induced in snug tight condition in 4 1/2 UNC bolts

Zone	Average Axial Stress MPa (ksi)	Standard Deviation MPa (ksi)	Average Bending Stress MPa (ksi)	Standard Deviation MPa (ksi)
1	6.9 (1.0)	6.1 (0.88)	22.8 (3.3)	13.1 (1.9)
2	27.9 (4.0)	5.9 (0.85)	41.4 (6.0)	20.0 (2.9)
3	36.5 (5.3)	7.0 (1.01)	40.0 (5.8)	26.9 (3.9)
4	35.2 (5.1)	8.2 (1.19)	37.2 (5.4)	29.0 (4.2)
5	20.7 (3.0)	8.6 (1.25)	24.8 (3.6)	11.7 (1.7)

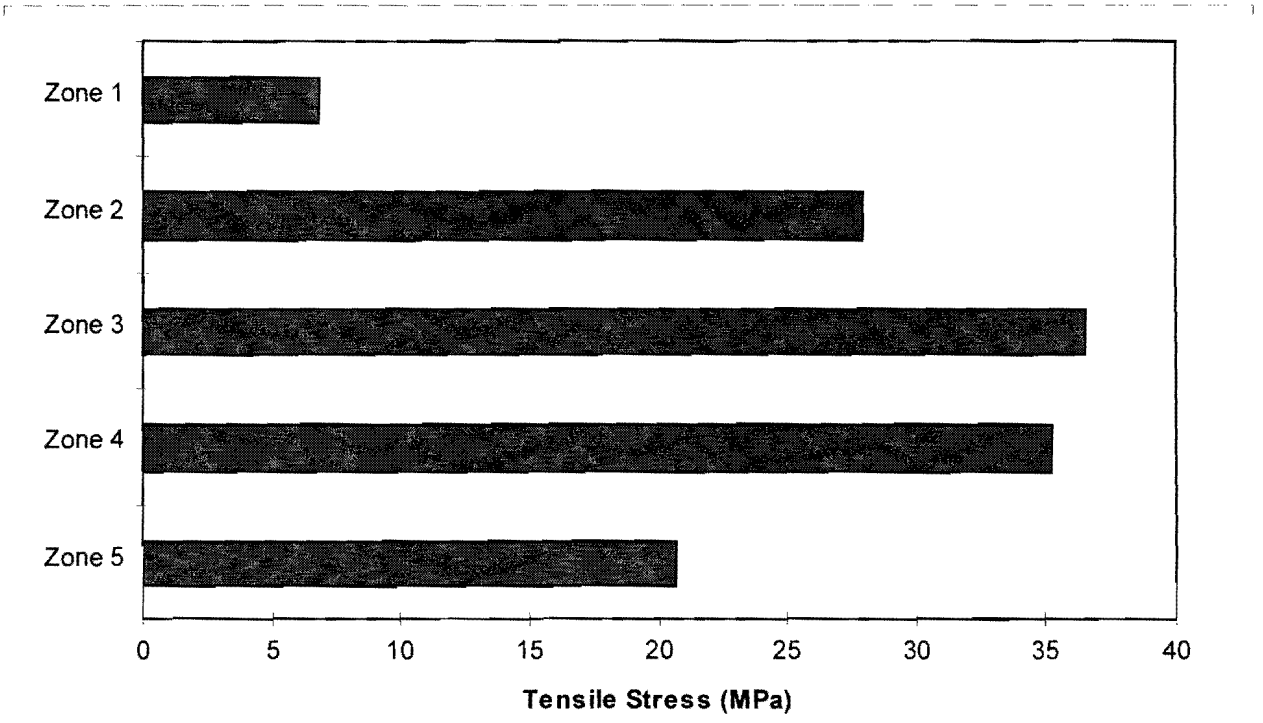

Figure 53 Axial stresses induced in snug tight condition, 4 1/2 UNC bolt.

Tightening to 30 Degrees Past Snug Tight The strains were measured while turning the nuts to 30 degrees past snug tight. The 30 degree past snug tight condition induced approximately a 159 MPa (23 ksi) preload stress. The data had considerable scatter for the different bolts, as the

high standard deviation of the data shows. Figure 54 the stress distribution in the bolt at 30 degrees past snug tight.

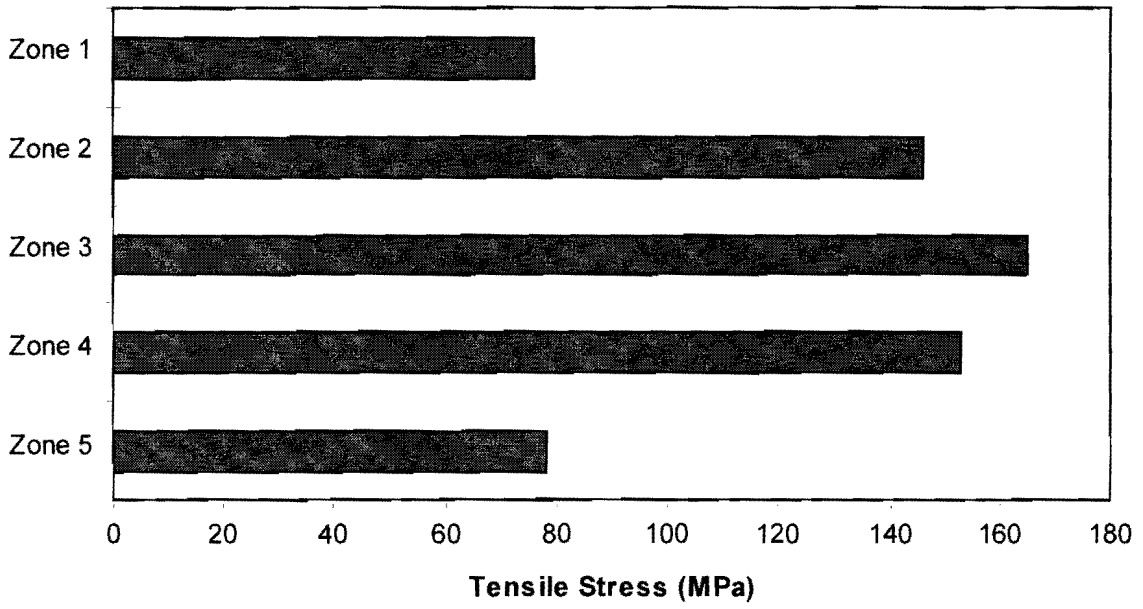

Figure 54 Axial stresses induced by turning 30 degrees past snug tight condition, 4 1/2 UNC bolt.

Tightening to 60 Degrees Past Snug Tight The strains were measured while turning the nuts to 60 degrees past snug tight. Figure 55 shows an example of the stresses induced in the five zones of the bolt during tightening. After the completion of all the tightening tests to 60 degrees past snug tight, the induced stresses were averaged in each of the five zones. Table 8 and Figure 56 show the results of the 60 degrees past snug tight tests on the 4 1/2 UNC bolts. The 60 degree past snug tight condition induced a maximum stress of approximately 470 MPa (68 ksi). This preload is 65 percent of yield. The data had considerable scatter for the different bolts, as the high standard deviation in the data indicates.

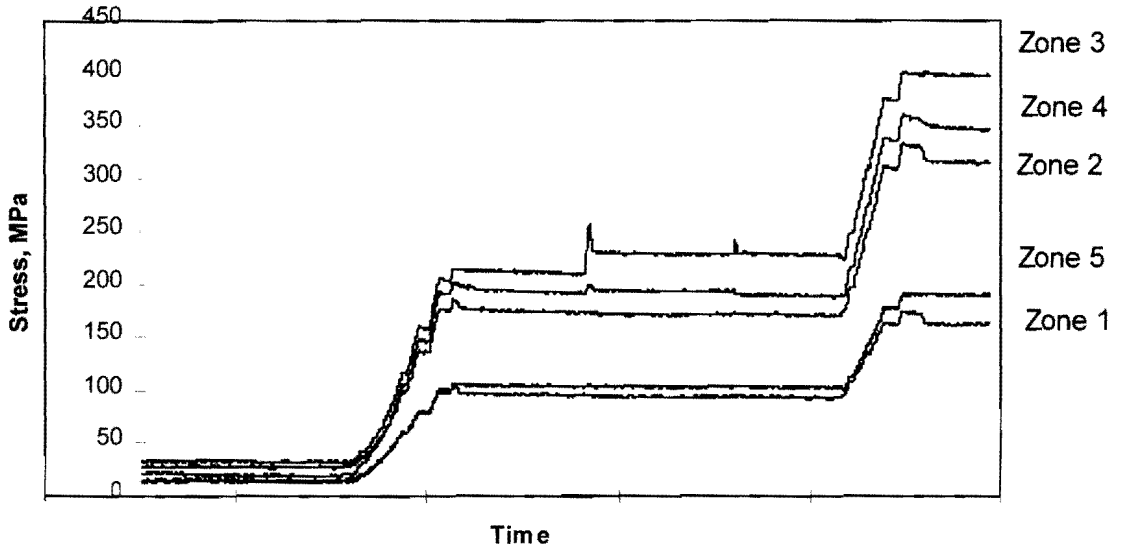

Figure 55 Axial tension stresses induced during tightening to 60 degrees past snug tight, 4 1/2 UNC bolts.

Table 8 Stresses induced at 60 degrees past snug tight, 4 1/2 UNC bolts

Zone	Average Tensile Stress MPa (ksi)	Standard Deviation MPa (ksi)	Average Bending Stress MPa (ksi)	Standard Deviation MPa (ksi)
1	150 (21.8)	47 (6.8)	-5 (-0.7)	36 (5.2)
2	354 (51.3)	71 (10.3)	30 (4.3)	29(4.2)
3	478 (69.3)	69 (10.0)	25 (3.6)	29 (4.2)
4	460 (66.7)	71 (10.3)	21 (3.0)	52 (7.6)
5	256 (37.2)	35 (5.1)	-48 (-6.9)	16 (2.3)

Using the three degrees of tightness tested, a relation between degree of rotation past snug tight and the axial stress induced can be graphed. Figure 57 shows this nonlinear relationship.

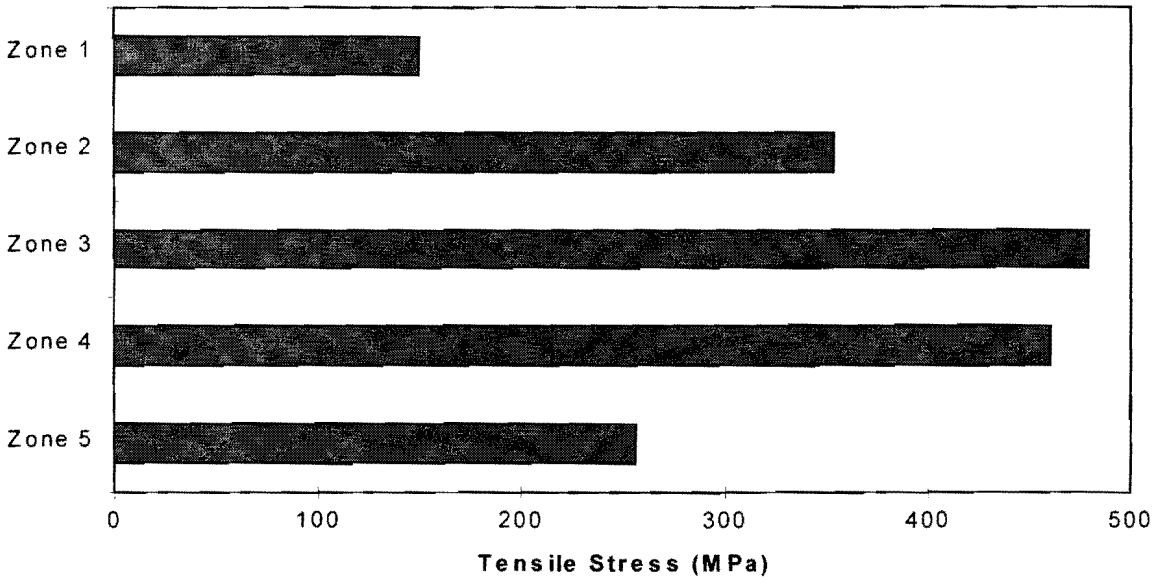

Figure 56 Tensile stresses induced at 60 degrees past snug tight, 4 1/2 UNC bolts.

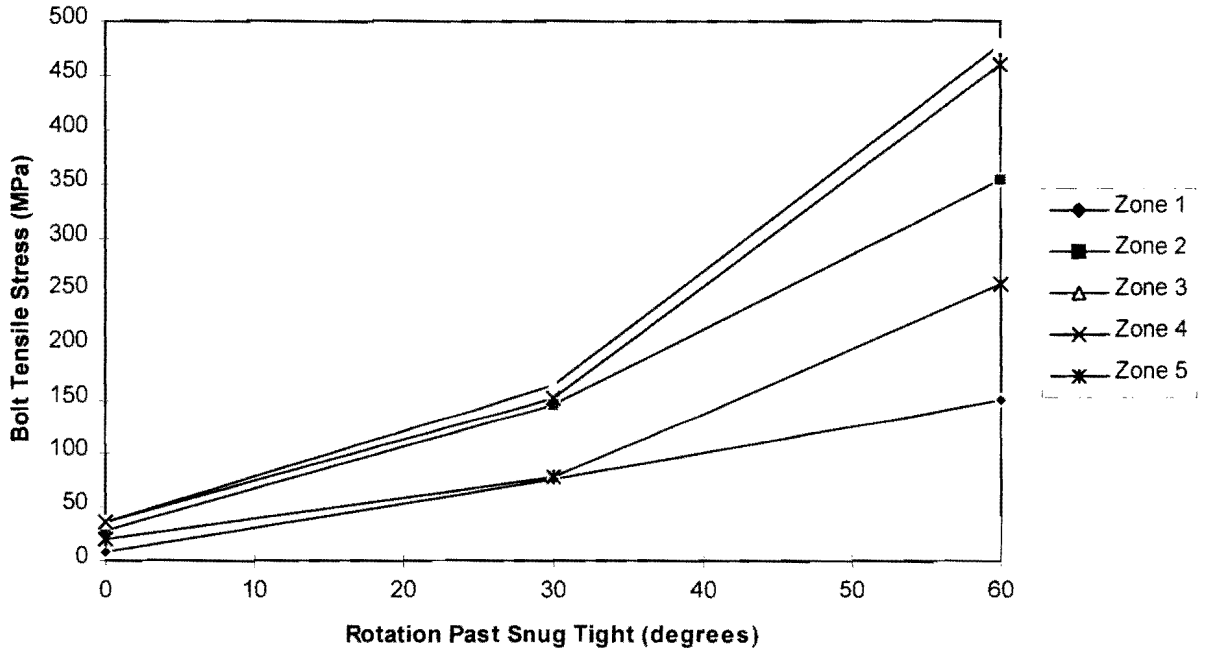

Figure 57 Relation between the rotation of the nut and induced tensile stress in the five zones instrumented--4 1/2 UNC bolt.

It is important to note that the 4 1/2 UNC bolts were grade 105 steel, with a specified minimum yield strength of 725 MPa (105 ksi). These results indicate that 4 1/2 UNC grade 55 bolts, with yield strength of 380 MPa (55 ksi), would yield when tightened to 60 degrees past snug tight.

8 UN Threads

Snug Tight Condition As the nuts were tightened to snug tight as described above, the strains induced in the bolts were measured. After the completion of all the snug tight tests, the stresses induced were averaged in each of the five zones. Table 9 shows the results of the snug tight tests on the 8 UN threaded bolts. The stresses induced in the 8 UN threaded bolts at snug tight were close to the stresses induced in the 4 1/2 UNC threaded bolts at snug tight. The maximum axial stress induced in the 8 UN threads was about 3 MPa (0.5 ksi) less than that of the 4 1/2 UNC threaded bolts. The stress distribution in the bolt caused by the snug tight condition can more easily be seen in the bar graph in Figure 58.

Table 9 Stresses induced in snug tight condition, 8 UN bolts

Zone	Average Tensile Stress MPa (ksi)	Standard Deviation MPa (ksi)	Average Bending Stress MPa (ksi)	Standard Deviation MPa (ksi)
1	10 (1.5)	6 (0.9)	5 (-0.7)	13 (1.9)
2	19 (2.7)	10 (1.4)	-16 (-2.3)	35 (5.3)
3	30 (4.4)	6 (0.9)	13 (-1.9)	54 (7.9)
4	31 (4.5)	8 (1.2)	12 (-1.8)	54 (7.8)
5	21 (3.1)	6 (0.8)	24 (-3.5)	61 (8.9)

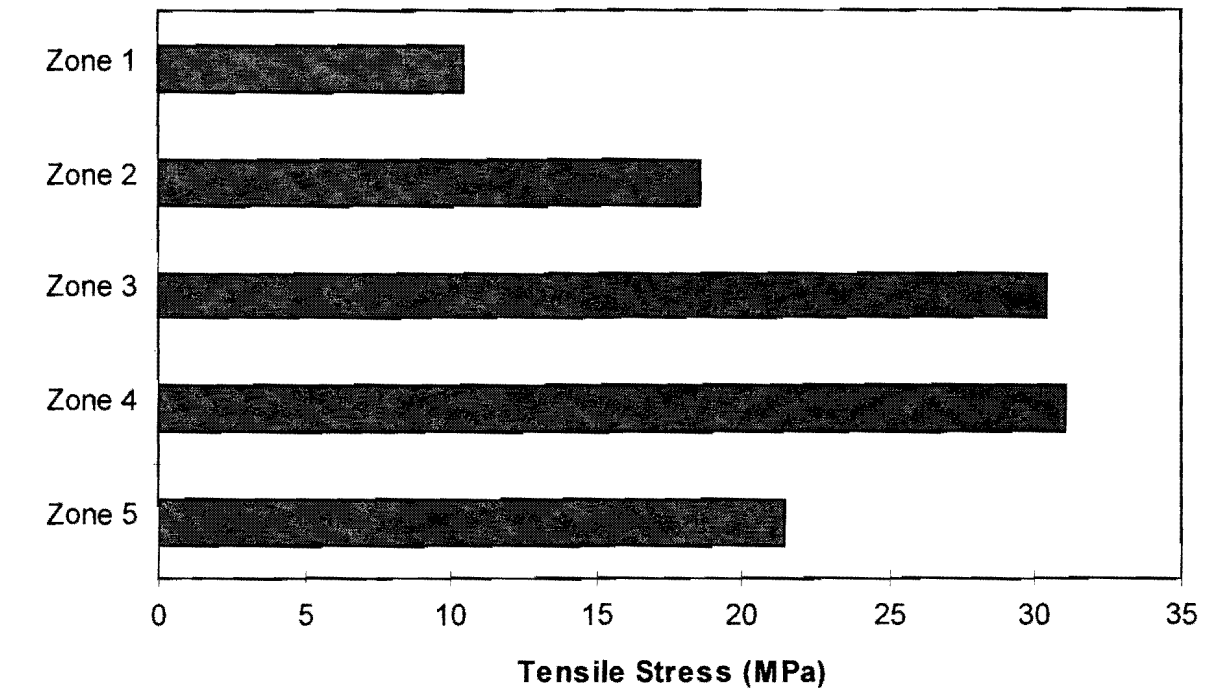

Figure 58 Axial stresses induced at snug tight condition, 8 UN bolts.

The axial stress induced by snug tight was consistent for the different bolts tested. However, the stresses increased slightly from one test to the next. For example, in the first test of bolt A, the maximum stress was 22 MPa (3.2 ksi), while the maximum stress for trial 3 was 30 MPa (4.4 ksi). This increase in stress per trial can be seen in Figure 59.

From Figure 59, it can be seen that the tensile stress induced in the bolt in the region between the double nuts tends to increase with each tightening. This increase is thought to be attributed to the fact that each trial lubricates the threads more thoroughly and crushes and straightens any imperfections in the nuts and bolts, causing a more efficient snug tight condition. The zinc coating was inspected after each snug tight test with a 10X magnifying glass, and no crushing or cracking was noticed.

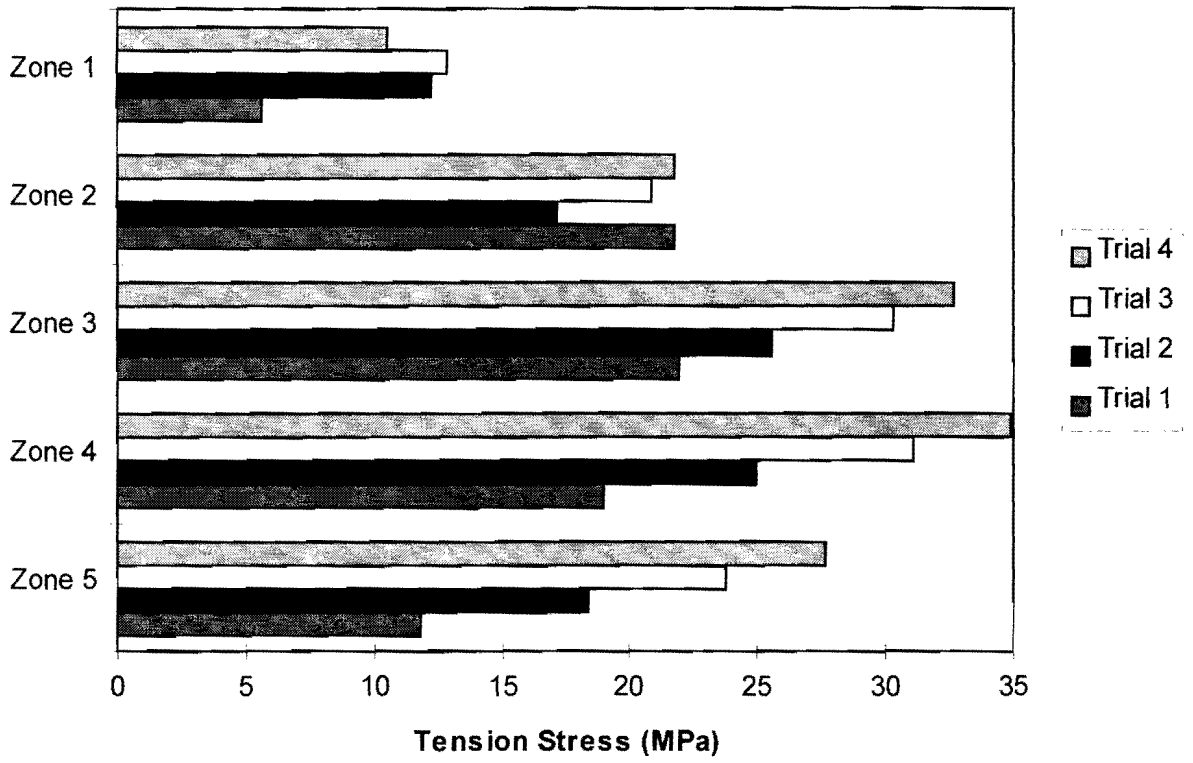

Figure 59 Induced preload stresses for repeated tightening trials, 8 UN bolts.

Also, researchers noticed that the induced bending stress did not increase from trial to trial. No pattern was found in the differences from trial to trial. However, the bending stresses induced were more variable from bolt to bolt. The most likely explanation for this variation is the potential bolt-to-bolt variation in alignment of bolt to base plate. Even though the bolts were carefully aligned using top and bottom templates, the hole tolerance in the templates allows for a slight misalignment. This potential misalignment is minimal, probably less than 0.004 mm/mm.

30 Degrees Past Snug Tight The strains in the bolts were measured while the nuts were turned 30 degrees past snug tight. The axial stresses induced in the bolt increased with each repeated tightening trial. For example, for Bolt E, in the first trial to 30 degrees past snug tight, the

maximum tensile stress induced in the bolt is 96 MPa (13.9 ksi). In trial 2, the same rotation induced 144 MPa (20.9 ksi). In the final trial, the maximum axial stress was 152 MPa (22 ksi). Figure 60 shows the difference between each consecutive trial.

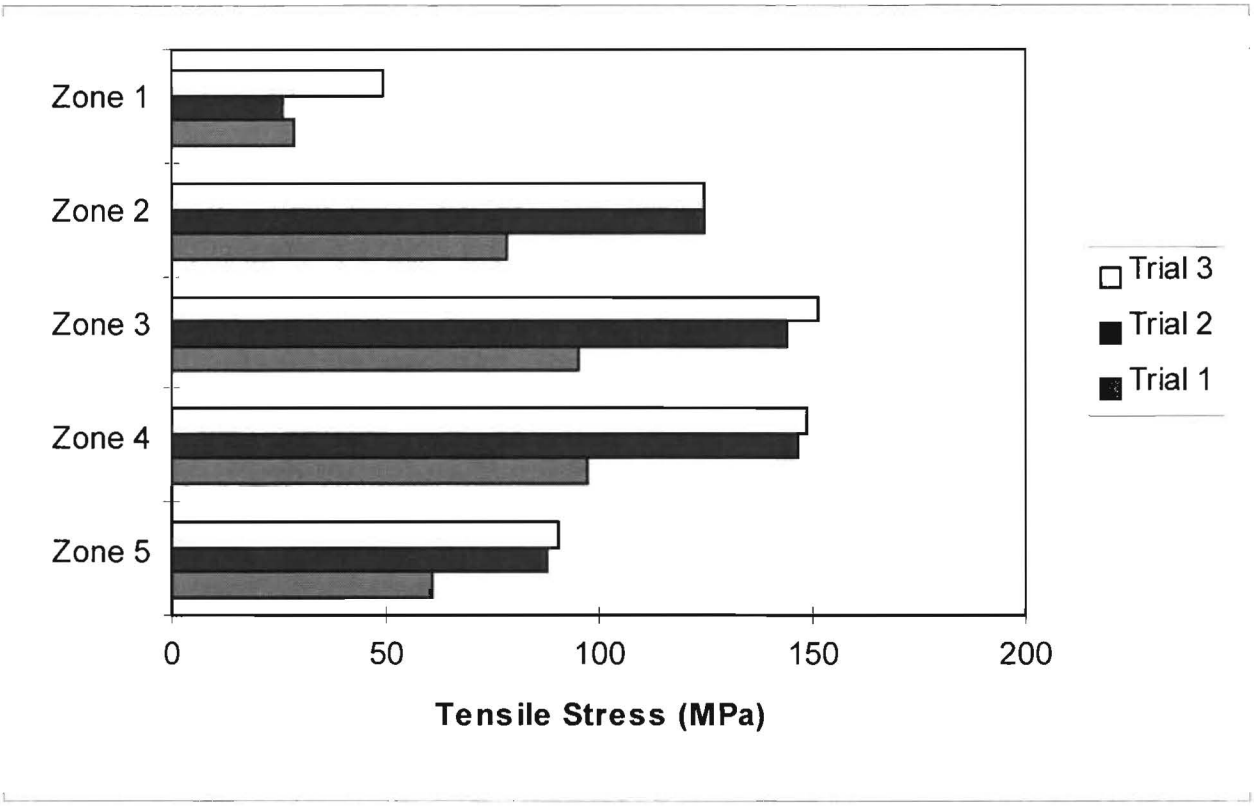

Figure 60 Induced axial stresses in repeated tightening to 30 degrees past snug tight condition, 8 UN bolts.

The maximum tensile stresses induced were considerably higher after the second and third tests. This increase in stress for the same amount of nut rotation is attributed to an increased nut rotation in the snug tight condition in repeated tightenings, resulting from improved lubrication and smoothing of thread irregularities with repeated tightening. In all tightening tests, the angle of rotation was measured from the snug tight reference. If a larger rotation occurs when reaching the snug tight condition in subsequent trials, a greater prestress would be obtained when the nut is turned an additional 30 degrees.

60 Degrees Past Snug Tight The strains in the bolts were measured while the nuts were rotated 60 degrees past the snug tight position. Again it was noticed that the maximum stresses induced in the bolt increased with each tightening trial. For example, for Bolt E, in the first trial to 60 degrees past snug tight, the maximum tensile preload stress induced in the bolt was 192 MPa (28 ksi). In trial 2, the tensile stress induced was 248 MPa (36 ksi), and in the final trial, the stress induced was 299 MPa (43 ksi). The difference between each consecutive trial can be seen in Figure 61. For this test, the tensile stress induced increased with each tightening trial. Unlike the 30 degree tests, there is also a large difference between the second and third trials. Again, one reason for this increase in stress for the same amount of nut rotation could be the variation in preload tightness obtained in the snug tight condition.

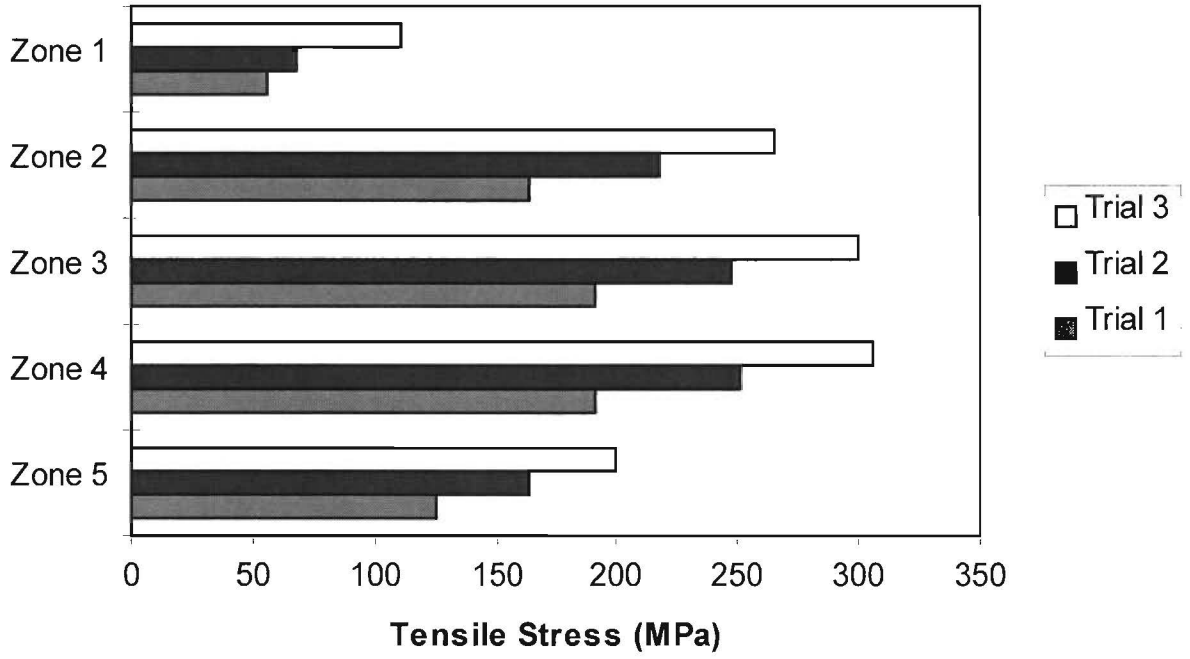

Figure 61 Measured preload stress in consecutive trials to 60 degrees past snug tight, 8 UN bolts.

Using the three degrees of tightness tested, a relation between degree of rotation past snug tight and the tensile stress induced in the region between the nuts can be graphed. Figure 62 shows this relation to be non-linear. The tensile stress in the region between the nuts for each level of tightness would be expected to fall between the two curves.

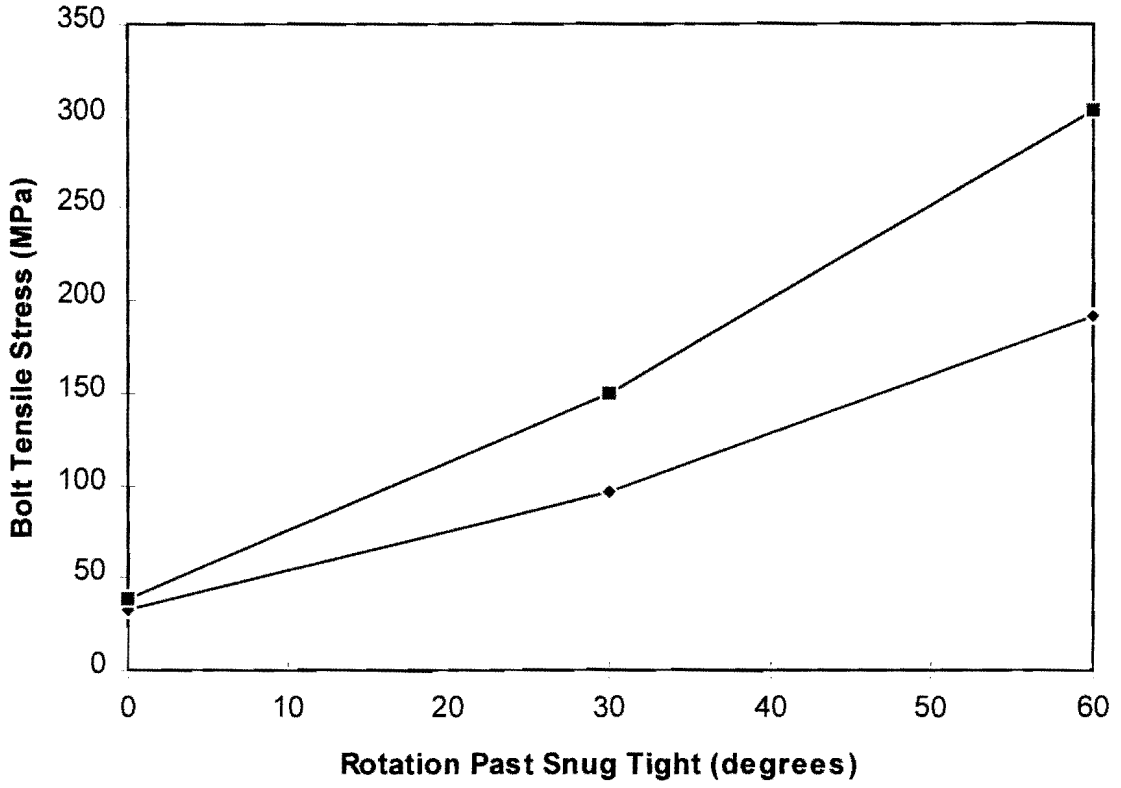

Figure 62 Relationship between axial prestress and nut rotation, 8 UN bolts.

90 Degrees Past Snug Tight When the 8 UN threaded bolts were tightened to 90 degrees past snug tight, the bolts yielded. The initial test plan called for tightening the nuts to 90 and 120 degrees past snug tight. However, the supplier shipped grade 55 anchor bolts instead of the specified grade 105 bolts. This error was not discovered until the specimens were built and in the process of testing. It is expected that the preload induced from 60 degrees past snug tight on the grade 55 bolts would be the same as for the grade 105 bolts. However, the grade 105 bolts could be tightened further without yielding. The yielding that occurred was local and was barely noticed during the removal of the nuts. The nuts were "sticky" when turned over the region of the bolt that yielded. The yielding did not appear to shorten significantly the fatigue life of the bolt. The section on fatigue results will discuss this.

Torque Requirements in the Tightening Procedure

4 1/2 UNC Bolts

The tightening torque was measured as described above. The nuts were taken to snug tight and then marked for the angle of rotation desired. For the 4 1/2 UNC threads, the nuts were turned to 60 degrees past snug tight in two equal stages. The nut was rotated approximately 30 degrees on the first stage, and the remaining angle of rotation in the second stage. Figure 63 shows maximum induced preload stress as a function of applied torque in a single representative test.

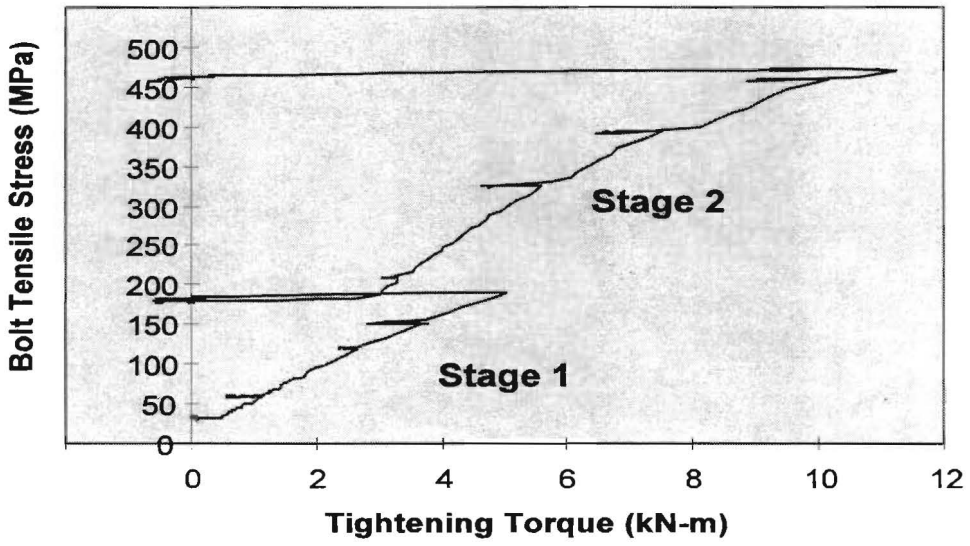

Figure 63 Relationship between axial prestress and applied torque, 4 1/2 UNC bolt.

As Figure 63 shows, the torque needed to rotate the nut drops off when the tightening procedure is stopped and restarted. There is bolt-to-bolt variation, and there is no unique relationship for any given bolt. Thus, it is impractical to try to ensure a specific prestress by calling for a specified torque. Also, it can be seen that the torque is a nonlinear function of axial stress. This shows that an increasing torque is needed for small increases in preload. Table 10 shows the results of all the tightening tests on 4 1/2 UNC bolts. To calculate the maximum average tensile stresses, the stresses measured in Zones 3 and 4 were averaged in each trial.

Table 10 Average torque and induced prestress at 60 degrees past snug tight, 4 1/2 UNC bolts

	Trial No.	Tightening Torque 10^6 N•mm (ft-lb)	Average Maximum Axial Stress in Bolt MPa (ksi)
Bolt C	1	6.81 (5,025)	440 (63.8)
	2	6.56 (4,835)	605 (82.7)
	3	5.05 (3,721)	408 (59.1)
Bolt E	1	9.14 (6,744)	373 (54.0)
	2	15.23 (11,231)	486 (70.4)
	3	18.32 (13,514)	539 (78.1)
Bolt G	1	10.62 (7,832)	549 (79.6)
	2	10.58 (7,806)	427 (61.9)
	3	11.23 (8,284)	432 (62.6)

When using the turn of the nut method, it was expected that once a nut was taken to 60 degrees past snug tight and subsequently loosened, the torque needed to re-tighten the nut might decrease because the threads become more thoroughly lubricated while tightening, due to crushing and straightening of any thread imperfections. This phenomenon was not observed in these tightening tests, however. In the first bolt tested, the torque did decrease for each trial, but the resulting tensile stress was highly variable. In the second bolt tested, the torque increased from each test, almost doubling from the first test to the second, while the stress induced also increased. In the third bolt tested, the tightening torque did not change significantly, while the stress induced dropped from the first and second tests. As is well known in the structural bolting industry, torques required to tighten are observed to vary significantly even for the same types of bolts.

The torque needed to loosen the nut after the fatigue tests was also measured in an attempt to determine whether the nuts had loosened during the test or if the preload in the bolt changed and to determine whether this technique might be used as a field inspection of nut tightness. To compare the torque needed to remove the nut to that needed to tighten the nut before cyclic loading, the tightening torque was measured before the test, and the loosening torque was measured after the specimen endured over two million cycles of fatigue loading. The

torque needed to remove the nut was less than that needed to tighten the nut to 60 degrees past snug tight. An example of this is shown in Figure 64. The two series show the tightening and loosening torque. The tightening torque is almost twice the loosening torque in this example. The loosening torque was highly variable. However, the nuts' locations were carefully marked before the fatigue test began, and the nuts showed no loosening rotation in any of the tests. Also, the stresses measured in the bolt did not decrease throughout the test.

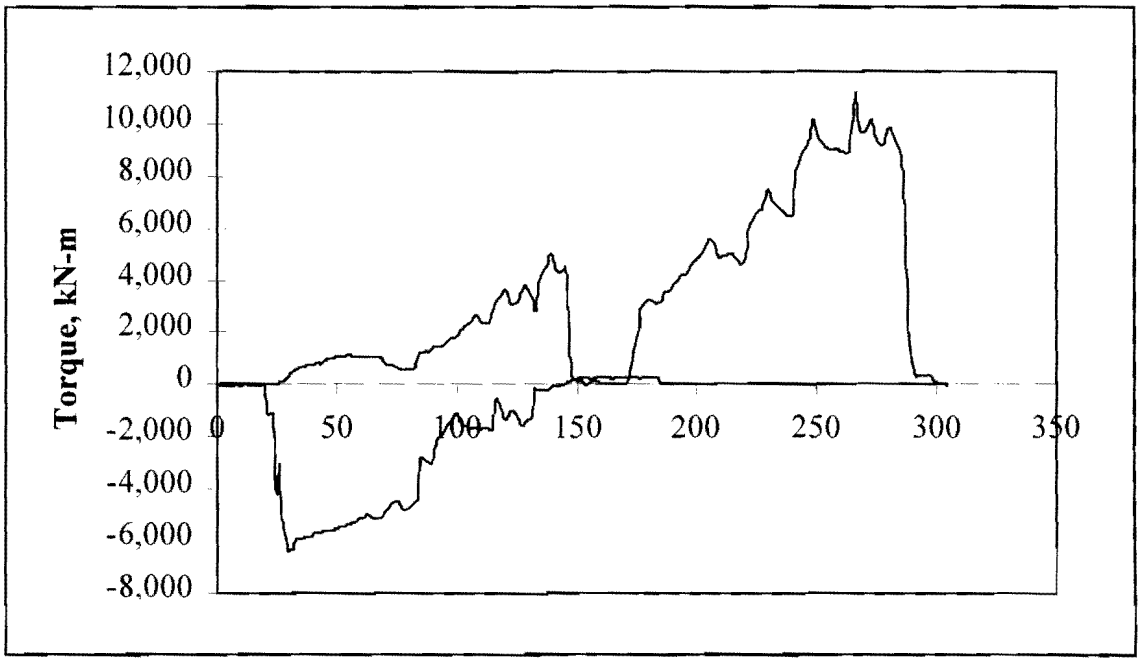

FIGURE 64 Torque required to loosen nut compared to tightening torque--4 1/2 UN.

8 UN Bolts

The torque required to tighten the nuts on the 8 UN threaded bolts was not measured due to equipment failure. These bolts were grade 55 steel, and could not be tightened to 60 degrees past snug tight without yielding. One person on a 3 m (10 ft) cheater pipe, with the bolt axis horizontal in the lab, developed the torque needed to tighten the nut to 60 degrees past snug tight. One person using a 3 m (10 ft) cheater pipe loosened the nuts, but the loosening torque was not measured.

Static Test Results

Once the specimen was in place and the pole was installed, the hydraulic actuator was connected to the pole. The static tests consisted of two parts. The first was to relate the pole base resultant moment to the bolt stresses. This relationship is used to determine the loads needed for the fatigue tests. The second part of the test was to study the effect of the bolt preloads on the cyclic live load stresses induced in the bolts from the column base moment.

Selection of Test Load

The column base resultant moments expected to induce desired test stresses in the bolts were calculated using the equivalent moment of inertia method. The loads and stresses calculated from this method were then compared with the static load tests of the specimen. In order to record the stresses in the bolts from just the column base moment, the bolts were not tightened enough to induce a preload stress. The nuts were tightened with a wrench just to the point of solid contact with the base plate but not to the snug tight condition. Static loads were then applied to the pole. Figure 65 shows the calculated stresses and measured stresses as functions of the column base moment. This figure shows that the calculated stresses match almost perfectly with the experimental stresses. This data was used to find the loads needed to induced the desired stress ranges in the fatigue tests.

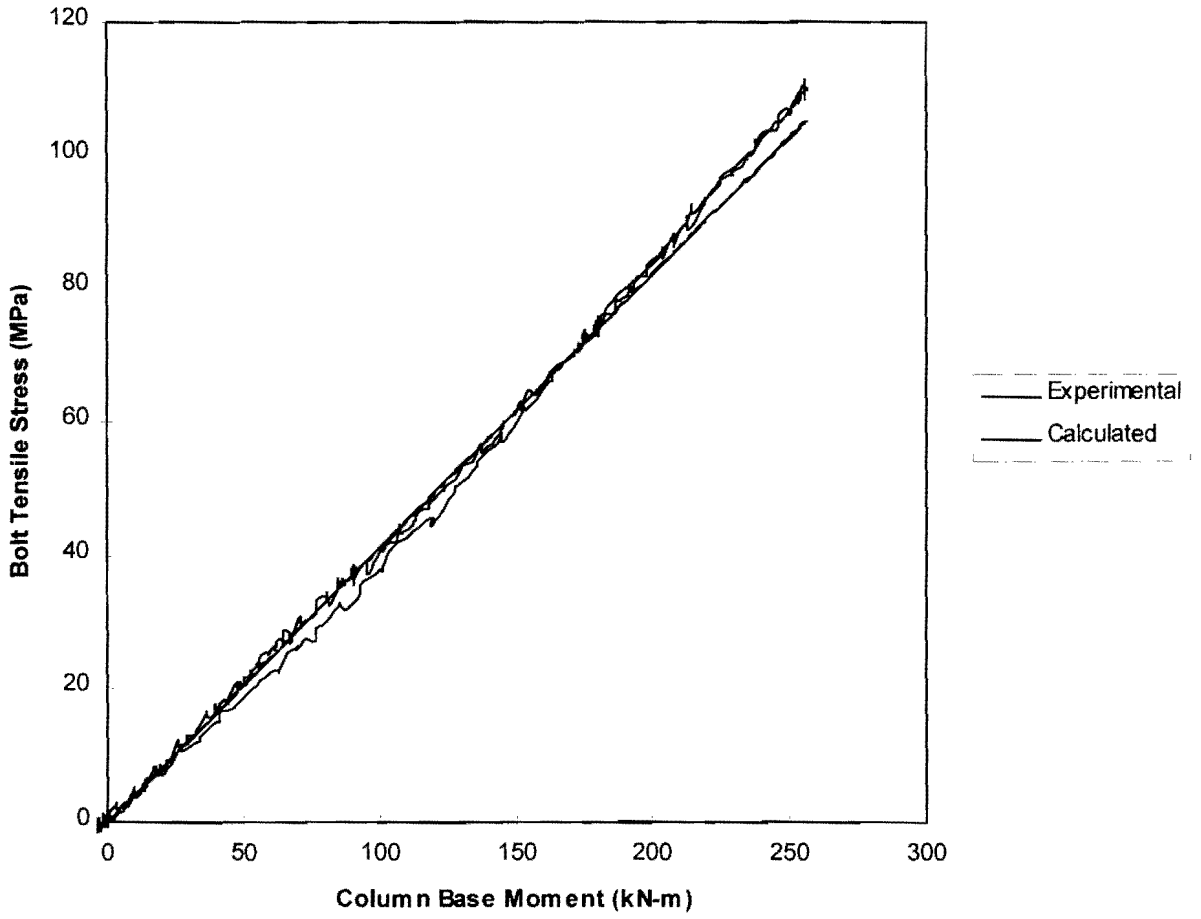

Figure 65 Relationship of maximum anchor bolt stresses to column base moment, 8 bolt pattern.

Pole to Baseplate Weld

A strain gage was placed as close to the weld from the pole to the base plate as possible to determine the nominal bending stresses in the vicinity of the weld caused by the pole base moment. Figure 66 shows the relationship between the pole base moment and the stresses in the top, and most critical, portion of the weld. This relationship is also linear. Therefore, once the pole base moment is known, the stresses in the weld can be found or vice versa. Because this is symmetric base, the compressive stresses can be interpolated from Figure 66.

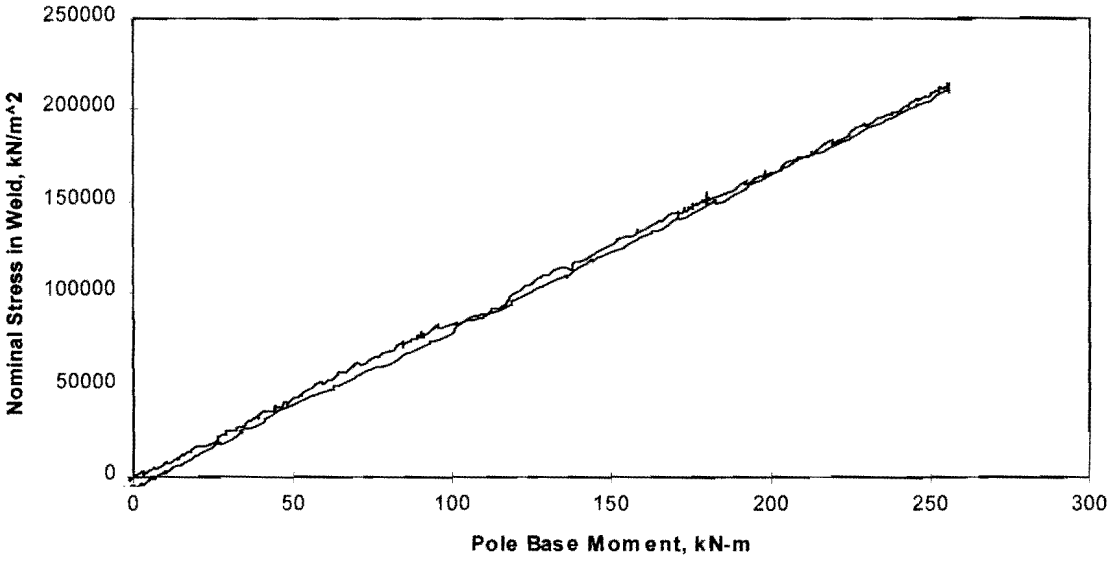

FIGURE 66 Measured pole-to-baseplate weld stresses as a function of column base moment, COSS.

When comparing Figures 65 and 66, it can be seen that the weld has a higher stress per pole base moment than the anchor bolts. For example, a 162,800 kN-mm (120 kip-ft) pole base moment caused a 140 MPa (19.5 ksi) stress in the weld and a 70 MPa (10 ksi) stress in the critical bolt. This weld detail is a Category C detail at best. These results would suggest that the weld is the critical connection of this anchorage system, an observation that was borne out in subsequent fatigue tests.

Effect of Preload on Bolt Stresses Induced by Column Base Moment

To determine the effect of bolt preload on the stresses induced by the column base moment, the nuts were turned to three different tightnesses: snug tight, 30 degrees past snug tight, and 60 degrees past snug tight. For each different degree of tightness, the pole was statically loaded. Figures 67, 68, and 69 show the stresses induced in the bolts from the pole base moment for the three different cases. These figures show that the live load stresses induced in the bolts due to the column base moment are reduced when the nuts are tightened.

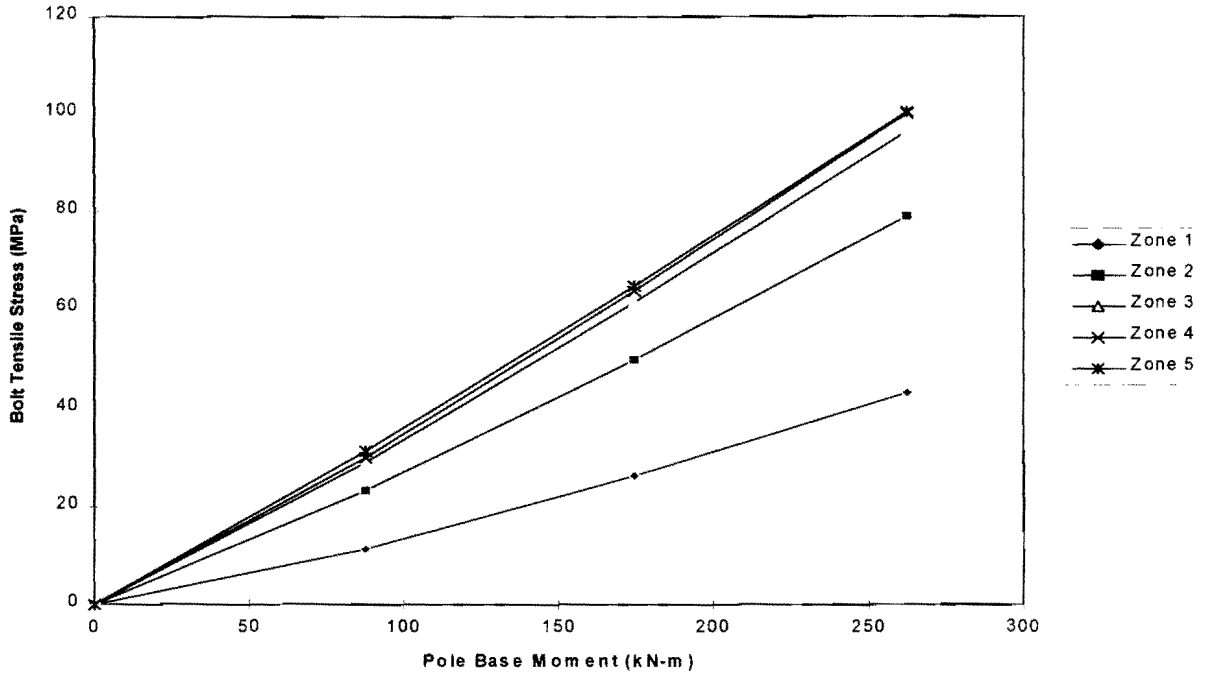

Figure 67 Relationship of critical COSS anchor bolt stresses and column base moment, snug tight condition.

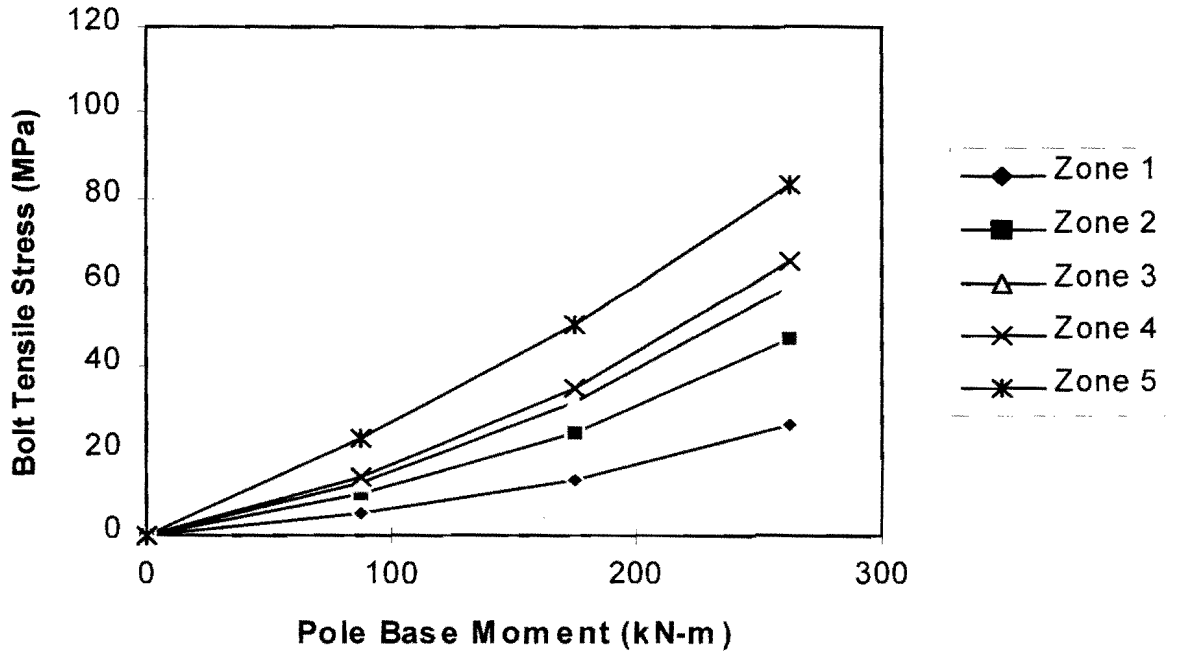

Figure 68 Relationship of COSS anchor bolt stresses to column base moment, 30 degrees past snug tight.

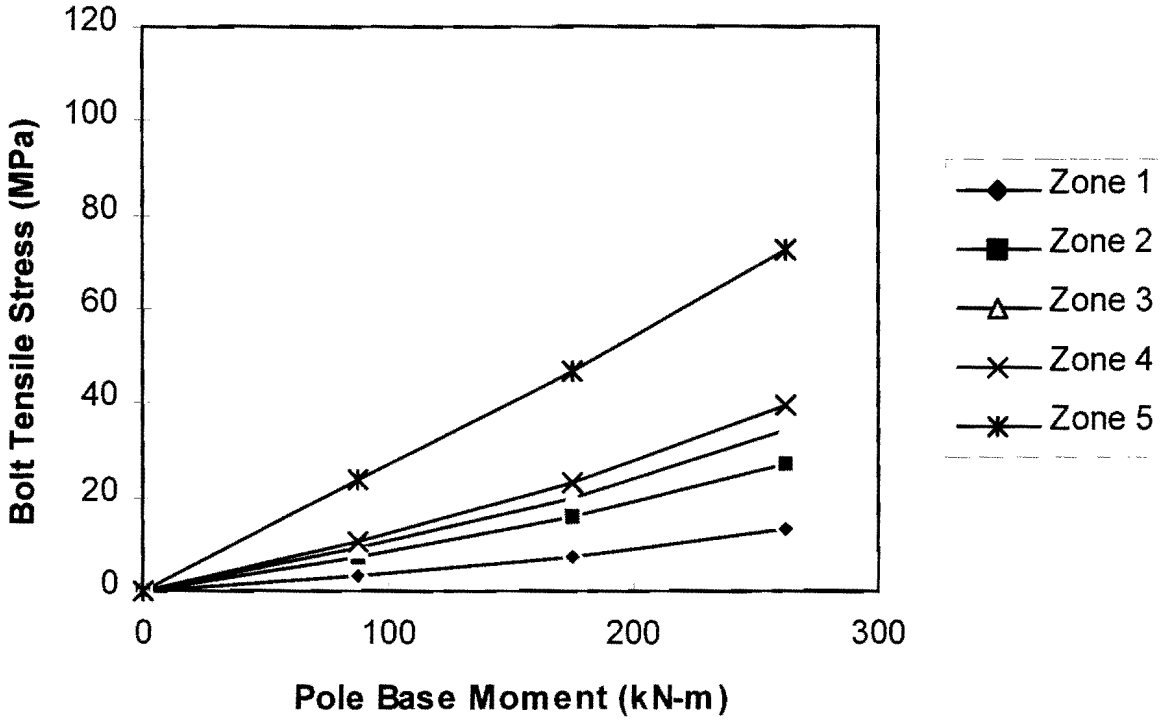

Figure 69 Relationship of COSS anchor bolt stresses to column base moment, 60 degrees past snug tight.

From these graphs, it can be seen that the more the nut is tightened, the lower the peak stress induced from the pole base moment. The zones that benefit the most from the preload are Zones 3 and 4, the region between the two nuts. It also can be seen that the zone that receives the highest stress is Zone 5, which is more susceptible to the stresses caused from the pole base moment.

Fatigue Test Studies

Three fatigue tests were conducted to study the effect of nut tightness on fatigue life of the 4 1/2 UNC bolts. In the first fatigue test, the nuts were tightened to 60 degrees past snug tight

condition. In the second fatigue test, the specimen was rotated 90 degrees so that the bolts originally on the neutral axis, which were not loaded during the first test, were oriented to carry the applied column base moments. After completion of this test, a third fatigue test was completed with the nuts loosened and retightened to a snug tight condition.

The stress range selected for the first fatigue test was 69 MPa (10 ksi). Previous research (Frank 1978) indicates that this connection, when tightened to 60 degrees past snug tight, can be classified as a Category C detail. However, according to a Lehigh study of the Michigan COSS bolts that failed (Fisher 1990), the service stress range that caused the failure was estimated to be approximately 69-83 MPa (10-12 ksi). In the present study, the 69 MPa (10 ksi) stress range was selected for the initial test based on preliminary data from field tests, which indicated that constant amplitude tests at this stress range would be a conservative approximation of an upper bound of actual wind loadings.

With the test stress range fixed, the mean loading was selected to cause peak stresses in the top bolt of 52 MPa (7.5 ksi) tensile and 17 MPa (2.5 ksi) compression. The bottom bolt peak stresses are reversed. The top bolt was used to model the bolt on the side away from traffic, considered to be the critical bolt in the connection, because of the mean stress corresponding to the weight of the cantilever arm in the COSS.

4 1/2 UNC Bolts

The 4 1/2 UNC nuts were tightened to 60 degrees past snug tight in the first test. The top and bottom bolts were loaded with a 70 MPa (10 ksi) stress range. The 17 MPa (2.5 ksi) mean tensile stress in the bottom bolt was chosen to simulate the bolt on the side opposite the cantilever by approximating dead load offset caused by the cantilever arm. With the top and bottom bolts having a 70 MPa (10 ksi) stress range, a 49 MPa (7.1 ksi) stress range was induced in the adjacent bolts in the 8-bolt pattern. Table 11 shows the stress range, mean stress and number of cycles on each bolt for the first fatigue test.

Table 11 Loading applied in first fatigue test of 4 1/2 UNC bolts

Bolt	Stress Range, σ_R MPa (ksi)	Mean Stress, σ_M, MPa (ksi)	Number of Cycles
A	69.0 (10.0)	-17.3 (-2.5)	2,156,023
B	49.0 (7.1)	-12.4 (-1.8)	2,156,023
C	0.0 (0.0)	-	-
D	49.0 (7.1)	12.4 (1.8)	2,156,023
E (critical)	69.0 (10.0)	17.3 (2.5)	2,156,023
F	49.0 (7.1)	12.4 (1.8)	2,156,023
G	0.0 (0.0)	-	-
H	49.0 (7.1)	-12.4 (-1.8)	2,156,023

No bolt failures were observed in the first fatigue test. However, the pole-to-baseplate weld failed twice. When a crack in the weld was discovered, the pole was removed, the weld was repaired, the pole was reinstalled in the fatigue test apparatus, and the fatigue test was continued. The pole-to-baseplate weld failures will be discussed in a following section. After the first fatigue test, all bolts were ultrasonically inspected for cracks. No cracks were detected.

For the second fatigue test, the specimen was rotated 90 degrees so that the bolts that were on the neutral axis during the first test carried the column base moments. The same mean stress and stress ranges used in the first test were applied in the second test. The bolts that were on the neutral axis had zero fatigue cycles at the beginning of the test. However, the adjacent bolts (B, D, F, and H) were also on the 45 degree plane in the second test. Therefore, the cycles from the second test were additive to the cycles in the first test on these bolts.

Table 12 shows the results after the second fatigue test. Because fatigue cycles are additive, this table shows all cycles on the bolts. Bolts A, C, E, and G only have cycles from one test because each bolt was on the neutral axis for the first test. Notice that bolts B, D, F, and H have cycles added from the first test.

Table 12 Results after second fatigue test on 4 1/2 UNC bolts; bolt C is critical

Bolt	σ_R, MPa (ksi)	Number of Cycles @ σ_M
A	0 (0)	2,156,023 @ σ_M =-17 MPa (-2.5 ksi)
B	49 (7.1)	2,156,023 cycles @ σ_M = -12 MPa (-1.8 ksi) and 2,001,320 cycles @ σ_M = 12 MPa (1.8 ksi)
C (critical)	69 (10)	2,001,320 @ @ σ_M = 17 MPa (2.5 ksi)
D	49 (7.1)	4,157,343 @ σ_M = 12 MPa (1.8 ksi)
E	0 (0)	2,156,023 @ σ_M = 17 MPa (2.5 ksi)
F	49 (7.1)	2,156,023 @ σ_M = 12 MPa (1.8 ksi) and 2,001,320 @ σ_M = -12 MPa (-1.8 ksi)
G	69 (10)	2,001,320 @ σ_M = -17 MPa (-2.5 ksi)
H	49 (7.1)	4,157,343 @ σ_M = 12 MPa (-1.8 ksi)

No anchor bolt failures occurred in the second fatigue test. After this fatigue test, all bolts were ultrasonically inspected for cracks. No cracks were detected on any bolt. At the conclusion of these two fatigue tests, four bolts had accumulated over two million cycles at a 70 MPa (10 ksi) stress range, and four bolts had accumulated over 4 million cycles at a 49 MPa (7.1 ksi) stress range. These points are plotted in Figure 70, with S-N curves representing AASHTO design categories C, D, and E. Each data point in Figure 70 represents two bolts.

The third fatigue test was a continuation of the second test, with the same anchor bolt configuration and loadings, but the nuts were loosened and retightened to snug tight only. Table 13 shows the results after the third fatigue test.

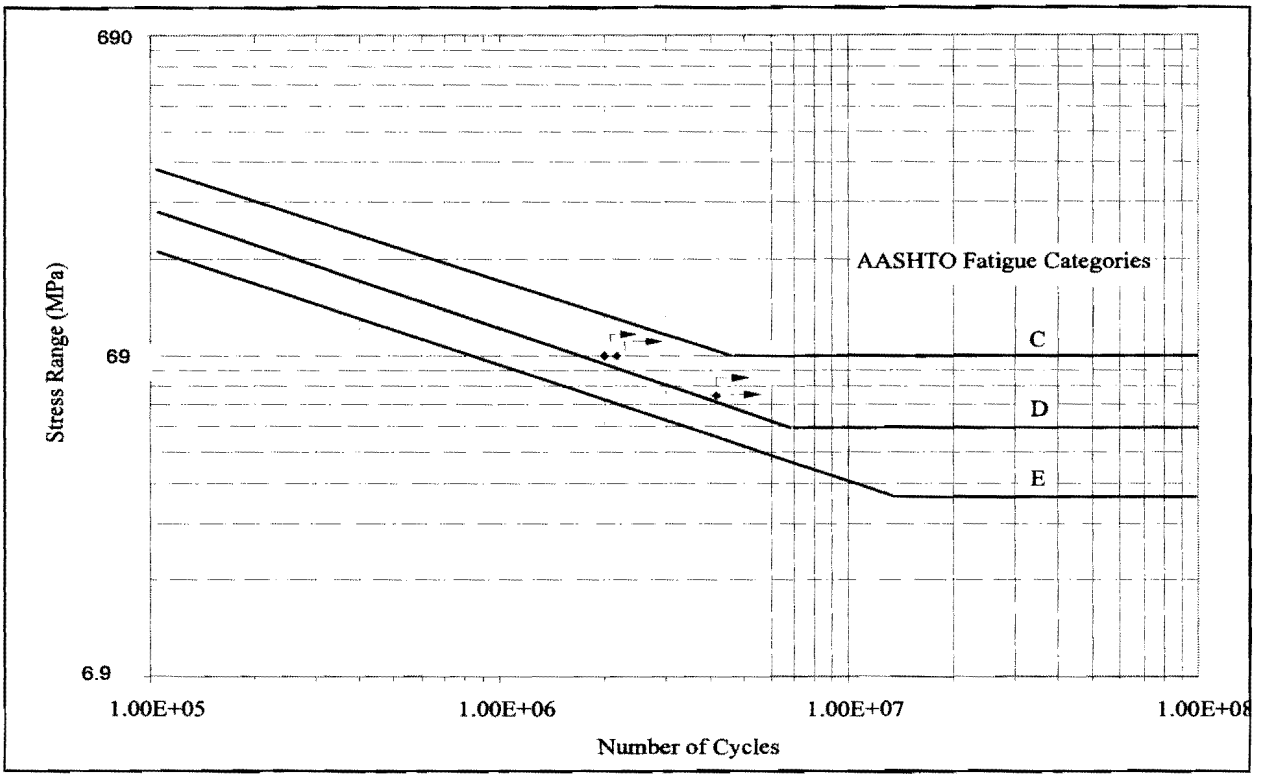

Figure 70 Fatigue test results for 4 1/2 UNC COSS bolt specimens.

Table 13 Results after third fatigue test on 4 1/2 UNC bolts; bolt C is critical

Bolt	σ_R, MPa (ksi)	Number of Cycles @ σ_M
A	0 (0)	2,156,023 @ σ_M =-17 MPa (-2.5 ksi) (from first test)
B	49 (7.1)	2,156,023 cycles @ σ_M = -12 MPa (-1.8 ksi) and 4,401,580 cycles @ σ_M = 12 MPa (1.8 ksi)
C (critical)	69 (10)	4,401,580 @ @ σ_M = 17 MPa (2.5 ksi)
D	49 (7.1)	6,557,603 @ σ_M = 12 MPa (1.8 ksi)
E	0 (0)	2,156,023 @ σ_M = 17 MPa (2.5 ksi) (from first test)
F	49 (7.1)	2,156,023 @ σ_M = 12 MPa (1.8 ksi) and 4,401,580 @ σ_M = -12 MPa (-1.8 ksi)
G	69 (10)	4,401,580 @ σ_M = -17 MPa (-2.5 ksi)
H	49 (7.1)	6,557,603 @ σ_M = 12 MPa (-1.8 ksi)

There were no anchor bolt failures in the third fatigue test. After the third fatigue test, all bolts were tested ultrasonically for cracks using ultrasonic equipment capable of detecting a 3 mm (1/8 in.) crack. No cracks were detected. After completion of the three fatigue tests, two bolts had experienced over 4.4 million cycles at a 69 MPa (10 ksi) stress range, two bolts had experienced over 2 million cycles at a 69 MPa (10 ksi) stress range, and four bolts had experienced over 6.5 million cycles at a 49 MPa (7.1 ksi) stress range. Figure 71 shows these results. Each point on the S-N curve in Figure 71 represents two data points.

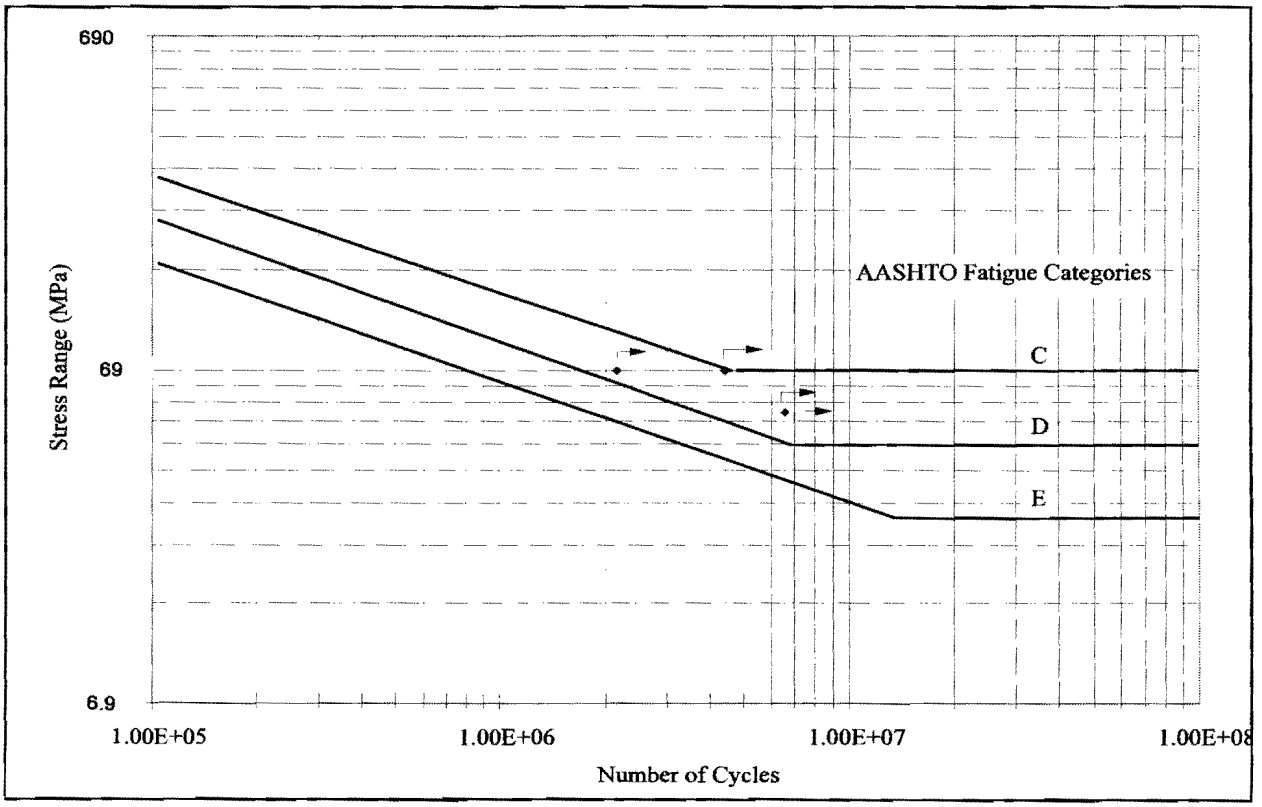

Figure 71 Results of third fatigue test on 4 1/2 UNC bolts.

As Figure 71 illustrates, this double nut connection, using 4 1/2 UNC threaded bolts tightened to 60 degrees past snug tight, can be classified at least as a Category D detail. Two of the bolts survived loading equivalent to AASHTO Category C, supporting the recommendation of others (Frank 1978) that Category C design allowable stresses can be used for this detail.

8 UN Threaded Bolts

The nuts were tightened to 60 degrees past snug tight in the first fatigue test. The 8 UN threaded bolts were loaded with a 97 MPa (14.1) ksi stress range on the top and bottom bolts. This higher stress range was selected because of the good performance of the 4 1/2 UNC bolts at the lower 69 MPa (10 ksi) stress range. The stress range was offset by 75% tensile and 25% compressive in the top bolt, simulating the bolt opposite the cantilever, to simulate the tensile offset caused in the field by the cantilever arm of the structure. Therefore, the bottom bolt stress range was 75% compressive and 25% tensile. With the top and bottom bolts having a 97 MPa (14.1 ksi) stress range, a 69 MPa (10 ksi) stress range was induced in the adjacent bolts. The stress range was increased to support a possible classification as a Category C detail. Figure 72 shows the orientation of the anchor bolts for the first fatigue test.

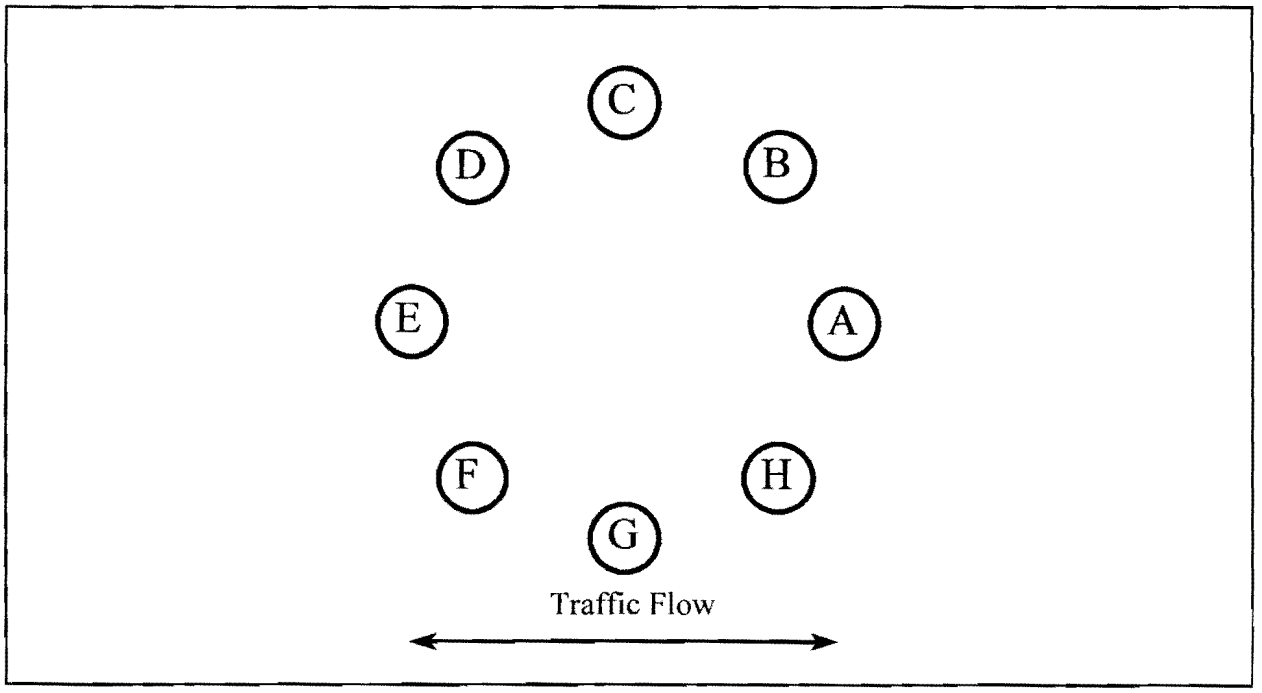

Figure 72 Orientation of 8 UN anchor bolts in first fatigue test.

The critical bolt C, with a 97 MPa (14.1 ksi) stress range fractured after 160,103 cycles. Once bolt C fractured, bolts B and D carried a 108 MPa (15.6 ksi) stress range. Bolts B and D

then fractured after 160,103 cycles at a 69 MPa (10 ksi) stress range and 77,407 cycles at a 108 MPa (15.6 ksi) stress range. Bolts A and E were then overloaded for 47,500 cycles at a 175 MPa (25.6 ksi) stress range before the test was stopped. Table 14 details the stress range, mean stress and number of cycles on each bolt for the first fatigue test.

Table 14 Results of first fatigue test on 8 UN bolts

Bolt	Stress Range, σ_R	Number of Cycles and Mean Stress, σ_M
A	0 MPa	--
	then 15 MPa (2.2 ksi)	77,407 @ 7.7 MPa (1.1 ksi)
	then 177 MPa (26 ksi)	47,500 @ 86 MPa (12.5 ksi)
B	69 MPa (10 ksi)	160,103 @ 17 MPa (2.5 ksi)
	then 108 MPa (16 ksi)	77,407 @ 37 MPa (5.3 ksi)
C	97 MPa (14 ksi)	160,103 @ 24 MPa (3.5 ksi)
D	69 MPa (10 ksi)	160,103 @ 17 MPa (2.5 ksi)
	then 108 MPa (16 ksi)	77,407 @ 37 MPa (5.3 ksi)
E	0 MPa	--
	then 15 MPa (2.2 ksi)	77,407 @ 7.7 (1.1 ksi)
	then 177 MPa (26 ksi)	47,500 @ 86 MPa (12.5 ksi)
F	69 MPa (10 ksi)	160,103 @ -24 MPa (-2.5 ksi)
	then 112 MPa (16 ksi)	77,407 @ -21 MPa (-3.1 ksi)
	then 133 MPa (19 ksi)	47,500 @ -32 MPa (-4.7 ksi)
G	97 MPa (14 ksi)	160,103 @ 24 MPa (-3.5 ksi)
	then 161 MPa (23 ksi)	77,407 @ -30 MPa (-4.4 ksi)
	then 258 MPa (37 ksi)	47,500 @ -79 MPa (-11.5 ksi)
H	69 MPa (10 ksi)	160,103 @ -17 MPa (-2.5 ksi)
	then 112 MPa (16 ksi)	77,407 @ -21 MPa (-3.1 ksi)
	then 133 MPa (19 ksi)	47,500 @ -32 MPa (-4.7 ksi)

After the first fatigue test, the specimen was rotated 90 degrees to test the bolts that were on the neutral axis during the first test. These bolts had a few cycles in their history due to the fracture during the first fatigue test. The specimen was oriented as in Figure 73.

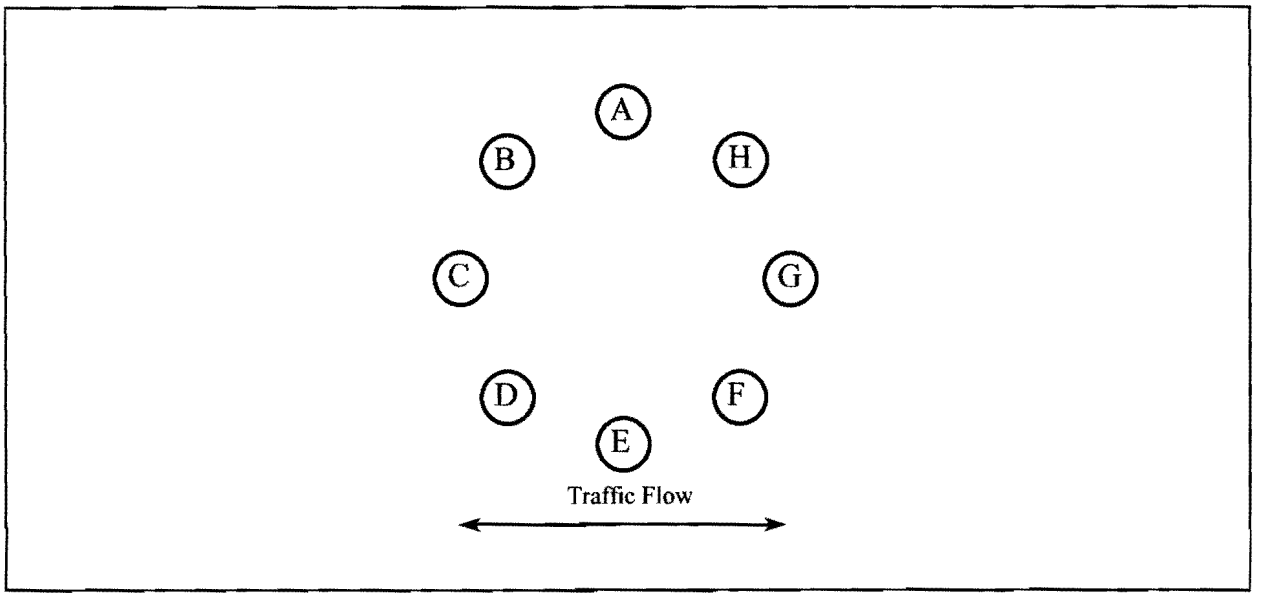

Figure 73 Orientation of specimen in second fatigue test of 8 UN threaded bolts.

Because bolts B, C, and D were broken in the first test, the only bolts tightened in the second test were A and E. The stress range was lowered to 69 MPa (10 ksi) for the second fatigue test. The top bolt simulating the bolt furthest from traffic again had a 75% tensile and 25% compressive offset stress range. The results of the second fatigue test are in Table 15.

Table 15 Load applied in second fatigue test on 8 UN bolts

Bolt	σ_R, MPa (ksi)	σ_M, MPa ksi)	Number of Cycles
A (critical bolt)	69 (10)	17 (2.5)	4,477,370
E	69 (10)	-17 (-2.5)	4,477,370

No bolts were broken in the second fatigue test. After 4.4 million cycles at a 69 MPa (10 ksi) stress range, the test was stopped. The bolts were inspected ultrasonically, and no cracks were detected in either bolt. This raised questions of the quality of the bolts that failed in the first fatigue test. One reason for this wide variance of fatigue life could be the fact that this stress range is right at the infinite life threshold. The third fatigue test was then set up to help determine the fatigue life of the 8 UN threaded bolts.

The third fatigue test had the same configuration as the second, only bolts A and E were loaded, but the stress range was increased to 97 MPa (14.1 ksi), as in the first test. The top bolt had a 75% tensile and 25% compressive offset. This was the same load that fractured the bolts in the first fatigue test. Table 16 shows the results of the third fatigue test.

Table 16 Results after third fatigue test on 8 UN bolts - bolt A - critical bolt

Bolt	σ_R, MPa (ksi)	σ_M, MPa (ksi)	Number of Cycles
A	98 (14.1)	24 (3.5)	1,465,230
E	98 (14.1)	-24 (-3.5)	1,465,230

The third fatigue test was stopped after a crack was detected with the ultrasonics. The top bolt, bolt A, had a 5 mm (3/16 in.) crack near the bottom surface of the leveling nut. After the crack was detected, the pole was removed. The bolt was cooled with liquid nitrogen and broken with the overhead crane to inspect the crack surface. Figure 74 shows a photograph of the crack surface.

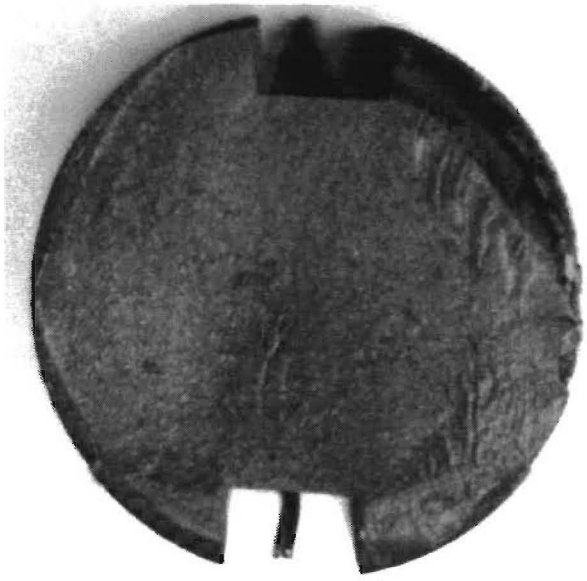

Figure 74 Photograph of fatigue crack surface in bolt A after third fatigue test.

For all three of the 8 UN fatigue tests, the effective stress ranges were calculated for each bolt. Miner's rule was used to determine the effective stress range for the given number of cycles at each stress range. Table 17 shows results of the calculations.

Table 17 Effective stress range for the three fatigue tests on the 8 UN bolts

Bolt	Effective Stress Range, σ_E, MPa (ksi)	Number of Cycles	Result
A	82 (11.9)	6,067,507	Crack Discovered
B	85 (12.4)	237,510	Fractured
C	97 (14)	160,103	Fractured
D	85 (12.4)	237,510	Fractured
E	82 (11.9)	6,067,507	No Crack Observed
F	99 (14.3)	285,010	Stopped testing No Crack Observed
G	165 (23.9)	285,010	Stopped Test No Crack Observed
H	99 (14.3)	285,010	Stopped Test No Crack Observed

The values of Table 17 were then graphed on an S-N Curve with the AASHTO fatigue categories, as is shown in Figure 75.

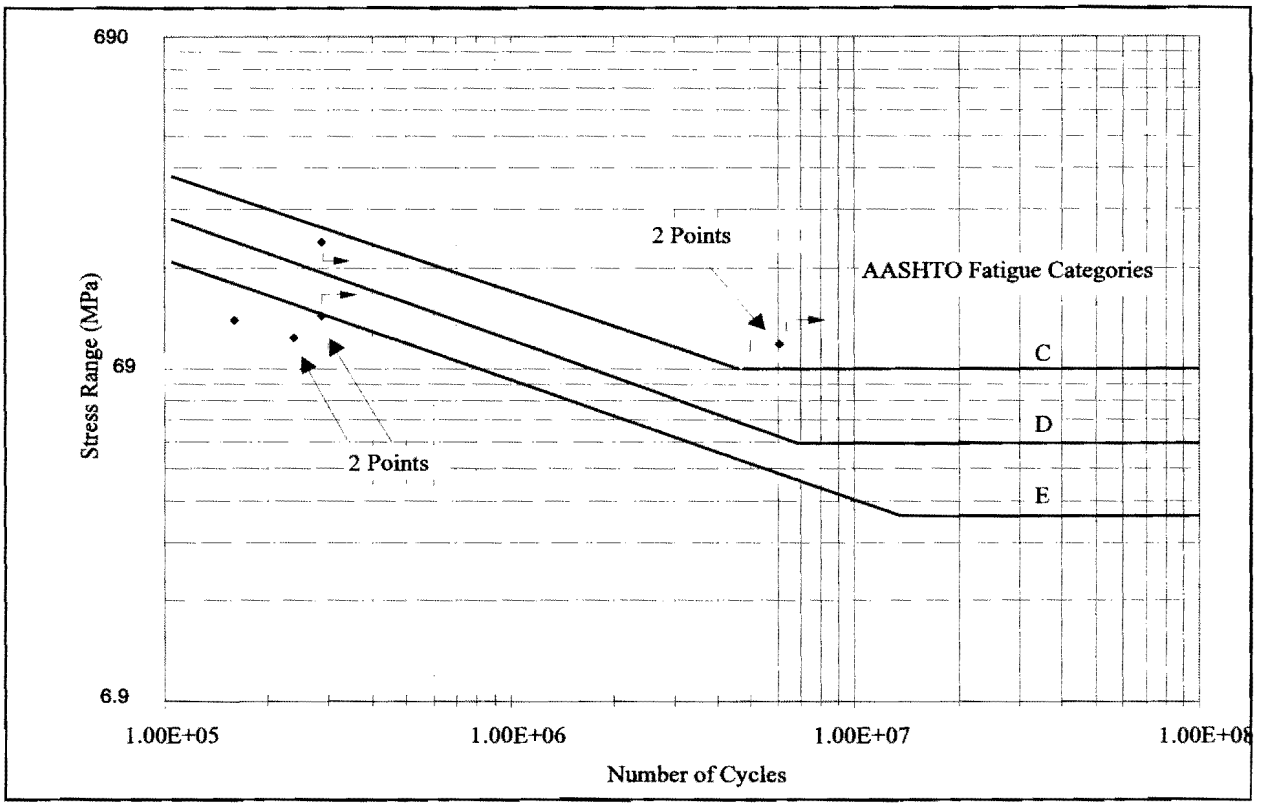

Fgure 75 Fatigue data on S-N curve after third fatigue test, 8 UN bolts.

Fatigue Performance of Pole-to-Baseplate Weld

According to the static test results, the weld experiences a higher stress range than the most critical anchor bolt. This weld detail is classified as a Category C detail as a maximum. By definition, a Category C detail can withstand a 69 MPa (10 ksi) stress range for an infinite life. To induce a 69 MPa (10 ksi) stress range in the topmost bolt, a 152 MPa (22 ksi) stress range is induced in the pole to baseplate weld. When a fatigue crack was first detected in the weld, the weld had experienced 649,473 cycles at a 152 MPa (22 ksi) stress range. The pole was removed and the weld was repaired. The weld was improved by replacing the two filet welds with a full penetration weld. The new weld was also ground and peened. These changes greatly improved the life of the weld. The second weld crack was detected after 1.3 million cycles of a 152 (22 ksi) stress range. Again, the cracked area was gouged and replaced with a full penetration weld. As Figure 76 shows, after the second repair, almost the entire original filet weld was replaced

with full penetration weld. After the second repair, the weld did not crack throughout the remainder of all the fatigue tests.

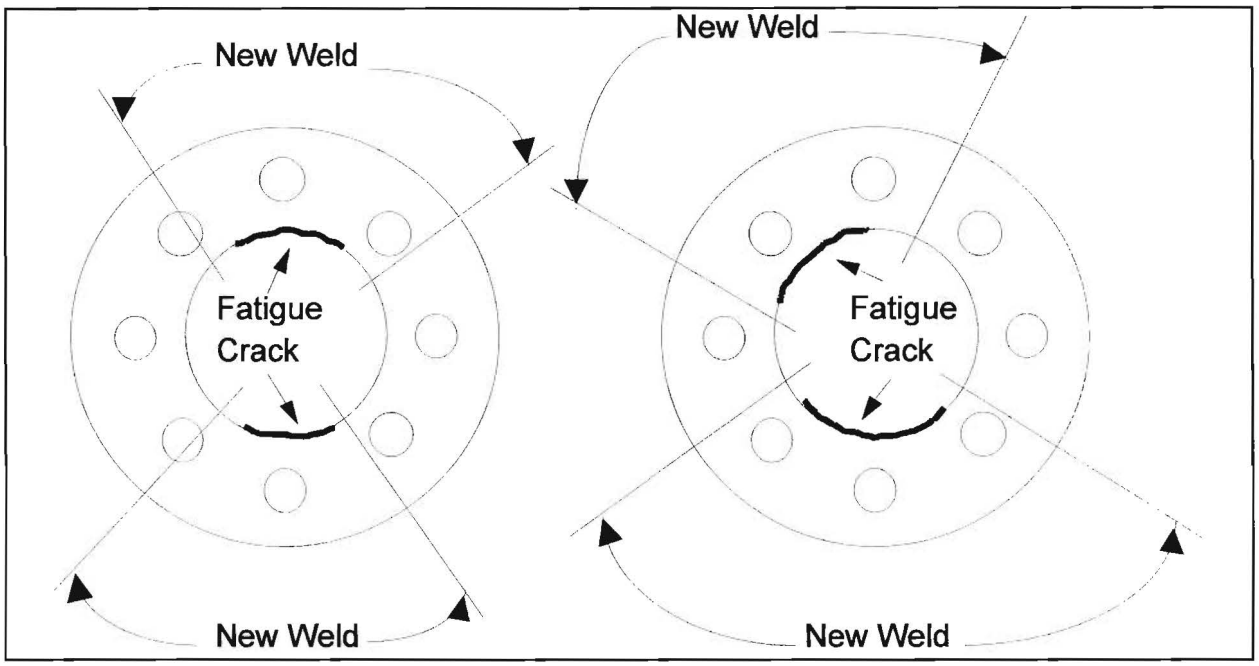

Figure 76 Crack and repair locations on pole-baseplate weld.

Effects of Various Parameters on Fatigue Life

Effect of Increased Shear on Fatigue Life Because of pole height limitations in the laboratory, the column base moment was induced by higher shear forces than expected in the field. The increase in the shear in the laboratory is a more severe loading than that in the field. The increase in shear causes a secondary bending stress in the bolts. The shear in the laboratory tests was about 5 times that expected of in the field, for the same column base moments. This secondary bending moment causes higher extreme fiber tensile stresses. The results obtained from the laboratory tests underestimate the strength of the structure because of the higher shear loading in the laboratory.

Effect of Notches Milled in the Bolts With the milling of the notches in the bolt, the stresses were increased at the tips of the notches, where the threads of the bolt interact with the nut. This lack of continuity of the threads causes a stress riser at the tip of the thread where the notch begins. This stress riser could cause problems with the initiation or propagation of a fatigue crack.

This increase in stress did not seem to affect the 4 1/2 UNC grade 105 bolts. Again, with the higher yield strength, this increase in stress is small in proportion to the yield strength. However, the notches did appear to affect the fatigue performance of the 8 UN grade 55 bolts. The crack started at the stress riser and caused premature failure in the first fatigue test. This stress increase would be a higher percentage of the yield strength of the grade 55 bolts than of the grade 105 bolts. Once the first bolt fractured, the remaining bolts were overloaded. One of the anchor bolts that failed did not have notches milled in it, but it was overloaded at a considerable stress.

In the second fatigue test on the 8 UN threads, the bolts did not fracture. The notches did not affect the fatigue life in this test. Even though the notches caused different stresses than in the unnotched bolts in the field, they were necessary for the measuring the stresses in the bolt. The notches caused a worse case loading than bolts in service, but were originally determined to be acceptable. However, due to the wide scatter of the data in the 8 UN fatigue tests, the notches were determined to be an unwanted variable. While these milled notches affected the fatigue tests of the grade 55 bolts, they did not cause failures on the grade 105 bolts. This would suggest that the grade 105 steel is more resistant to higher stress ranges in the bolt.

Effect of Thread Pitch on Fatigue Life Due to the error by the supplier, who supplied grade 55 bolts instead of grade 105, it is hard to compare the performance of the different thread pitches due to the different grades of steel. From a fatigue standpoint, the 8 UN threads give the bolt a higher area and, therefore, lower stress range in service.

Effect of Preload on Fatigue Life The static tests, showed that the preload affected the bolt in the region between the nuts. The higher the preload, the lower the pole live load stress. This reduced stress range will increase the fatigue life of the bolt. This preload should also help prevent nut loosening, therefore preventing any banging of the baseplate on the nuts, which would cause impact loading. However, this preload does not protect the region under the bottom nut, as these failures and finite element modeling have shown.

Nut Loosening Studies

After nut tightening and before each fatigue test, the baseplate was carefully marked to determine the orientation of the anchor bolt nuts before initiation of cyclic loading. During the fatigue tests, the marks were inspected to determine if the nuts had rotated. The live load stresses in the bolt were also monitored to determine if the nuts had loosened. Loosening would be manifested by an increase in the live-load stress ranges induced in the bolt. After the completion of each of the fatigue tests, the nuts were inspected to determine if they had rotated from the original position. The nuts did not move from their original position in any of the fatigue tests, including one series when the nuts were only snug tight.

With minimal preload apparently sufficient to prevent the nuts loosening, the nut does not need to be welded to the baseplate, except to prevent vandalism. This would facilitate the inspection of the tightness of the nuts in future inspections and retightening, if necessary.

Methods of Inspection of Nut Tightness

Inspection techniques to detect nut tightness were unsuccessful in differentiating between nuts tightened to snug tight condition and nuts turned past snug tight. Ultrasonics were used to try to determine how tight the nut was by the change in responses from the ultrasonic waves. The nuts were tightened to different levels of tightness, and ultrasonic waves were transmitted through

both the nuts and longitudinally down the bolt. No significant differences in the returning ultrasonic signals were observed with different degrees of nut tightness.

A subjective method sometimes used in field inspection (Wong 1990) was also evaluated. In this method, the nut is struck with a 0.7 kg (1.5 lb) hammer, and the inspector subjectively evaluates the sound of the impact. If the sound is "dull," the nut is determined to be not tightened. If the sound is a higher-pitched ring, the nut is indicated to be tightened. The degree of tightness is not determined.

To evaluate this method, several nuts were tightened to 60 degrees past snug tight. Each nut was then hit with a 0.7 kg (1.5 lb) hammer. The inspector carefully noted the sound of the impact. This process was repeated several times to determine the sound of a nut tightened to 60 degrees past snug tight. The nut was then loosened and tightened to snug tight. The nut was then struck with the hammer, and any difference in the sound of the impact was carefully noted. Finally, the same test was conducted on nuts tightened by hand, ie. less than snug tight. The results of this test are obviously subjective, but in the tests conducted here, the method failed to prove useful in detecting the difference between nuts in a snug tight condition and nuts tightened past snug tight. Both nuts tightened to snug tight and nuts tightened to 60 past snug tight gave off a sound which could be described as a sharp clang. After several repeated tests, it was determined that the difference in the sounds from the snug tight condition and the 60 degrees past snug tight could not be distinguished audibly. When the hammer struck the hand-tightened nut, a noticeably different, duller sound was heard, compared to the sounds observed in tests of nuts in the snug tight and tightened conditions. While this field inspection technique could indicate the difference between a hand-tightened nut and a nut tightened with a wrench, the technique was determined to be of negligible real value in the tightness of a large-diameter anchor bolt nut.

The most useful field inspection technique seems likely to be loosening and retightening with a hammer and slug wrench. When the exact degree of tightness is not important, as in many double-nut system applications, the wrench can be placed on the nut to be inspected, and an attempt to loosen by hand will indicate nuts that are less than snug tight. The use of a 7.2 kg (16 lb) hammer to loosen the nut will give some indication of how tightly the nut is tightened, if the number of turns it rotates before it can be further loosened by hand is noted. Retightening to the

desired degree of tightness can be accomplished with the same equipment, after cleaning and lubricating the nut and bolt threads and bearing surfaces. This technique was successfully evaluated with the laboratory specimens, although the absence of environmental effects prevented corrosion from being a problem in the lab tests. Also, retightening to the same turn-of-the-nut specification can result in increased bolt preload, compared to earlier tightening efforts. This was not a problem in the laboratory specimens. In order to utilize this method, any tack welds of the nut to the washer must be removed.

LABORATORY STUDIES--HMIP SPECIMENS

Experiment Design

Laboratory investigation of HMIP specimens focused on testing two 0.91 m (36 in.) diameter twelve bolt patterns with 4 1/2 UNC and 8 UN threads. Testing was not completed on the 8 UN specimen before the end of the contract period. The 8 UN anchor bolts used in this specimen were suspected to be lower strength grade 55 steel, f_y = 380 MPa (55 ksi) bolts as found in the 8 UN COSS specimen. All tested anchor bolts were 57 mm (2.25 in.) diameter grade 105 steel, f_y = 724 MPa (105 ksi). The 4 1/2 UNC specimen is seen in Figure 77.

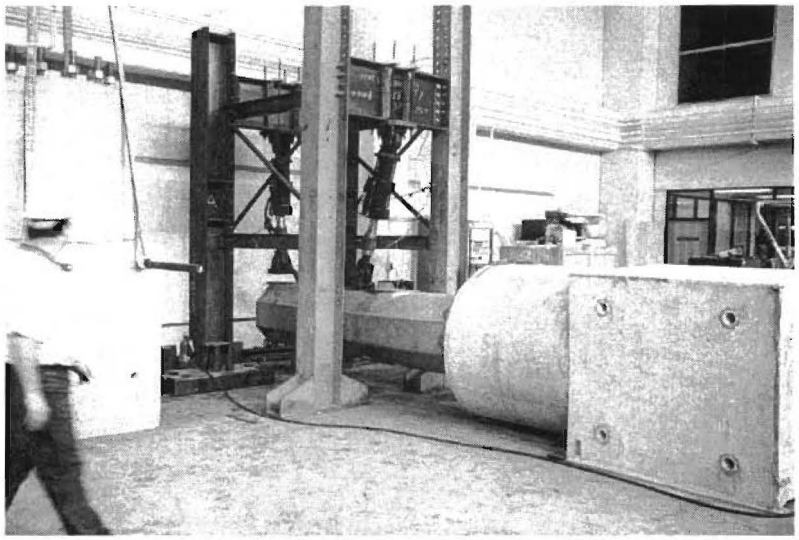

FIGURE 77 Photograph of HMIP 4 1/2 UNC laboratory specimen.

Specimen Design

HMIP specimens were designed using standard TxDOT HMIP plans for 129 km/hr (80 mph), 46 m (150 ft) eight-sided poles. The HMIP portion of the specimen was a 3.65 m (12 ft) octagonal cross section with a 13 mm (1/2 in.) wall thickness (see Appendix A). The pole was identical to production poles, except in two respects. First, the access port was eliminated as being unnecessary. Second the ground sleeve was eliminated at the suggestion of the supplier and with

the approval of the project advisors in the interest of economy as the test objective was evaluation of the anchor bolt performance, not pole performance. The section of the specimen containing the anchor bolts was designed according to TxDOT standards. The bottom portion of the specimen was secured to the testing lab floor using four 1.8 m (72 in.) threaded rods. Specimens were designed to rotate about the longitudinal axis so that two different loading configurations could be used to load the same bolt pattern. Specimens were designed to be statically and dynamically loaded to determine effects of bolt preload on fatigue life of the anchor bolts.

HMIP Loading Configuration

To simulate the low shear, high moment character of the environmental loads seen by HMIP structures, two 250 kN (55 kip) capacity hydraulic rams were connected to the HMIP pole via reinforced through-pole connections near the midpoint and far end of the 3 m (10 ft) pole section. Figure 78 depicts this loading configuration. Equal and opposite ram forces were applied for all static and cyclic loading resulting is the application of a force couple (bending moment) with minimal transverse shear force.

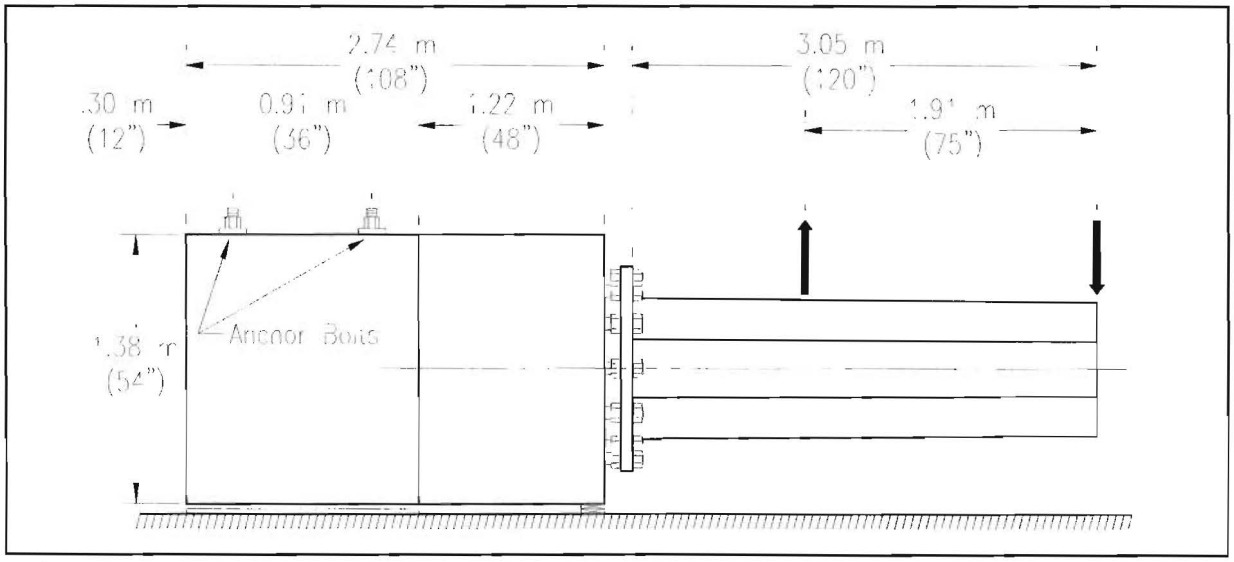

FIGURE 78 Loading configuration for HMIP 4 1/2 UNC laboratory specimen.

HMIP Instrumentation

Sixty-two data channels were recorded during testing of the HMIP specimen. Two channels monitored ram loads, two channels monitored strain in the HMIP pole section, two monitored strain at the base of the top bolt below the double nutted connection, and fifty-six channels monitored anchor bolt strains. All anchor bolts in the HMIP specimen were instrumented with strain gages in different sections of the double-nutted connection.. Bolts were arranged and labeled as shown in Figure 79.

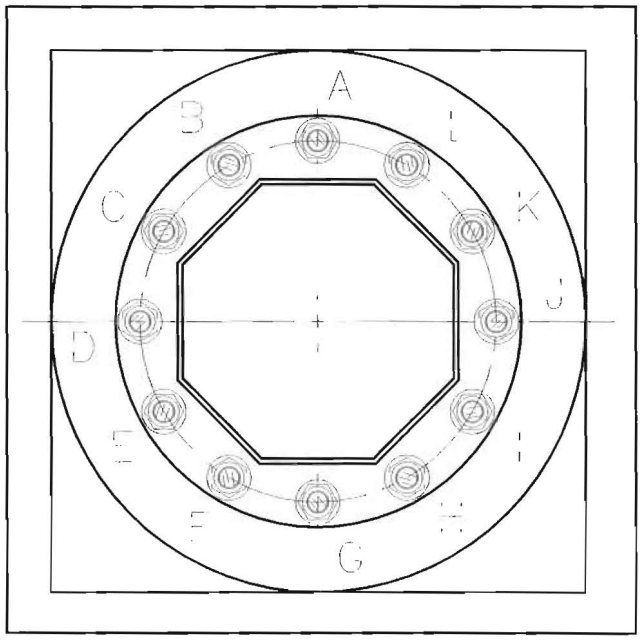

FIGURE 79 Anchor bolt locations for HMIP 4 1/2UNC laboratory specimen.

Longitudinal keyways were milled on opposite sides of the bolt for placement of strain gages, allowing the leads to pass beneath the nuts. Bolts A, D, G, and J were each instrumented with ten gages attached in pairs on opposite sides of the bolt cross-section as seen in Figure 80. Two gage pairs were located in the region covered by the top nut, the next two gage pairs were in the region spanned by the baseplate, between the nuts, and the last gage pair was located in the region covered by the leveling nut. Monitoring all gages separately allowed extraction of tension and bending stresses at each longitudinal location.

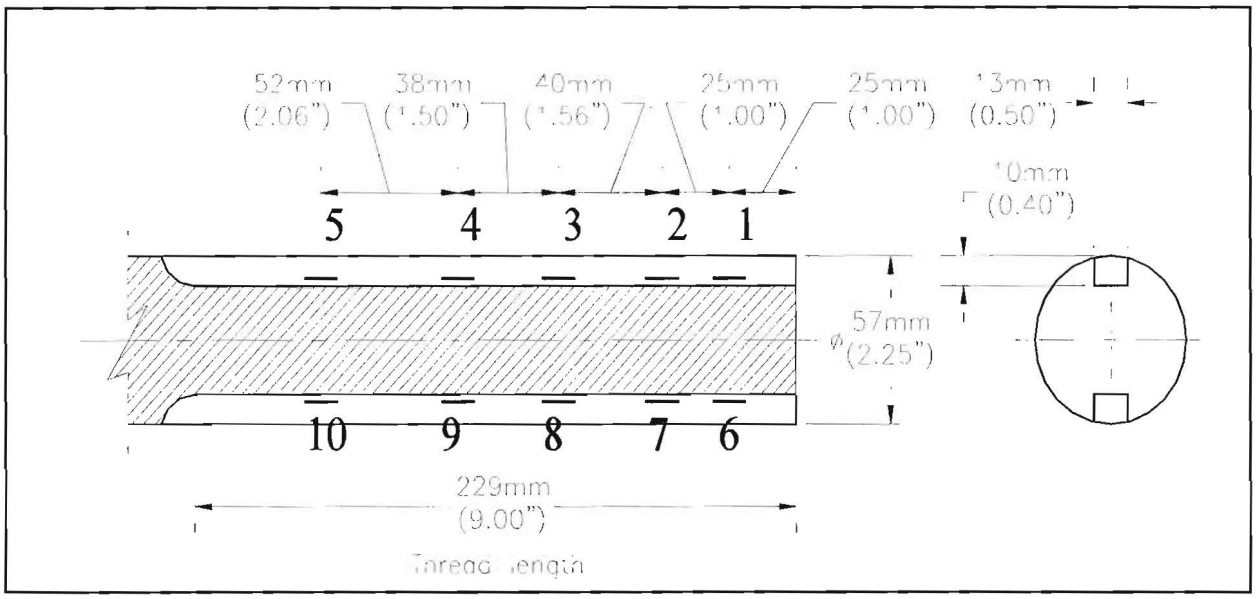

FIGURE 80 Location of strain gages along bolts A, D, G, J - HMIP 4-1/2 UNC laboratory specimen.

Bolts B, C, E, F, H, I, K and L were instrumented with two unpaired gages in the same keyway channel as seen in Figure 81. One gage was located in the region covered by the top nut, and the second gage was located at the midpoint of the baseplate region. These gages only provided data on tensile stresses under the assumption of zero bending stress in the bolt in these two regions.

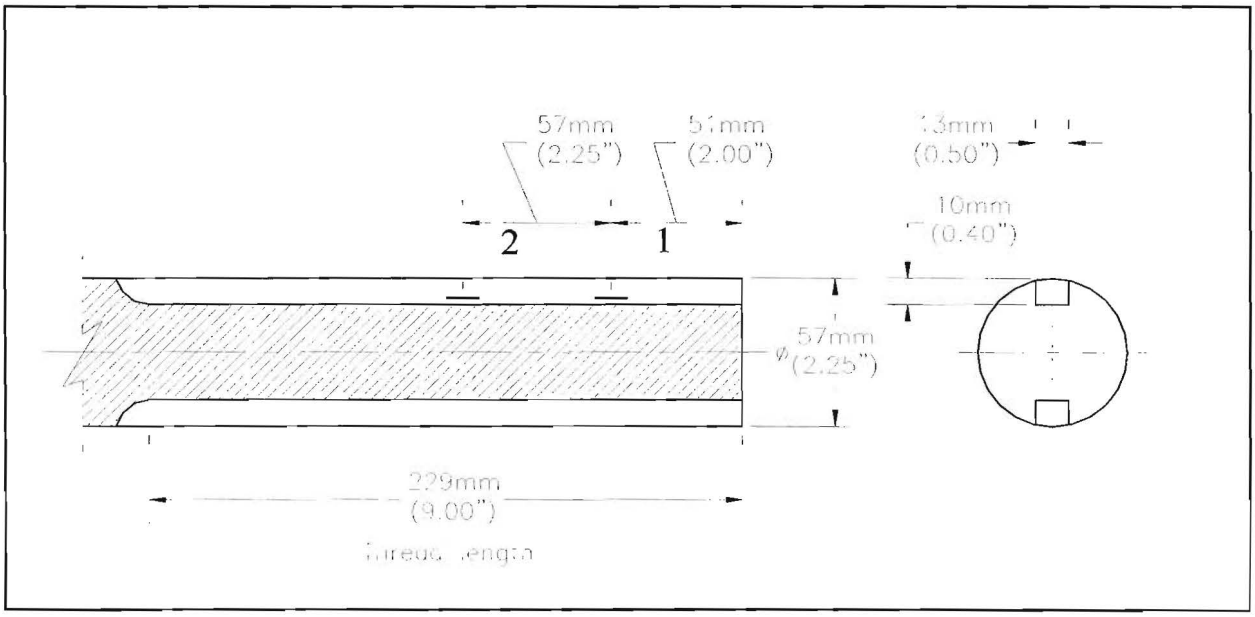

FIGURE 81 Location of strain gages along bolts B, C, E, F, H, I, K, L - HMIP 4 1/2 UNC laboratory specimen.

Laboratory Study Procedures

Three test types were accomplished, tightening, static loading, and fatigue loading. The objective of the tightening tests was to determine the variation in preload induced in the anchor bolts due to repeated tightening and loosening of one double-nut connection. Static load tests established the relationship between the applied ram force couple and anchor bolt forces and stresses. The fatigue test validated the AASHTO fatigue category designation for double-nut connection with preloaded bolts. The fatigue test stress range was chosen after study of expected service loads and fatigue category classification results of COSS specimen data. As noted earlier, previous research (Frank 1978) indicates that this bolt detail can be classified between AASHTO Category E and Category C, depending upon the nut tightness. Under current specifications, AASHTO Category C details can be used for connections that experience more than two million cycles of stress ranges of 70 MPa (10 ksi) (AASHTO 1985). In the current HMIP fatigue study, applied cyclic loads were selected to stress bolts most distant from the neutral axis (Bolts A and G) to a range of 87 MPa (12.5 ksi) with a zero mean stress.

Laboratory Testing of HMIP 4 1/2 UNC Anchor Bolt Specimens

Laboratory investigation of HMIP 4 1/2 UNC anchor bolts was divided into three phases. Tightening tests determined variation in anchor bolt preloads using the turn-of-the-nut method and established effects of repeatedly tightening and loosening one top nut in a fully preloaded connection. Static load tests established the relationship between the applied ram force couple and resulting anchor bolt stresses. A 2,000,000 cycle fatigue test validated the AASHTO fatigue category designation of preloaded HMIP 4 1/2 UNC double-nutted connection.

Tightening Tests

Extensive tightening tests were conducted on COSS laboratory specimens to establish acceptable procedures for tightening double nutted connections in the field. The procedures established in the COSS tightening tests were extended to HMIP specimens, and this report records the results of these experiments. All nuts were tightened one-sixth turn past snug tight.

Differences between COSS and the HMIP connection seen in Figure 77 led to some differences in resulting HMIP stress levels and tightening procedures. The larger bolt diameter of 57 mm (2.25 in.) versus 51 mm (2.00 in.) for laboratory COSS specimens required higher tightening torque levels. HMIP double-nutted connections exhibited lower preload stress for the same turn of the nut, 60 degrees. This is attributed primarily to the thicker 76 mm (3.00 in.) HMIP baseplate which resulted in a more flexible connection than the 51 mm (2.00 in.) COSS baseplate connections. HMIP specimens contained twelve double-nutted anchor bolts versus eight bolts in COSS specimens. This reduced the available tightening room and resulted in variations in the tightening order of individual bolts. The twelve bolt HMIP connection tended to lockup the lower leveling nut of bolts near the end of the tightening order. Other preloaded bolts in the connection compressed the baseplate against the remaining leveling nuts, which locked up the leveling nuts and prevented their loosening prior to retightening the connection to final preload stress level.

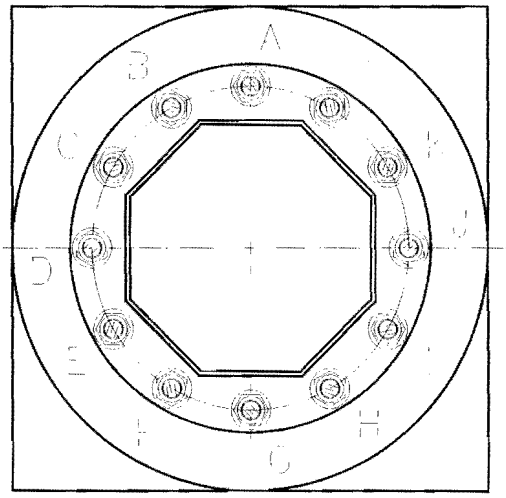

FIGURE 82 Bolt pattern of 4 1/2 UNC HMIP laboratory specimen.

Significant variations in longitudinal bolt stress were found in all bolts. This was attributed to several causes. Variation due to strain gage position was consistent with the expected stress build up in the anchor bolts as you pass through the nut regions toward the baseplate region. Highest snug tight and preload stresses were found in the baseplate regions of all bolts. Significant bending stresses were found in the four bolts with ten-gage instrumentation. These stresses are probably present in all bolted connections and are attributed to misalignment of the anchor bolts and the non-parallel character of actual nut-washer-baseplate surfaces.

Tightening Procedure

After leveling and adjustment of the HMIP pole specimen, all bolts were brought to a snug tight condition by hand tightening with a knocker wrench. Bolts were then brought to the designated preload condition of one-sixth turn past snug tight using a knockerwrench and a 2.75 m (9 ft) cheater bar. An overhead crane was used to turn each nut the last 15 to 20 degrees. Table 18 lists the order of tightening used to reach snug tight and preloaded conditions for the twelve bolt HMIP pattern identified in Figure 79.

Table 18 Bolt tightening order for 4 1/2 UNC HMIP laboratory specimen

Tightening Order	Anchor Bolt	Tightening Order	Anchor Bolt
1	A	7	B*
2	G	8	F*
3	D	9	K*
4	J	10	I*
5	L	11	C*
6	H*	12	E*

*Level nut locked-up

Measured stress levels for the snug tight condition are tabulated in Tables 19, 20 and 21. The axial and bending component of stress for bolts A, D, G and J are shown in Tables 19 and 20, respectively. Locations 3 and 4 are in the baseplate region, which exhibits the highest stress levels. Significant variations are noted at the snug tight condition of these bolts. Stress levels ranged from 19 MPa (2.8 ksi) to 202 MPa (29.3 ksi) with a mean of 92 MPa (13.4 ksi) The bending component of the longitudinal stressed ranged from 88 MPa (12.8 ksi) to 15 MPa (2.2 ksi) with a mean of 44 MPa (6.4 ksi). Stresses in two-gage bolts showed significant variation, ranging from 66 MPa (9.6 ksi) to -11 MPa (-1.6 ksi) with a mean of 27 MPa (4.0 ksi).

Table 19 Bending component of snug-tight stress in HMIP laboratory specimen, bolts A, D, G, J

Bolt	Location									
	1		2		3		4		5	
	MPa	(ksi)	MPa	(ksi)	MPa	(ksi)	MPa	(ksi)	MPa	(ksi)
A	30	(4.3)	53	(7.7)	34	(4.9)	25	(3.7)	22	(3.1)
D	51	(7.4)	81	(11.7)	88	(12.8)	86	(12.5)	59	(8.5)
G*	---	---	---	---	---	---	---	---	---	---
J	18	(2.7)	19	(2.7)	15	(2.2)	15	(2.1)	9	(1.4)
Mean	33	(4.8)	51	(7.4)	46	(6.6)	42	(6.1)	30	(4.3)
Std. Dev.	14	(2.0)	25	(3.7)	31	(4.5)	31	(4.6)	21	(3.0)

*Lost data

Table 20 Axial component of snug-tight stress in HMIP laboratory specimen bolts A, D, G, J

Bolt	Location									
	1		2		3		4		5	
	MPa	(ksi)	MPa	(ksi)	MPa	(ksi)	MPa	(ksi)	MPa	(ksi)
A	94	(13.6)	171	(24.8)	195	(28.4)	202	(29.3)	128	(18.6)
D	16	(2.3)	21	(3.0)	20	(2.8)	19	(2.8)	-3	-(0.5)
G*	---	---	---	---	---	---	---	---	---	---
J	38	(5.6)	54	(7.8)	59	(8.5)	59	(8.6)	37	(5.4)
Mean	49	(7.2)	82	(11.9)	91	(13.2)	93	(13.6)	54	(7.9)
Std. Dev.	33	(4.7)	65	(9.4)	75	(10.9)	78	(11.4)	55	(8.0)

*Lost data

Table 21 Snug tight stresses in HMIP laboratory specimen, bolts B, C, E, F, H, I, K, L

Bolt	Location			
	1		2	
	MPa	(ksi)	MPa	(ksi)
B	44	(6.4)	41	(6.0)
C	48	(6.9)	47	(6.8)
E	7	(1.0)	14	(2.0)
F	-25	-(3.6)	-11	-(1.6)
H	-24	-(3.4)	8	(1.1)
I	-4	-(0.5)	10	(1.5)
K	53	(7.7)	45	(6.5)
L	71	(10.3)	66	(9.6)
Mean	21	(3.1)	27	(4.0)
Std. Dev.	37	(5.4)	26	(3.8)

Tightening was repeated, and all bolts brought to preloaded condition of one-sixth turn past snug tight. Stresses at this level showed less variation than in the snug tight case. Tables 22, 23 and 24 tabulate indicated stress levels at the preloaded condition. The axial component of stress in bolts A, D and J ranged from 371 MPa (53.8 ksi) to 471 MPa (68.4 ksi) with a mean of 432 MPa (62.7 ksi) The bending component of the longitudinal stresses ranged from 13 MPa (1.8 ksi) to 98 MPa (14.2 ksi) with a mean of 50 MPa (7.2 ksi). Stresses in two-gage bolts showed significant variation ranging from 210 MPa (30.5 ksi) to 449 MPa (65.0 ksi) with a mean of 371 MPa (53.8 ksi).

The top nuts on three bolts in the pattern, C, D, and E, were individually loosened after all bolts were brought to the preloaded condition. These nuts were then retightened to evaluate the effect of retightening on the stress levels in individual double-nutted connections. A significant increase in preload stress occurred. Stresses increased on average 85 MPa (12.2 ksi) with a standard deviation of 22 MPa (3.3 ksi). The mean preload stress in these bolts was 400 MPa (58 ksi). When retightened, the nuts did not return to their original snug tight position. After rotation of one-sixth turn, all nuts were rotated 10 to 15 degrees beyond their prior position.

This rotation agrees with the stress increase noted above. During testing, the pole was removed for repair. All nuts tended to return to their respective preload when the pole was reinstalled. The increase in preload stresses did not occur when all nuts started at a loose state.

Table 22 Axial component of preload stress in HMIP laboratory specimen bolts A, D, G, J

Bolt	Location									
	1		2		3		4		5	
	MPa	(ksi)	MPa	(ksi)	MPa	(ksi)	MPa	(ksi)	MPa	(ksi)
A	216	(31.3)	388	(56.4)	446	(64.7)	453	(65.8)	277	(40.2)
D	190	(27.6)	325	(47.1)	390	(56.5)	371	(53.8)	211	(30.6)
G*	---	---	---	---	---	---	---	---	---	---
J	230	(33.4)	415	(60.2)	461	(66.9)	471	(68.4)	302	(43.9)
Mean	212	(30.8)	376	(54.6)	432	(62.7)	432	(62.7)	263	(38.2)
Std. Dev.	17	(2.4)	38	(5.5)	31	(4.5)	44	(6.4)	39	(5.6)

*Lost data

Table 23 Bending component of preload stress in HMIP laboratory specimen, bolts A, D, G, J

Bolt	Location									
	1		2		3		4		5	
	MPa	(ksi)	MPa	(ksi)	MPa	(ksi)	MPa	(ksi)	MPa	(ksi)
A	1	(0.1)	14	(2.0)	13	(1.8)	50	(7.2)	65	(9.4)
D	86	(12.5)	114	(16.5)	85	(12.3)	98	(14.2)	20	(2.9)
G	---	---	---	---	---	---	---	---	---	---
J	39	(5.7)	16	(2.3)	21	(3.1)	37	(5.3)	40	(5.8)
Mean	42	(6.1)	48	(6.9)	40	(5.7)	61	(8.9)	42	(6.0)
Std. Dev.	35	(5.1)	47	(6.8)	32	(4.7)	26	(3.8)	19	(2.7)

Table 24 Preload stresses in HMIP laboratory specimen, bolts B, C, E, F, H, I, K, L

Bolt	Location			
	1		2	
	MPa	(ksi)	MPa	(ksi)
B	342	(49.6)	416	(60.3)
C	352	(51.1)	392	(56.9)
E	285	(41.3)	359	(52.1)
F	138	(20.0)	210	(30.5)
H	276	(40.0)	323	(46.9)
I	306	(44.4)	377	(54.7)
K	422	(61.3)	440	(63.8)
L	396	(57.4)	449	(65.1)
Mean	314	(45.6)	371	(53.8)
Std. Dev.	88	(12.8)	77	(11.2)

Static Tests

Static tests were conducted to determine the stress level induced in anchor bolts due to the ram force couple applied to the HMIP pole. These tests were conducted before and after development of preload in the anchor bolt connections. Significant bending stresses in anchor bolts made interpretation of non preload data difficult, but tensile stresses in the baseplate region of anchor bolts tended to agree with beam bending theory. Gages below the double-nutted connections confirmed the applicability of bending theory to the preloaded connections. As expected, preloaded connections exhibited significantly reduced anchor bolt stress variations in the baseplate region during the fatigue test.

Fatigue Test

A two million cycle fatigue test was conducted to establish the AASHTO fatigue category of the preloaded double-nutted connection in HMIP poles. The fatigue test stress range was chosen after study of expected service loads and fatigue category classification results of COSS specimen data. As noted, previous research (Frank 1978) indicated that bolt detail can be classified between AASHTO Category E and Category C, depending on nut tightness. Under current specifications, AASHTO Category C details can be used for connections that experience more than two million cycles of stress ranges of 70 MPa (10 ksi) (AASHTO 1985). In the current HMIP fatigue study, applied cyclic loads were selected to stress bolts most distant from the neutral axis (bolts A and G) to a range of 87 MPa (12.5 ksi) with a mean stress of 0.0 MPa. The second tier of bolts, B, L, F and H experienced a stress range of 75 MPa (10.8 ksi). This test established six data points for evaluation of the fatigue category of these connections. Table 25 summarizes the stress history of the 4 1/2 UNC anchor bolts of the HMIP specimen utilized in this test. Table 26 summarizes the AASHTO fatigue category established for each bolt in the fatigue test conducted here. A total of six bolts were cycled to AASHTO Category D. The fatigue test totaled 2,1760,000 cycles. The first 1.5 million cycles were conducted using the fixtures described earlier. During the last 600,000 cycles, a single ram was used at the end of the pole specimen. This was done to reduce stress concentrations at the mid-point through-hole connections that had repeatedly failed in fatigue. Although this increased the transverse shear stress in the anchor bolts, the level was relatively low and did not appear to affect the test. All angular positions of all top nuts were indexed to monitor any loosening that might occur during the fatigue test. No rotation or loosening of nuts was observed.

Table 25 Anchor bolts stress in fatigue test of HMIP 4 1/2 UNC laboratory specimens

Bolt	Stress Range, σ_R MPa	(ksi)	Mean Stress, σ_M, MPa	(ksi)	Number of Cycles
A	86	(12.5)	0	(0.0)	2,176,000
B	75	(10.8)	0	(0.0)	2,176,000
C	43	(6.3)	0	(0.0)	2,176,000
D	0	(0.0)	0	(0.0)	2,176,000
E	43	(6.3)	0	(0.0)	2,176,000
F	75	(10.8)	0	(0.0)	2,176,000
G	86	(12.5)	0	(0.0)	2,176,000
H	75	(10.8)	0	(0.0)	2,176,000
I	43	(6.3)	0	(0.0)	2,176,000
J	0	(0.0)	0	(0.0)	2,176,000
K	43	(6.3)	0	(0.0)	2,176,000
L	75	(10.8)	0	(0.0)	2,176,000

Table 26 AASHTO fatigue category of anchor bolts in fatigue test of HMIP 4 1/2 UNC laboratory specimens

Bolt	Stress Range, σ_R MPa	(ksi)	Number of Cycles	AASHTO Fatigue Category
A	86	(12.5)	2,176,000	D
B	75	(10.8)	2,176,000	D
C	43	(6.3)	2,176,000	E'
D	0	(0.0)	2,176,000	--
E	43	(6.3)	2,176,000	E'
F	75	(10.8)	2,176,000	D
G	86	(12.5)	2,176,000	D
H	75	(10.8)	2,176,000	D
I	43	(6.3)	2,176,000	E'
J	0	(0.0)	2,176,000	--
K	43	(6.3)	2,176,000	E'
L	75	(10.8)	2,176,000	D

No anchor bolt failures were observed in the fatigue test. However, the pole-to-baseplate weld failed once, and the through-pole ram connection near the mid-point of the HMIP pole failed repeatedly. Cracks in the fillet weld at the pole base were discovered after 200,000 cycles. The pole was removed and the weld repaired. After repair, the weld was tapered, recessed and peened to reduce residual tensile stresses in the toe region of the weld. No failures occurred in the weld over the remaining portion of the fatigue test. The weld failure regions are indicated in Figure 83. Photographs of the weld failures near bolts B and L are shown in Figures 84 and 85, respectively. Strain gages were installed at the base of the pole below bolt A and on a corner near bolt B. A stress range of 159 MPa (23 ksi) was recorded on the corner of the pole near bolt B. This stress range does not include local stress concentrations at the weld. The fillet weld at the pole base is an AASHTO fatigue Category E detail, and the fatigue test conducted here confirms this designation. The improvements made to the weld appear to have raised the AASHTO fatigue category to at least level C.

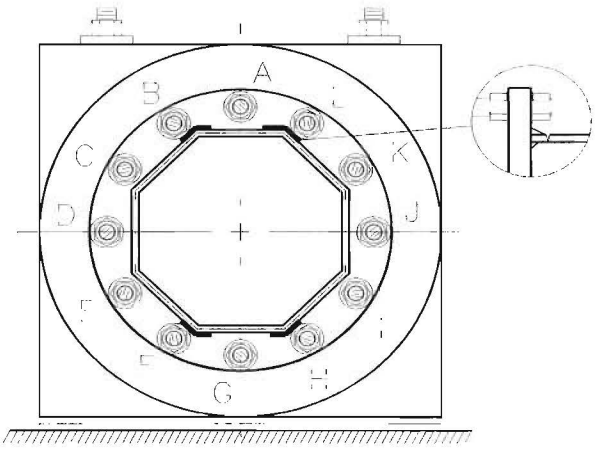

FIGURE 83 Fatigue induced cracks at toe of fillet weld in HMIP 4 1/2 UNC laboratory specimen.

FIGURE 84 Photograph of fatigue crack adjacent to bolt B in HMIP 4 1/2 UNC laboratory specimen.

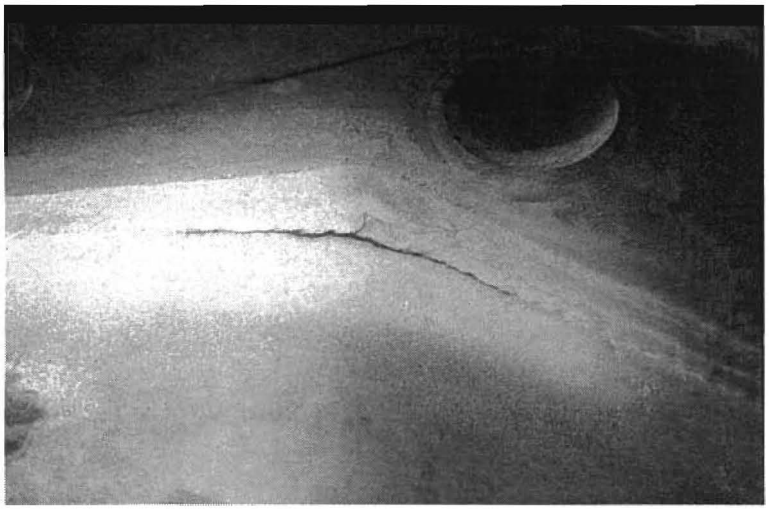

FIGURE 85 Photograph of fatigue crack adjacent to bolt L in HMIP 4 1/2 UNC laboratory specimen.

The mid-point connection failed repeatedly near the holes drilled in the pole for the through-pole connections. Figure 86 shows typical fatigue induced cracks found in this connection during testing. These cracks were repaired by drilling out the crack tip and gouging and rewelding the

cracks. Near the end of testing a cover plate was installed over the cracked section, and the mid-point ram was removed. Cycling of the base connection was completed using only the ram at the end of the pole. This increased the shear stress in the pole but reduced the stresses in the mid-point region, since application of the transverse ram load was eliminated.

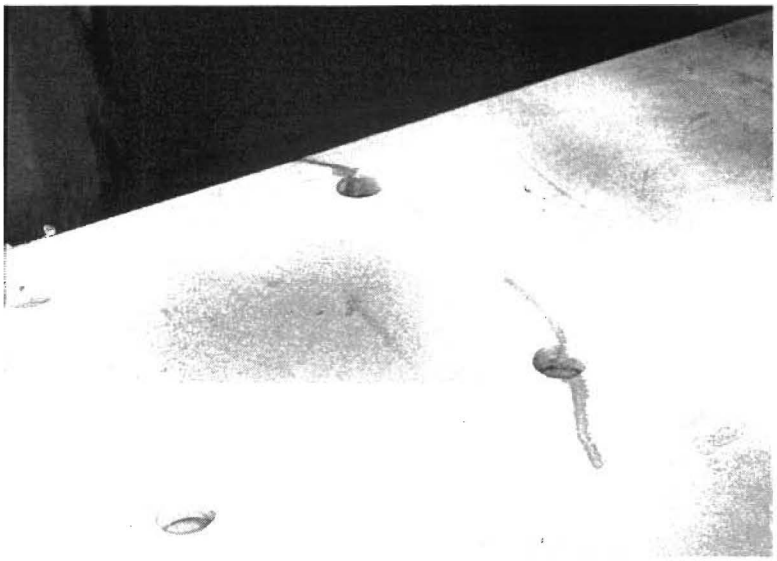

FIGURE 86 Fatigue cracks near holes for mid-point connection in 4 1/2 UNC HMIP laboratory specimen.

CONCLUSIONS

This study investigated the tightening procedures used to tighten anchor bolts past snug tight, the preload induced at different degrees of tightness, and the effects of preload on fatigue life. The findings and conclusions of this study are listed as follows:

- Regarding the desirability of tightening nuts to induce a preload, it is concluded that:

1. The large-diameter anchor bolts tested indicated an infinite fatigue life when loaded at a 70 MPa (10 ksi) stress range.
2. When the large-diameter bolts tested were tightened to 60 degrees past snug tight, no nut loosening was observed in any fatigue test. Observable nut rotation did not occur. If creep or relaxation in the bolt, nut, or galvanizing occurred, its signficance was negligible.
3. The large-diameter anchor bolt details tested when the nuts are tightened to 60 degrees past snug tight can be classified as an AASHTO Category D detail.
4. The preload reduces the live load stress in the region between the nuts. A finite element study of the double nut anchor bolt detail indicates stress concentrations of approximately 1.4 occur in both snug tight connections and preloaded connections. In a misaligned bolt, the stress concentrations rise to nearly 3. It was determined that the addition of a preload two times greater than the maximum bolt axial stress amplitude shifts the location of failure from the region between the top and bottom nuts to a location below the bottom nut. A 40% reduction and relocation of the maximum stress range causes this shift. A preload of between one-third and twice the maximum axial stress amplitude reduces the stress range approximately 25% to 40%. A preload less than one-third the maximum axial stress moves the location of failure back to Location 1 and reduces the stress range from 25% to 0% when there is no preload. These observations are in general agreement with findings in previous studies of double nut anchor bolt connections and in general agreement with laboratory observations in the present study.

- Regarding the methods useful for achieving a preload:

5. One person using a 7 kg (16 lb) sledgehammer and knocker wrench can tighten the nuts

effectively to a preload of 400 to 450 MPa (60 to 65 ksi).

6. The torque required to turn large-diameter anchor bolts to 60 degrees past snug is too large to be reliably applied in the field with a 3 m (10 ft) long cheater pipe.

7. The torque required to tighten the nuts to specified rotation was not consistent from bolt to bolt or even on the same bolt, indicating that the use of a calibrated torque wrench is not a reliable way to achieve a repeatable preload.

- Regarding the methods potentially useful for inspecting nuts for tightness in the field:

8. The method of striking the nut with a hammer to determine nut tightness is very subjective and probably not practical for detecting the difference between large-diameter nuts that are snug tight and nuts that are tightened past snug tight. Nuts that are less than snug tight omit a noticeably duller sound than nuts that are snug tight, however. The effect of spot welding the nut to the washer and to the base plate on this inspection technique was not investigated.

9. Ultrasonic testing methods were not successful in quantifying or verifying the tightness of the double nut system.

10. The use of a 7 kg (16 lb) hammer and slug wrench is a practical method to test for tightness of grade 105 bolts.

- General conclusions from the laboratory tests include:

11. The weld between the pole and baseplate is the critical connection concerning fatigue failure.

12. The 8 UN threaded bolts exhibited a higher preload when the nuts were tightened, loosened, and re-tightened.

- Regarding field performance of the monitored HMIP and COSS structures:

13. Many of the cyclic stresses which cause fatigue damage of large-diameter anchor bolts in COSS and HMIP structures may be attributed to vortex shedding. In both structures instrumented in the present study, however, these stresses are determined to be so small that they can be discounted in the fatigue design of HMIP structures. Based on the monitored behavior of a test HMIP structure over a period of 0.3 yr, it was determined that the anchor bolts should have an infinite life in their current snug tight position.

14. The dynamic properties of the test HMIP structure were determined and an analytical model was developed to predict the effective stress range seen in the anchor bolts due to vortex shedding. The model predicted the effective stress range observed in experimental data within 11 %.

- Regarding the significance of misaligned bolts:

15. From the numerical studies, it was observed that misaligned snug tight and preloaded double nut anchor bolt configurations are expected to give degraded performance with regard to fatigue. Higher stress ranges are seen in the snug tight condition when the bolt is misaligned, and some of the beneficial effect of the preload is lost in the preloaded misaligned bolt. Because anchor bolts in HMIP structures see relatively low stress ranges, the beneficial fatigue effects from preloading are generally not needed. It is therefore concluded that bolt alignment is more critical than bolt preload when considering the fatigue behavior of large-diameter anchor bolts in HMIP structures.

RECOMMENDATIONS

- The following recommendations are offered:

1. The Department should adopt a standard specification for tightening of large-diameter anchor bolts by the contractor at the time of installation. A draft specification is given in Appendix D.
2. The Department should identify 20-30 selected COSS structures for field inspection. Candidate structures should be selected based on time in service in geographical areas subject to frequent high wind load conditions. The field inspections should include ultrasonic inspection of all anchor bolts for defects, the inspection of the nuts for tightness using a slug wrench and sledgehammer, and inspection of the pole-to-baseplate weld for fatigue cracks. This latter inspection should be accomplished visually using a dye-penetrant technique, or ultrasonically, depending on the capabilities available. The findings of this field inspection should be reviewed to determine whether additional field inspection or research is recommended.

Recommendations for Further Research

- Based on the findings of the current research, the following topics are suggested for further research:

3. Analysis of stress range histogram data from the test HMIP structure indicated that the pole-to-baseplate welded connection was critical with regard to fatigue. Also, both the HMIP and COSS pole-to-baseplate welds cracked repeatedly during laboratory tests where they were used to apply fatigue loadings to anchor bolts. Because of these observations, any further research regarding fatigue of HMIP or COSS should include evaluation of the weld detail.
4. A more complete vortex shedding model should be developed in order to more accurately predict the cross wind forces induced by this phenomenon.

REFERENCES

AASHTO (1985) "Standard specifications for structural supports for highway signs, luminaires and traffic signals," American Association of State Highway and Transportation Officials, Washington, DC.

AASHTO (1994) "Standard specifications for structural supports for highway signs, luminaires and traffic signals," American Association of State Highway and Transportation Officials, Washington, DC.

ABAQUS (1995) ABAQUS Users Manual Vols. 1 & 2, Ver. 5.4. Hibbitt, Karlson & Sorenson, Inc. Providence, RI.

Abraham, R.C. (1996) "Tightening procedures for large-diameter anchor bolts," Thesis in Progress, Texas A&M University.

AISC (1989), Manual of Steel Construction, 7th ed., American Institute of Steel Construction, New York.

AWS (1984) "Structural Welding Code--Steel," 8th ed., American Welding Society.

Bedolla, R. (1994) F. Benson interview at his East Nueces County Maintenance Office, December 1, 1994, Corpus Christi District, Texas Department of Transportation.

Bickford, J. H. (1987) "Rating the safety of high-strength bolts," *Machine Design*, 111- 112.

Blevins, R.D. (1990) Flow-Induced Vibration, 2nd ed., Van Nostrand Reinhold.

Burkett, K. and J. Yang (1994) F. Benson interview at Design Division Office, December 20,

1994, Texas Department of Transportation, Austin, Texas.

Clough, R.W. And J. Penzien (1993) Dynamics of Structures, McGraw Hill.

Culp, J.D., M. Witteveen, and H.L. Wong (1990) "Action plan for cantilever sign problem--report to management," Michigan Department of Transportation.

Dann, R. T. (1975) "How much preload for fasteners?" *Machine Design*, 66-69.

Fisher, J.W. (1990) Letter to James D. Culp, P.E., Center for Advanced Technology For Large Structural Systems at Lehigh University, July 12, 1990.

Fisher, F. L. and K. H. Frank (1978) "Axial tension fatigue strength of anchor bolts," Report No. 172-2F. Center for Highway Research, University of Texas at Austin.

Fisher, J. W. (1990) " Preliminary report to James D. Culp concerning the studies and assessment of anchor bolts that developed fatigue cracks which lead to failure," Department of Civil Engineering, Lehigh University, Lehigh, PA.

Fisher, J. W. (1990) "Report to James D. Culp concerning the studies and assessment of anchor bolts that developed fatigue cracks which lead to failure," Department of Civil Engineering, Lehigh University, Lehigh, PA.

Frank, K.H. (1978) "Fatigue of anchor bolts," Center for Highway Research, Report 172-2F, The University of Texas at Austin.

Hasselwander, G.B., J. O. Jirsa, and J. E. Breen (1974) "A Guide to the selection of high-strength anchor bolt material," Center for Highway Research Report 29-1, The University of Texas at Austin.

Higgins, C. C. and R.E. Klingner (1991) "Effect of environmental cycling on the strength of short retrofit anchor bolts," Center for Highway Research Report 1208-1F, The University of Texas at Austin.

Hinkle, C. (1995) F. Benson telephone interview, January 12, 1995, Thomas and Betts, Memphis, TN.

Lockmann, H. W. (1981) "Tightening of heavy bolted joints - advantages of the hydraulic method of tightening--Part 1," Sheet Metal Industries, 214-221.

Lower, B. R. and L. J. Pearson (1982) "Static and dynamic properties of anchor bolts for sign supports," Report No. R-1197, Materials and Technology Division, Michigan Department of Transportation.

Lower, B. R. and L. J. Pearson (1987) "Static and dynamic properties of anchor bolts for sign supports--Final report," Report No. R-1283, Materials and Technology Division, Michigan Department of Transportation.

Lower, B. R. and L. J. Pearson (1987) "Static and dynamic properties of anchor bolts for sign supports--Draft," Research Laboratory Section of the Materials and Technology Division Research Report No. R-1283, Michigan Department of Transportation.

Maruyama, K. and M. Nakagawa (1985) "Proposal of new torque control method and new design system in bolted joint," Bull. P.M.E. (T.I.T.), No. 55, 25-29.

McCrum, R. (1993) "Brief summary of michigan's research work with anchor bolts on cantilevered sign structures," Materials and Technology Division, Michigan Department of Transportation.

McDonald, J. R., K.C. Mehta, W. Oler, and N. Pulipaka (1995) "Wind Load Effects on Signs, Luminaires and Traffic Signal Structures," Wind Engineering Research Center Report No. 1303-F (Draft), Texas Tech University.

MDOT (1994) "Procedure for the inspection of sign structures," Materials and Technology Division, Michigan Department of Transportation.

MDOT (1994) "Special Provisions for Sign and Light Standard Anchor Bolts," Michigan Department of Transportation Bureau of Highways Specification SP8.07(A).

MDOT (1994) "Special Provision for cantilever sign support erection," Michigan Department of Transportation, Bureau of Highways.

MDOT (1994) "Cantilever anchor bolt tightening procedure," Materials and Technology Division, Michigan Department of Transportation.

Meyers, B. (1995) F. Benson interview at King Ranch Gas Plant Headquarters Office, February 24, 1995, Exxon Corporation King Ranch Gas Plant, King Ranch, Kleberg County, Texas.

Miner, M.A. (1945) "Cumulative damage in fatigue," Journal of Engineering Mechanics, Vol. 67, ASME, New York.

Nava, F. and P. Wheeler (1994) F. Benson interview, December 1, 1994, V. C. Huff and Saxet Fabrication respectively, Corpus Christi, TX.

Ness, B. W. and R. D. Till (1992) "Cantilever sign structure inspection final report," M&T Report No. R-1319, Materials and Technology Division, Michigan Department of Transportation.

Peterson, R.E. (1974) Stress Concentration Factors, John Wiley & Sons.

Polasek, M. (1994) F. Benson telephone interview on November 30, 1994, Central and South West Services, Tulsa, OK.

Product Engineering (1977) "Thread forms and torque systems boost reliability of bolted joints," Product Engineering, 37-41.

Siavelis M. P. and J. N. Hosteny (1984) "Fastener loosening: the effects," Assembling Engineering, 36-38.

South, J.M. (1994) "Fatigue analysis of overhead sign and signal structures" Physical Research Report Number 115, Illinois Department of Transportation, Bureau of Materials and Physical Research.

Till, R. (1992) "M DOT mates," Materials and Technology Engineering and Science, Michigan Department of Transportation, Issue No. 62.

Turner, D. and R. Stone (1994) F. Benson interview at Traffic Signal Offices, November 3, 1994, Corpus Christi District, Texas Department of Transportation.

Walton, N.E. and N.J. Rowan (1969) "Final Report: Supplementary Studies in Highway Illumination," Texas Transportation Institute Research Report 75-13F, Texas A&M University, College Station.

Wong H. L., J. D. Culp and M. Witteveen (1990) "Action plan for cantilever sign problem--Report to Management," Materials and Technology Division, Maintenance Division, and Design Division, Michigan Department of Transportation.

Wong, S. and H. Painter (1994) F. Benson interview at Traffic Signal Office, December 15, 1994, Houston District, Texas Department of Transportation.

APPENDIX A--SCHEMATIC DRAWINGS OF HMIP AND COSS SECTIONS

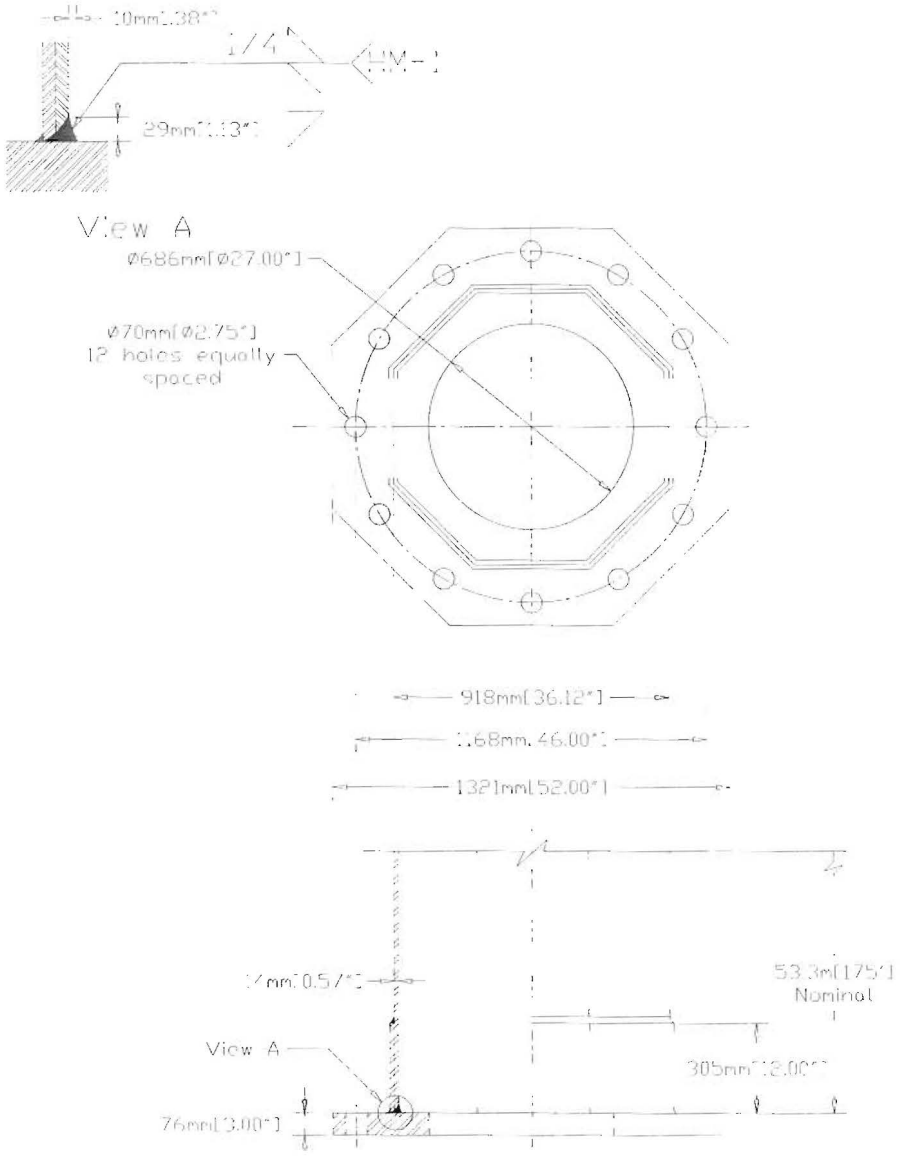

Figure A-1 Schematic drawing of HMIP bottom segment and base plate used in field study.

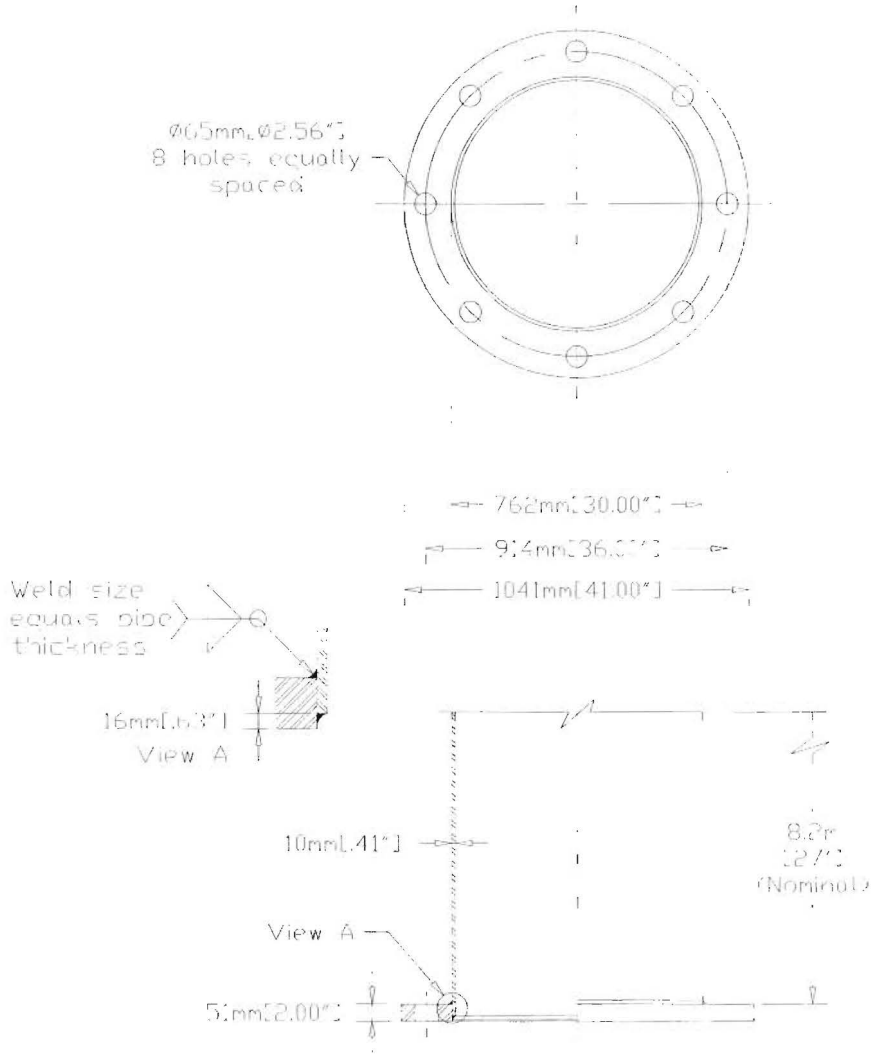

Figure A-2 Schematic drawing of COSS structure tower and base plate used in field study.

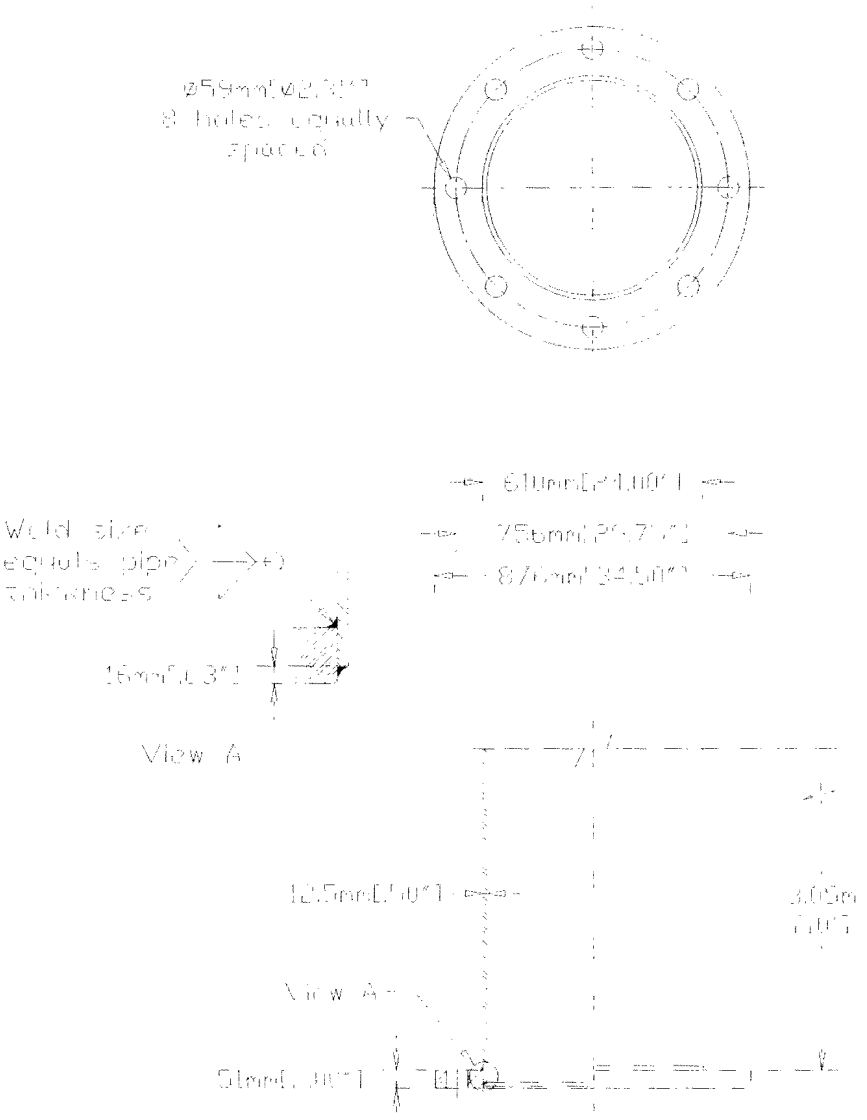

Figure A-3 Schematic drawing of COSS specimen used in laboratory study.

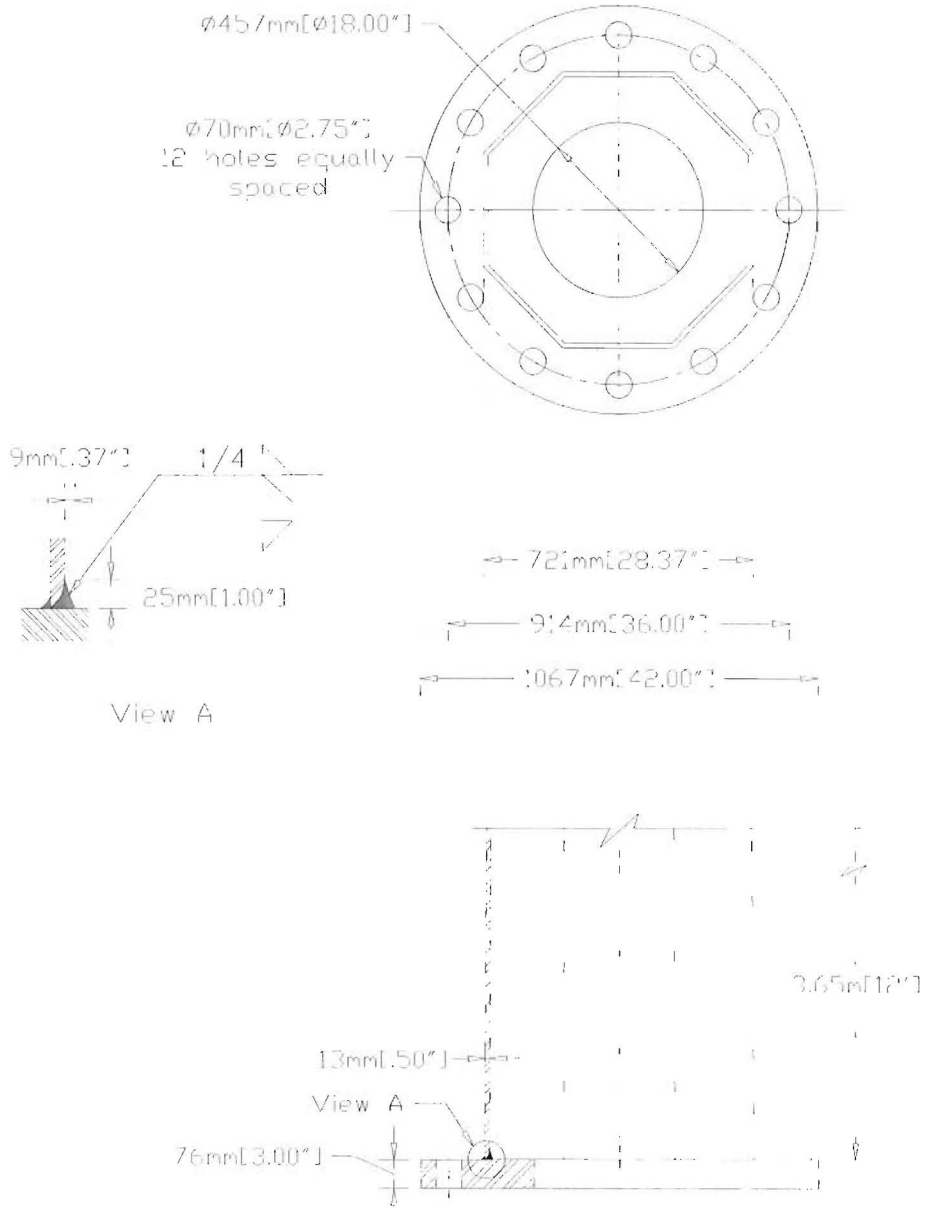

Figure A-4 Schematic drawing of HMIP specimen used in laboratory study.

APPENDIX B--VORTEX SHEDDING LOAD MECHANISM AND HMIP STRUCTURES

VORTEX SHEDDING LOAD MECHANISM AND HMIP STRUCTURES

INTRODUCTION TO VORTEX SHEDDING

Vortex shedding is a phenomenon which can occur when a fluid flows past a bluff body. Vortex shedding occurs in HMIPs when vortices, or swirling pockets of air, are alternately shed from the crosswind sides of the pole. These vortices cause oscillating pressures on the pole and these pressure differentials in turn induce transverse vibrations into the structure. A visual representation of the vortex shedding phenomenon can be seen in Figure B-1. Here, the crosswind deflections caused by a wind speed, U, are denoted as A_y, and the equivalent pole diameter is D_e. A more detailed description of the vortex shedding process is given by Blevins (Blevins 1990):

> "As a fluid particle flows toward the leading edge of a cylinder, the pressure in the fluid particle rises from the free stream pressure to the stagnation pressure. The high fluid pressure near the leading edge impels flow about the cylinder as boundary layers develop about both sides. However, the high pressure is not sufficient to force the flow about the back of the cylinder at high Reynolds numbers. Near the widest section of the cylinder, the boundary layers separate from each side of the cylinder surface and form two shear layers that trail aft in the flow and bound the wake. Since the innermost portion of the shear layers, which is in contact with the cylinder, moves much more slowly than the outermost portion, the shear layers roll into the near wake, where they fold on each other and coalesce into discrete swirling vortices. A regular pattern of vortices, called a vortex street, trails aft in the wake. The vortices interact with the cylinder and they are the source of the effects called vortex-induced vibration."

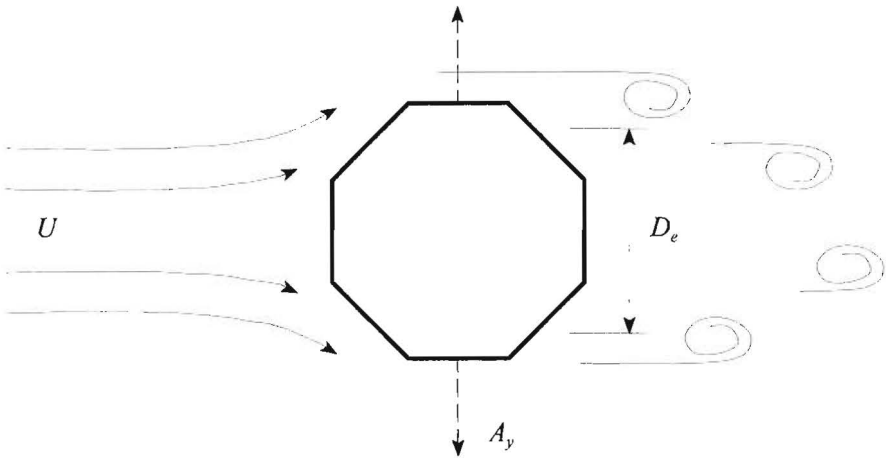

Figure B-1 Representation of vortex shedding.

The vortex shedding phenomenon is a function of the Reynolds number. The Reynolds number is nondimensional term that represents the ratio between the inertial force and the friction force on a body. The fluid is air, and the body is the HMIP. Now the Reynolds number is given by:

$$Re = \frac{UD_e}{\nu},$$

where:

Re	=	Reynolds number,
U	=	wind speed, m/s (ft/s),
D_e	=	equivalent pole diameter, m (ft), and
ν	=	kinematic viscosity of air = 1.681×10^{-3} m^2/s (1.564×10^{-4} ft^2/s).

For Reynolds numbers between 300 and 1.5×10^5, the flow is termed subcritical. Vortex shedding caused by subcritical flow is characterized by strong and periodic crosswind vibrations. Alternatively, for Reynolds numbers between 1.5×10^5 and 3.5×10^6, the flow is termed transitional flow. Vortex shedding caused by transitional flow is characterized by turbulent boundary layers and a drop in the drag coefficient. Finally, for Reynolds numbers greater than

3.5×10^6, the flow is termed supercritical. Vortex shedding caused by winds in the supercritical range again show periodic vibrations caused by a turbulent boundary layer. Wind speeds between 0 m/s and 22 m/s (0 mph and 50 mph) are common conditions that induce vortex shedding and give Reynolds numbers in the subcritical to transitional range.

Another dimensionless parameter used to characterize fluid flow in the process of vortex shedding is the Strouhal number which relates the dominant vortex shedding frequency, the wind speed, and the equivalent pole diameter. The Strouhal number is given by:

$$S = \frac{f_s D_e}{U} ,$$

where:

S = Strouhal number and

f_s = vortex shedding frequency, Hz.

Vortex shedding in the transitional range occurs at $S \approx 0.2$. The current AASHTO design guide for sign and signal structures suggests using $S = 0.15$ (AASHTO 1994). The Strouhal number is a function of the diameter and can be approximated by the equivalent pole diameter.

PREDICTION OF VORTEX SHEDDING FORCES

Because a HMIP is a linearly tapered, octagonal cross-sectioned structure, its response to vortex shedding is much more complex than the method presented here. Because it is tapered, the HMIP does not respond as a prismatic structure; rather, sections of the pole respond differently in the presence of wind induced vibrations. The approximate prediction method presented relates an HMIP to a circular cantilevered pole of equivalent stiffness based on the calculated equivalent properties. This method has been used in previous research projects (South 1994), and current AASHTO specifications use a similar approach with regards to crosswind forces acting on a structure (AASHTO 1994). This gives validity to the method presented, but the reader is advised that this is an approximation of the vortex shedding phenomenon and is given as a comparison to

current AASHTO methods.

First, consider the forces acting on the HMIP in the windward direction. The forces imposed in this direction are caused by drag effects and are given by:

$$F_D = \frac{1}{2}\rho U^2 D_e C_D \ ,$$

where:

F_D = drag force per unit length, N/m (lb/ft),

ρ = density of air = 9.85×10^{-4} kg/m^3 (0.002378 slug/ft^3), and

C_D = drag coefficient.

Current AASHTO guidelines suggest using $C_D = 1.2$ for octagonal cross sections (AASHTO 1994). In general, the drag coefficient increases with increasing cross wind vibration. A new expression for the drag coefficient increased by vortex shedding effects is given as:

$$C_D' = C_D\left[1 + \left(\frac{A_y}{D_e}\right)\right] \ ,$$

where:

C'_D = increased drag coefficient and

A_y = cross wind deflection, m (ft).

Now, the force on the HMIP in the windward direction can be expressed as:

$$F_D = \frac{1}{2}\rho U^2 D_e C_D' \ .$$

The ultimate goal is to find the equivalent static forces which must be applied to the pole in order to simulate the stresses induced in the bolts by vortex shedding. These forces can be considered to be caused by lift effects. This lift force is caused by varying pressures on the sides of the pole induced by the shedding vortices and can be expressed as:

$$F_L = \frac{1}{2}\rho U^2 D_e C_L \ ,$$

where:

F_L = lift force per unit length, N/m (lb/ft) and

C_L = lift coefficient.

Now, the lift coefficient must be found.

Two methods exist to predict vortex shedding induced vibrations by determination of the lift coefficient. The first model is a linear harmonic model which does not incorporate feedback effects. This model assumes that the vortex shedding response is sinusoidal and the forces due to the vibration are given by:

$$F_L = \frac{1}{2}\rho U^2 D_e C_L' \sin(\omega_s t) \quad ,$$

where:

ω_s = $2\pi f_s$ = circular vortex shedding frequency, rad/s and

t = time, s.

This response reaches a maximum at resonance and here, solution of the equation of motion yields an expression for the lift coefficient as:

$$C_L = \frac{4\pi S^2 \delta_r A_y}{D_e} \quad ,$$

where δ_r is the reduced damping term. Because this method idealizes the vortex shedding process as purely sinusoidal and does not include feedback effects, the second procedure is preferred.

The reduced damping term is defined as:

$$\delta_r = \frac{2m_e(2\pi\xi)}{\rho D_e^2} \quad ,$$

where:

m_e = equivalent mass per unit length, kg/m (slug/ft) and

ξ = damping factor.

This expression is the mass ratio times the structural damping factor. In general, when the

reduced damping increases, the crosswind vibrations decrease.

The second method for predicting vortex shedding induced vibrations is called the wake oscillator model. This model assumes that the vortex shedding process is self-excited and can be modeled by a simple, nonlinear oscillator. This method assumes:

1) Inviscid flow provides a good approximation for the flow field outside near the wake.
2) There exists a well-formed, two-dimensional vortex street with a well-defined shedding frequency.
3) The force exerted on the cylinder by the flow depends on the velocity and acceleration of the flow relative to the cylinder.

This method is useful because the crosswind vibrations can be expressed in terms of the reduced damping in the wake oscillator model. These vibrations are:

$$\frac{A_y}{D_e} = \frac{0.07\Gamma_n}{(1.9 + \delta_r)S^2}\sqrt{0.3 + \frac{0.72}{(1.9 + \delta_r)S}},$$

where Γ_n is the dimensionless mode factor for mode n. For a cantilevered uniform beam the first three mode factors are: $\Gamma_1 = 1.305$, $\Gamma_2 = 1.499$, $\Gamma_3 = 1.537$. Only the first three modes are assumed to cause significant vortex shedding responses. Using the equivalent pole properties, the HMIP can be approximated as a cantilevered uniform beam. Now, the lift coefficient, C_L, can be found by the following relationship:

$$C_L = 0.35 + 0.60\left(\frac{A_y}{D_e}\right) - 0.93\left(\frac{A_y}{D_e}\right)^2.$$

This equation is a fit of experimental data by Blevins (1990).

Large amplitude crosswind vibrations, A_y, are experienced when the wind causes a vortex shedding frequency near the natural frequency of the HMIP. This situation occurs when:

$$f_s = \frac{SU}{D_e} \approx f_n ,$$

where f_n is the structure natural frequency for mode n. This situation is known as lock-in and is caused by the effect of the cross section motion on the wake of the flow. The lock-in band is the range of frequencies over which the pole vibration controls the vortex shedding frequency. The lock-in band gives the critical behavior of a structure responding to vortex shedding effects. A response can be obtained for each wind speed, however. The structure is behaving in the lock-in band when:

$$0.6 \leq \frac{f_n}{f_s} \leq 1.4 .$$

The frequency in which the vortices are shed per wind-induced cycle is equal to the modal natural frequency of the pole which is excited. It is interesting to note that the vortices are shed from the opposite side of the pole experiencing the maximum displacement when the structure natural frequency is slightly below the vortex shedding frequency. On the other hand, when the structure frequency is slightly higher than the vortex shedding frequency, the vortex is shed from the same side experiencing maximum displacement.

Now that the lifting or vortex shedding forces can be calculated, the anchor bolt stresses are determined by determining the column base moment as:

$$M = 6F_L L_e D_e \left(500 F_L L_e D_e\right) ,$$

where M is the column base moment, in N-mm (lb-in.). The anchor bolt stresses can be found as:

$$\sigma = \frac{Mc}{I} ,$$

where:

σ = anchor bolt stress, MPa (psi),

c = distance of bolt from the neutral axis, mm (in.), and

I = moment of inertia of bolt group, mm^4 (in^4).

A summary of the analytical procedure to predict anchor bolt stresses is summarized in Figure B-2. This method provides an estimation of the stress seen in an anchor bolt due to vortex shedding induced vibrations. The stress range calculated by the model is taken as twice the stress in the anchor bolt and is comparable to the effective stress range. The stress range estimated by the model at each wind speed can be seen in Table B-1. The majority of these expected stress ranges fall below 7 MPa (1 ksi). This result is in agreement with the stress range histogram data presented from the test HMIP structure.

Basic Input Parameters

1. Equivalent pole diameter, D_e
2. Equivalent pole length, L_e
3. Equivalent mass per unit length, m_e
4. Moment of inertia of bolt, I
5. Structure natural frequencies, f_n , n = 1,2,3
6. Fluid density, ρ
7. Fluid kinematic viscosity, v
8. Structural damping, ξ
9. Assume Strouhal number, S = 0.2
10. Wind speeds, U

Reduced Damping

1. Calculate reduced damping, δ_r

$$\delta_r = \frac{2m_e(2\pi\xi)}{\rho D_e^2}$$

Vortex Shedding Frequencies

1. Calculate stationary vortex shedding frequencies, f_s, for each wind speed

$$f_s = \frac{SU}{D_e}$$

Nondimensional Parameters

1. Calculate Reynolds number, Re, for each wind speed

$$R_e = \frac{UD_e}{\upsilon}$$

2. f_n/f_s for each wind speed for modes n = 1, 2, 3

Check For Significant Amplitudes

1. Is $0.6 \le f_n/f_s \le 1.4$?
   If YES then proceed
   If NO then go to next mode

Figure B-2 Flow chart to determine vortex shedding stresses (continued next page).

Resonant Amplitude

1. Compute A_y/D_e for each mode

$$\frac{A_y}{D_e} = \frac{0.07\Gamma_n}{(1.9 + \delta_r)S^2}\sqrt{0.3 + \frac{0.72}{(1.9 + \delta_r)S}}$$

Lift Coefficient

1. Calculate lift coefficient, C_L for each mode using A_y/D_e for that mode

$$C_L = 0.35 + 0.60\left(\frac{A_y}{D_e}\right) - 0.93\left(\frac{A_y}{D_e}\right)^2$$

2. Take C_L to be the maximum value from mode 1, 2, or 3

Lift Force

1. Compute the lift force, F_L

$$F_L = \frac{1}{2}\rho U^2 D_e C_L$$

2. Take C_L to be the maximum value from mode 1,2, or 3

Base Moment

1. Compute the base moment, M

$$M = 6F_L L_e D_e\left(500F_L L_e D_e\right)$$

Anchor Bolt Stress

1. Compute the anchor bolt stress

$$\sigma = \frac{Mc}{I}$$

Figure B-2 Continued.

Table B-1 Prediction of vortex shedding stress ranges.

Wind Speed		Stress Range		Wind Speed		Stress Range	
m/s	mph	MPa	psi	m/s	mph	MPa	psi
0.4	1	0.00	0.4	11.6	26	2.02	293.3
0.8	2	0.01	1.7	12.0	27	2.18	316.3
1.3	3	0.03	3.9	12.5	28	2.30	333.8
1.7	4	0.05	6.8	12.9	29	2.47	358.1
2.2	5	0.07	10.8	13.4	30	2.64	383.2
2.6	6	0.11	15.6	13.8	31	2.82	409.2
3.1	7	0.15	21.2	14.3	32	3.01	436.0
3.5	8	0.19	27.8	14.7	33	3.20	463.7
4.0	9	0.24	35.1	15.2	34	3.40	492.2
4.4	10	0.30	43.4	15.6	35	3.60	521.6
4.9	11	0.36	52.5	16.0	36	3.81	551.8
5.3	12	0.43	62.5	16.5	37	4.02	582.9
5.8	13	0.51	73.3	16.9	38	4.24	614.8
6.2	14	0.59	85.0	17.4	39	4.47	647.6
6.7	15	0.67	97.6	17.8	40	4.70	681.3
7.1	16	0.77	111.1	18.3	41	4.94	715.7
7.6	17	0.87	125.4	18.7	42	5.18	751.1
8.0	18	0.97	140.6	19.2	43	5.43	787.3
8.4	19	1.08	156.6	19.6	44	5.69	824.3
8.9	20	1.20	173.5	20.1	45	5.95	862.2
9.3	21	1.32	191.3	20.5	46	6.22	901.0
9.8	22	1.45	210.0	21.0	47	6.49	940.6
10.3	23	1.58	229.5	21.4	48	6.77	981.0
10.7	24	1.72	249.9	21.9	49	7.05	1022.3
11.1	25	1.87	271.2	22.3	50	7.34	1064.5

This model is compared to a representative trace of wind speed and anchor bolt stress data. One set of data was collected on February 26, 1996. On this day, the wind was out of the south gusting between 5 m/s (11 mph) and 8 m/s (18 mph). The wind speed variation with time can be seen in Figure B-3. The stress data for the west anchor bolt can be seen in Figure B-4 and shows the vortex shedding induced cyclic stresses.

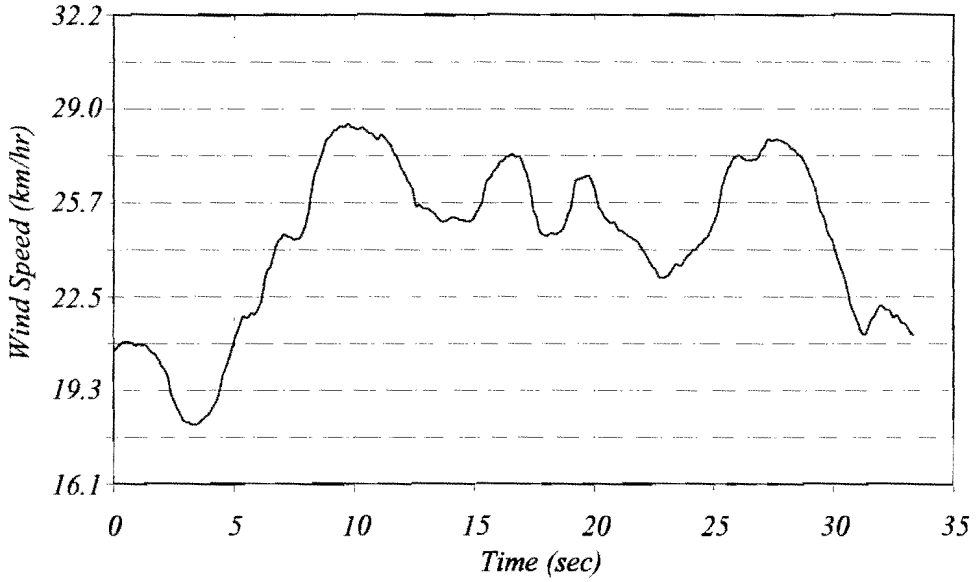

Figure B-3 Wind speed variation with time, February 26, 1996.

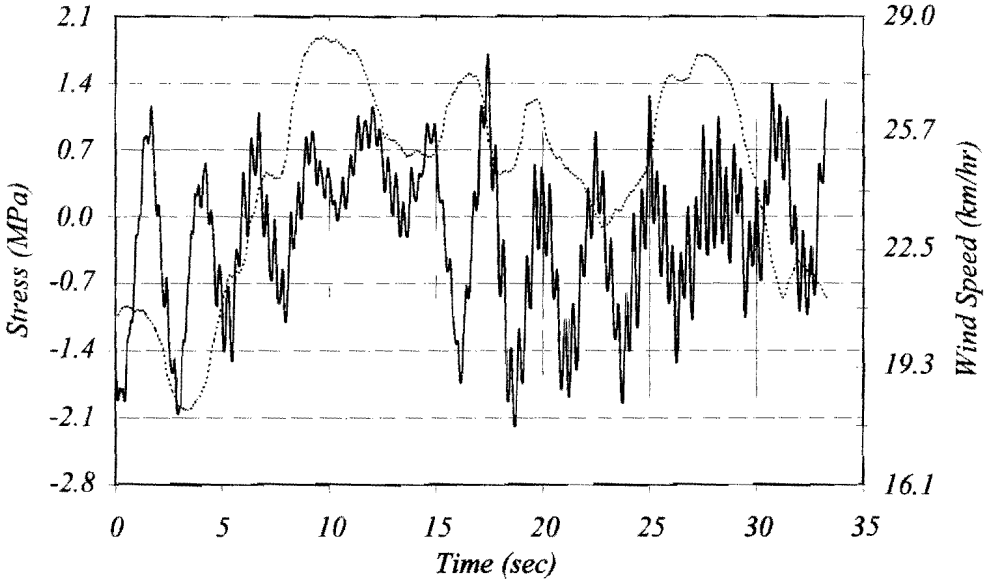

Figure B-4 West bolt stress variation with time, February 2, 1996.

When the data in Figure B-4 is analyzed to determine the number of stress cycles, an effective stress range can be calculated. For this set of data, the effective stress range is 1.1 MPa (156 psi). The average wind speed of the data in Figure B-3 is 6.7 m/s (15 mph). The estimated stress range using this wind speed with Table B-1 is 0.7 MPa (98 psi), which gives a difference of 46 percent. On the other hand, if the maximum wind speed of 8.0 m/s (18 mph) seen in Figure B-3 is used, the estimated stress range is 1.0 MPa (141 psi). This value is within 11 percent of the effective stress range seen from the representative trace.

Current AASHTO design guidelines for sign and signal structures incorporate a method to account for vortex shedding induced vibrations in response to fatigue design. A simplified formula that applies a pressure to the cross-wind sides of the pole is given as:

$$P_t = \frac{P}{2\beta},$$

where:

P_t = transverse wind pressure, Pa (lb/ft^2),

P = nongusted wind pressure, Pa (lb/ft^2), and

β = structural damping.

The nongusted wind pressure is given as :

$$P = 0.00256 U^2 C_d C_h (0.0473 U^2 C_d C_h) ,$$

where:

C_d = drag coefficient = 1.3 and

C_h = height coefficient = 1.5.

AASHTO suggests calculating the transverse wind pressure based on the critical wind speed for a given mode. AAHSTO suggests using $1/2\beta = 100$, which assumes a damping = 0.005 (0.5%). This method assumes that vortex shedding only occurs at the critical velocity for each mode, but crosswind vibrations can be calculated for each wind speed. When this is done and the anchor bolt stresses and stress ranges are calculated as shown previously, a comparison of the two methods can be presented. The comparison of the presented analytical approximation and the AASHTO recommendation for expected anchor bolt stress ranges can be seen in Figure B-5.

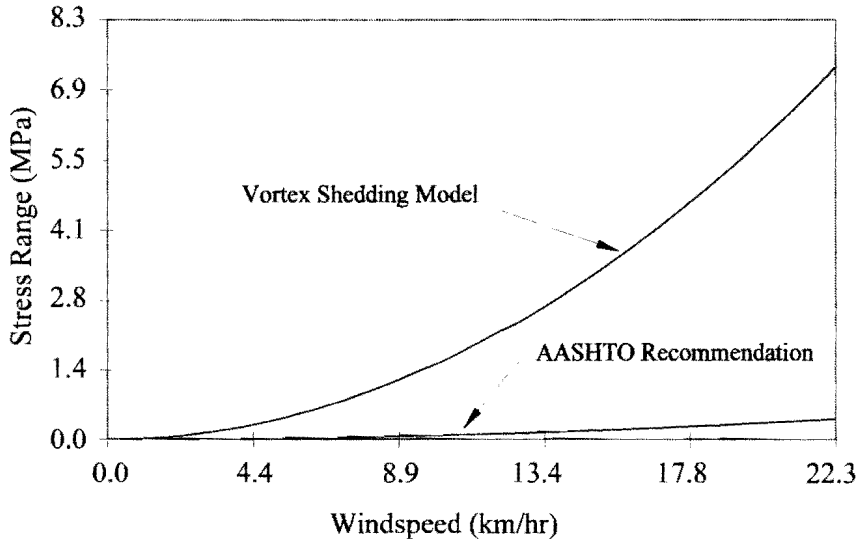

Figure B-5 Comparison of vortex shedding model and AASHTO recommendations.

Galloping is defined as an instability of structures in currents. All noncircular cross

sections are susceptible to galloping because the fluid force changes with orientation to the flow. This phenomenon can cause large scale vibrations and instability if the oscillating fluid force tends to increase the vibration. A structure in susceptible to galloping when:

$$\frac{U}{f_n D_e} > 20 .$$

For the first mode of vibration, the HMIP is susceptible to galloping at wind speeds above 3.6 m/s (8 mph). For the second mode, galloping could theoretically occur at wind speeds above 12 m/s (27 mph). The HMIP is not susceptible to galloping in modes three and four.

In conclusion, the phenomenon of vortex shedding has been introduced and its effects on HMIP structures have been studied. The analytical model to predict vortex shedding induced stresses in HMIP anchor bolts provides a reasonable estimation of the effective stress range seen in the anchor bolts at a given wind speed. The predicted stress ranges compare in magnitude to the stress range histogram data collected on the test structure. This model can be used with either an average yearly wind speed or a wind speed histogram to estimate the effective stress ranges in anchor bolts and estimate a structural fatigue life in addition to using the critical wind speeds. However, because of the low stress ranges caused by the vortex shedding phenomenon, vortex shedding is not critical for fatigue in HMIP structures and can be discounted in fatigue design.

APPENDIX C--EVALUATION OF DYNAMIC CHARACTERISTICS OF HMIP STRUCTURE

EVALUATION OF DYNAMIC CHARACTERISTICS OF HMIP STRUCTURE

The dynamic vibrational properties of the pole strongly influence the HMIP anchor bolt stresses induced by wind forces and vortex shedding forces. When an HMIP is acted upon by a dynamic load such as wind, the magnitudes of the anchor bolt stresses are a function of how the pole reacts to the input forces. The vortex shedding response is a function of the modal characteristics of the structure, therefore, the important pole dynamic properties include modal frequencies, modal shapes, and structural damping, ξ. In order to predict the anchor bolt stresses due to vortex shedding, these properties must be found.

The dynamic properties of the test pole at the Riverside Campus of Texas A&M University were evaluated by recording free vibration response time histories of strain gage voltage versus time. The input forcing function was achieved by pulling on the south light assembly cable. This cable is used to raise and lower the lighting assembly. The response time history data was recorded for all strain gages. A trace of the North bolt response is shown in Figure C-1. The modal frequencies of the pole can be determined by converting this trace from the time domain into the frequency domain. This conversion is done by way of a Fast Fourier Transform (FFT). A spectral density plot shows the response signal as a function of frequency and is achieved by plotting the real part of the FFT versus frequency. The spectral density plot for the input signal of Figure C-1 can be seen in Figure C-2.

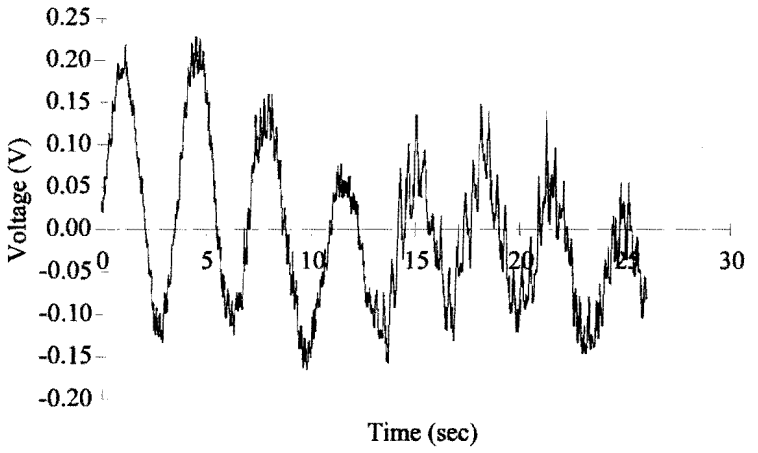

Figure C-1 Strain gage voltage versus time for North Bolt, HMIP.

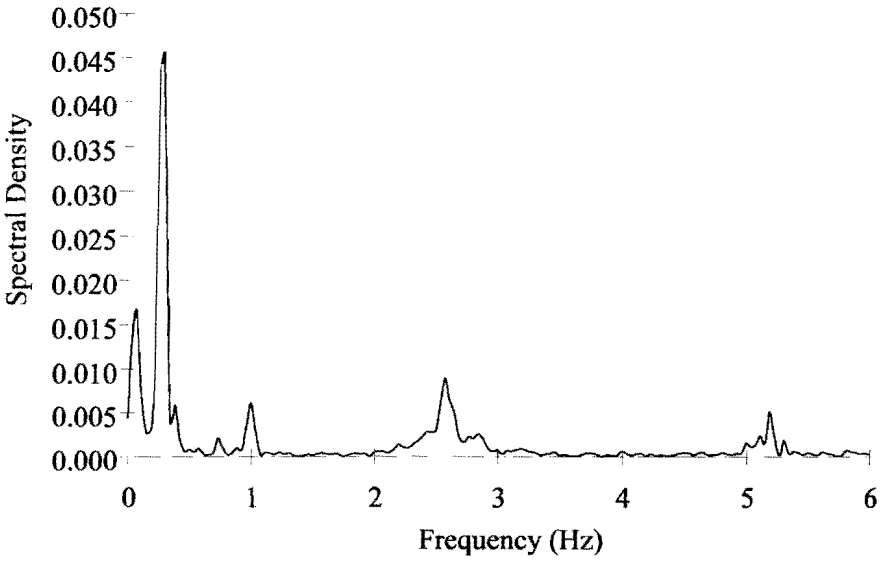

Figure C-2 Spectral density plot for data in Figure C-1.

The spikes seen in Figure C-2 show the regions of frequency that dominate the input traces. These are the natural frequencies of the pole. This spectral density plot shows a

clustering around the 0 Hz to 0.25 Hz range. This response is due to the conditions in which the test data was obtained. Data was collected on a day when the wind speed was near 2.3 m/s (5 mph). This low frequency response is the structural response to slightly varying wind and must be filtered out in order to properly see the fundamental frequencies alone. The data obtained from the North anchor bolt seen in Fig. 1 is passed through a 0.25 Hz high pass filter. This new trace can be seen in Figure C-3 and its spectral density plot, shown in Figure C-4, is used to determine the lowest four natural frequencies of the HMIP.

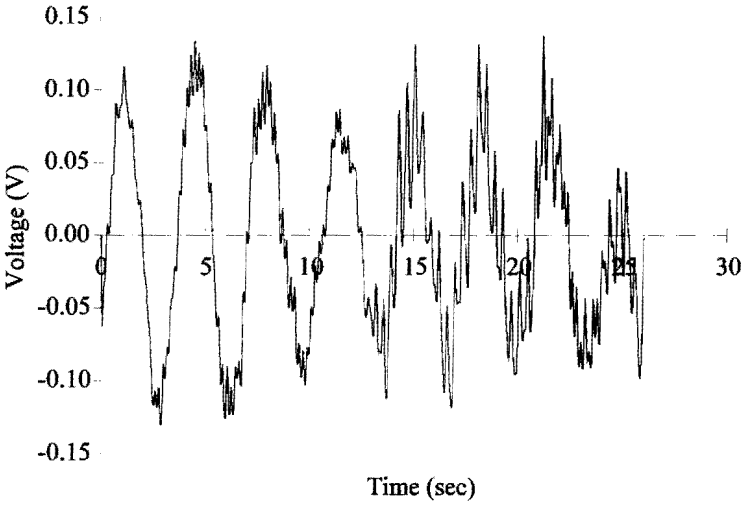

Figure C-3 High pass filtered data of Figure C-1.

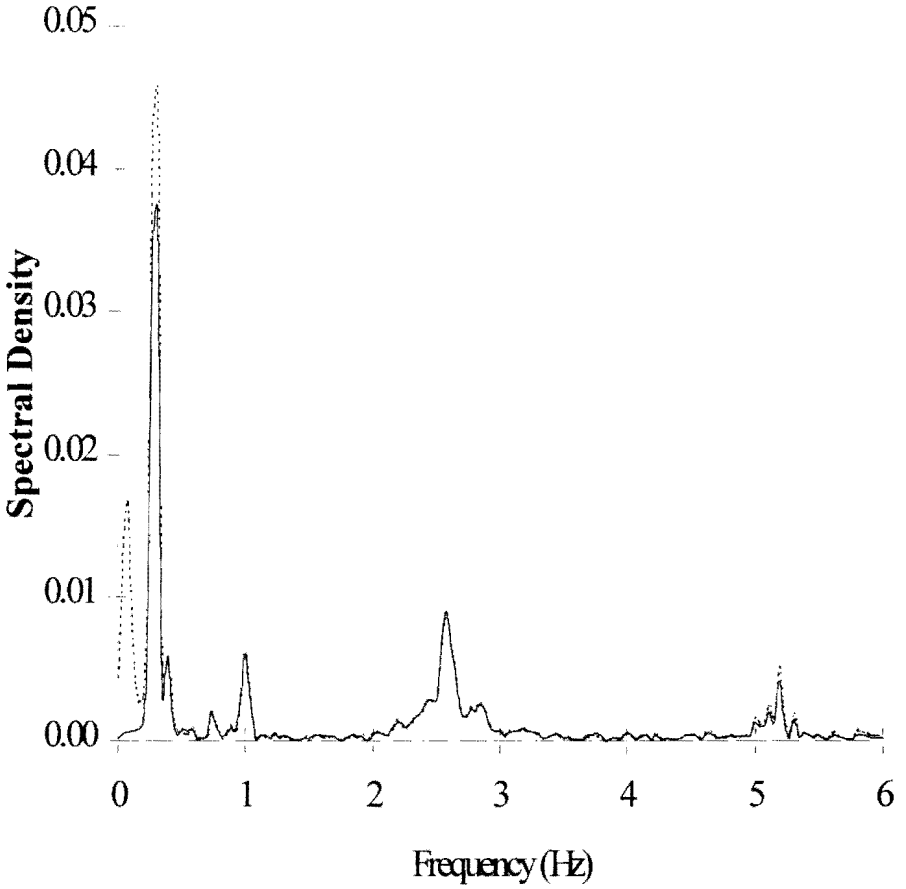

Figure C-4 Spectral density plot for data in Figure B-3.

An eigenvalue analysis of the pole was also performed to predict the natural frequencies. The analysis was done by breaking the pole into six different sections and assumes a 409 kg (900 lb) lumped nodal mass at the top of the HMIP to simulate the lights and lighting structure. The values obtained by this analysis correlate closely to the first four modes seen from the free vibration test data in Figure C-4. The higher modes of vibration have high frequencies and are not found in this analysis. Table C-1 shows a summary and comparison of the first four modes. Figure C-5 shows the mode shapes for the first four modes.

Table C-1 Summary and comparison of natural frequency data.

Mode	Modal Frequency (Hz) Free Vibration Data	Modal Frequency (Hz) Eigenvalue Analysis	Difference (%)
1	0.32	0.33	1.5
2	1.02	1.12	9.3
3	2.58	2.67	1.7
4	5.19	5.07	2.3

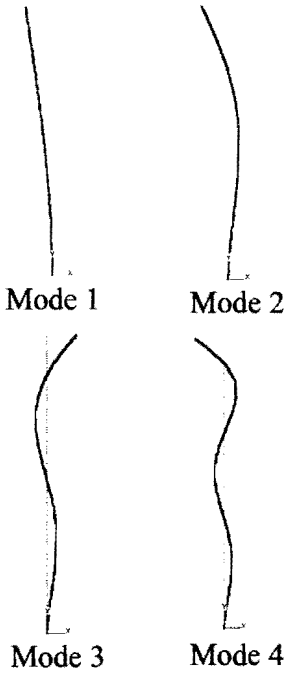

Figure C-5 Mode shapes of HMIP.

Structural damping gives a measure of the rate of energy dissipation in a structure. To obtain the structural damping, ξ, the natural log decrement method (Blevins 1990) is used

in which

$$\xi = \frac{\ln \frac{v_n}{v_{n+m}}}{(m-n)2\pi},$$

where:

ξ = structural damping,

v_n = maximum response for peak n, and

v_{n+m} = maximum response for next peak $n+m$.

The input signal of Figure C-3, however, cannot be used with this method. To properly use the natural log decrement method, the first mode of vibration must be isolated. Isolation of this mode is accomplished by passing the data of Figure C-1 through a bandpass filter. The bandpass filter combines a low pass filter with cutoff at 0.5 Hz and a high pass filter with cutoff and 0.25 Hz. Figure C-6 shows the resulting filtered data. Using the natural log decrement method with Figure C-6 gives a structural damping of 0.024 (2.4%). This is higher than the suggested AASHTO value of $\xi = 0.005$ (0.5 %) for sign and signal structures (AASHTO 1994).

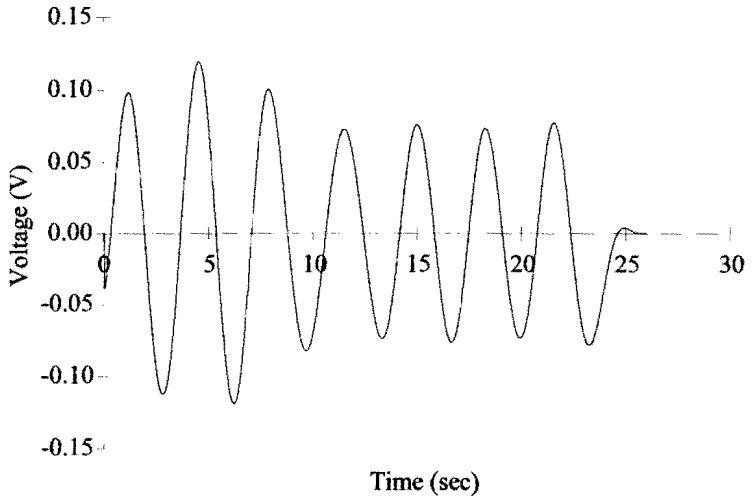

Figure C-6 Band pass filtered data of Figure C-1.

EQUIVALENT POLE PROPERTIES

To develop a vortex shedding model, properties other than natural frequencies, mode shapes, and damping must be determined. These other pole properties include diameter, length, wall thickness, mass per unit length, and moment of inertia. The typical HMIP is composed of thin-walled, tapered octagonal sections. HMIPs are typically installed in heights of 30 500 mm (100 ft), 38 000 mm (125 ft), 45 700 mm (150 ft), and 53 300 mm (175 ft). These different lengths are achieved by combination of three 1010 mm (33.3 ft) sections plus addition of the desired number of 7600 mm (25 ft) sections to obtain the desired height. Normally, TxDOT specifies poles designed for 36 m/s (80 mph) or 45 m/s (100 mph) wind speeds. The 45 m/s (100 mph) pole has larger diameters and thicker wall sections. The test HMIP at the Riverside Campus is designed for a wind speed of 45 m/s (100 mph).

Because a HMIP is a complex, octagonal cross-sectioned, linearly tapered structure, and vortex shedding simulation is based on a simple prismatic, circular cross-section, the pole properties must be calculated based on a pole of equivalent stiffness. First, an equivalent pole diameter is calculated as (AASHTO 1994):

$$D_e = \frac{D_t - D_b}{2},$$

where:

D_e = equivalent pole diameter, mm (ft),
D_t = flat-to-flat dimension at the top of the pole, mm (ft), and
D_b = flat-to-flat dimension at the bottom of the pole, mm (ft).

Here, the equivalent diameter represents the distance between separation points of the shear layers in the fluid flow. Similarly, the equivalent pole length is given by (AASHTO 1994):

$$L_e = L\sqrt{\frac{2D}{D_t + D_b}},$$

where:

L_e = equivalent pole length, mm (ft) and

L = length of HMIP, mm (ft).

The equivalent wall thickness can be found using a weighted average method as:

$$t_e = \frac{\sum_{i=1}^{N_s} t_i L_i}{\sum_{i=1}^{N_s} L_i},$$

where:

t_e = equivalent wall thickness, mm (ft),

N_s = number of pole sections,

t_i = thickness of section *i*, mm (ft), and

L_i = length of section i, mm (ft).

The equivalent mass per unit length can be found by first determining the equivalent area as (AASHTO 1994):

$$A_e = 6.63 R_e t_e = 6.63\left(\frac{D_e}{2} - \frac{t_e}{2}\right)$$

$$\left(A_e = 6.63 R_e t_e = 6.63\left(\frac{D_e}{2} - \frac{t_e}{2}\right) \right),$$

where:

A_e = equivalent area, mm^2 (ft^2) and

R_e = equivalent radius, mm (ft).

Now, the equivalent mass per unit length can be calculated as:

$$m_e = \frac{A_e \gamma + \frac{W}{L_e}}{g},$$

where:

m_e = equivalent mass per unit length, kg/m (slug/ft),

γ = weight density of the pole = 77 000 N/m^3 (490 lb/ft^3),

W = weight of light structure, N (lb), and

g = acceleration due to gravity = 9.81 m/s^2 (32.2 ft/sec^2).

Finally, the moment of inertia at the anchor bolt detail must be calculated. This calculation involves the determination of the moment of inertia for each bolt plus the contribution due to the parallel axis theorem. The moment of inertia of each bolt is given by:

$$I_b = \frac{\pi R_b^4}{4},$$

where:

I_b = moment of inertia of one bolt, in^4 (mm^4) and

R_b = equivalent radius of a single bolt, in (mm).

And:

$$R_b = \frac{\left(\varphi - \frac{0.9743}{n}\right)}{2},$$

where:

φ = diameter of bolt, mm (in.) and

n = number of threads per millimeter (threads per inch).

The contribution to the moment of inertia of the bolt detail due to the parallel axis theorem involves the equivalent area of the bolt given by:

$$A_b = \frac{\pi}{4}\left(\varphi - \frac{0.9743}{n}\right)^2,$$

where:

A_b = equivalent area of a single bolt, mm^2 (in.^{2}).

Now, the total moment of inertia can be given as:

$$I = \sum_{i=1}^{N_b} I_b + (A_b y_i^2),$$

where:

N_b = number of bolts in the bolt group and

y_i = vertical distance from the neutral axis to bolt N_b, mm (in.).

Table C-2 summarizes these properties.

Table C-2 HMIP equivalent properties.

Pole Property	S.I. Value	U.S. Customary Value
Equivalent diameter, D_e	0.55 m	1.82 ft
Equivalent length, L_e	31.79 m	104.31 ft
Equivalent wall thickness, t_e	1.14×10^{-2} m	3.73×10^{-2} ft
Equivalent mass per unit length, m_e	173.3 kg/m	3.62 slug/ft
Moment of inertia, I	4.78×10^{9} mm^4	11484 in^4

APPENDIX D--Proposed Specification for Tightening Large-Diameter Anchor Bolts

(Proposed)

TIGHTENING LARGE-DIAMETER ANCHOR BOLTS IN COSS AND HMIP FOUNDATIONS

1. Description This item shall govern for tightening nuts on double-nut anchor systems using 4.5 mm (1.75 in.) diameter and larger anchor bolts to secure Cantilever Overhead Sign Structures (COSS) or High Mast Illumination Poles (HMIP) to drilled shaft foundations in accordance with the details and dimensions shown on the plans or as directed by the Engineer. Proper performance of the double-nut anchor bolt system under static and cyclic loadings requires that a preload be built into the anchor bolts by a specified nut tightening procedure. Failure to follow the specified procedure can result in inadequately tightened bolts or excessively tightened bolts. Inadequately tightened bolts can lead to fatigue failures and/or loosening of the nuts under cyclic loading. Overly tightened bolts may deform plastically, necessitating removal and replacement.

2. Materials All materials furnished, assembled, fabricated or installed under this item shall be new, unless otherwise indicated, and in strict accordance with the details shown on the plans. Specified nuts shall be installed on the anchor bolts by the fabricator and shipped assembled on the anchor bolts. Anchor bolt threads shall be protected to prevent damage during shipping and handling.

3. Inspection of anchor bolts after construction of the drilled shaft After construction of the drilled shaft foundation, the anchor bolts must be inspected visually to verify that projecting length of bolts, bolt pattern and orientation of pattern, bolt alignment, bolt galvanizing, are as shown in the plans. Bolt pattern must be inspected by comparison of the top template to the baseplate of the structure to be erected. More than 3 mm (1/8 in.) misalignment of the holes in the baseplate of the structure and the holes in the template must be reported to the Engineer. Individual bolts must not be misaligned more than 3 mm/m (1/8 in. in 3 ft). Any misaligned bolts must be approved by the Engineer. Straightening of misaligned bolts by bending is not permitted, unless at the specific direction of the Engineer. Inspection must also verify that

proper anchor bolt nuts are provided as called out on the plans and that the threads on the bolts have not been damaged during construction. For inspection, the nuts should be turned off and back onto the bolts by one worker using a wrench only. Any damage that requires more than minimal effort must be called to the attention of the Engineer for possible correction.

4. Lubrication of the Anchor Bolts Once the inspection of the bolts is completed, the threads of the anchor bolts should be cleaned and lubricated with beeswax. This should be done the day of erection. If erection is delayed more than 24 hours after the bolts are lubricated, this cleaning and lubricating must be repeated.

5. Bolt Tightening Sequence The pole shall be erected and bolt tightening completed with all cantilevered elements removed. The bolts must be tightened in the sequence specified at each step which calls for tightening. For an eight-bolt pattern, denote the bolts 1-8, in clockwise order viewed from above, beginning with bolt 1 on the side away from the heaviest cantilevered element. The tightening sequence is 1, 5, 2, 6, 8, 4, 7, 3. For a twelve-bolt pattern, denote the bolts 1-12, in clockwise order viewed from above, beginning with bolt 1 on the side away from the heaviest cantilevered element. The tightening sequence is 1, 7, 2, 8, 12, 6, 3, 9, 11, 5, 4, 10.

6. Tightening Methods Two methods are acceptable: impact tightening and static tightening. Tools used to tighten the nuts by the impact tightening method shall be box end "slug" or "knocker" wrenches in the size of the nuts to be tightened, and a 7 kg (16 lb) sledgehammer. Tools used to tighten the nuts shall be "spud" wrenches in the size of the nuts to be tightened, and a pipe or extension handle at least 3 m (10 ft) in length suitable for extending the handle of the wrench and applying the torque required to turn the nuts as specified herein. In the impact tightening method, the wrench is driven with the hammer until the specified nut rotation is achieved, using the specified tightening sequence. In the static tightening method, the wrench is turned by the force of three or more workers until the specified nut rotation is achieved, using the specified tightening sequence.

7. Tightening Procedures The bottom nuts shall be installed on the bolts, one on each bolt. Using the top template as a guide, level the top template by adjusting the bottom nuts so that the template rests on each nut and the distance between the top of the concrete shaft and the bottom surface of the bottom nut is approximately 12 mm (0.5 in.). Remove the template, lubricate the bearing surface of the bottom nuts and washers with beeswax, and erect and plumb the structure as specified elsewhere. Adjust the bottom nuts so that each is bearing equally on the washer or baseplate. With all cantilevered elements removed, and with the plumbed structure supported by a crane, lubricate the bearing surfaces of the top nuts and washers and install the washers and top nuts and turn them onto the bolts so that each top nut is hand-tight against the washer or baseplate. Using a wrench, turn the bottom nuts up in the specified sequence to a snug tight condition--snug tight is defined to be the condition where the nut is in full contact with the baseplate, and it may be assumed that the full effort of a workman on a 300 mm (12 in.) wrench results in a snug tight condition. Verify that the structure is still plumb and still supported by the crane. In the specified sequence, turn the top nuts down to the same snug tight condition. Once the snug tight condition is achieved, preload is induced by either the static or impact tightening method. The tightening in either case is by the turn-of-the-nut method; the reference positions of the nuts in the snug tight condition must be marked with a suitable marking on one flat, with a corresponding reference mark on the baseplate at each bolt to indicate their individual positions.

In the specified sequence, fit the wrench on the nut to be turned and turn the nut down until the nut has been turned 30 degrees (one-half of a hex nut "flat") past snug tight. Tighten each top nut in the specified sequence to 30 degrees past snug tight. Repeat this process turning each top nut an additional 30 degrees down until each top nut has been tightened 60 degrees past snug tight.